To the Graduate Council:

I am submitting herewith a dissertation written by David F. Swaile entitled "Alternate Methods of Laser-Based Fluorometric Detection In Capillary Electrokinetic Separations." I have examined the final copy of this dissertation for form and content and recommend that it be accepted in partial fulfillment of the requirements for the degree of Doctor of Philosophy, with a major in Chemistry.

Michael J. Sepaniak, Major Professor

We have read this dissertation
and recommend its acceptance

Accepted for the Council:

Associate Vice Chancellor
and Dean of The Graduate School

ALTERNATE METHODS OF LASER-BASED FLUOROMETRIC DETECTION IN CAPILLARY ELECTROKINETIC SEPARATIONS

A Dissertation

Presented for the

Doctor of Philosophy

Degree

The University of Tennessee, Knoxville

David F. Swaile

December 1991

DEDICATION

For Beverly Ann.

ACKNOWLEDGMENTS

This work would not have been possible without the help and encouragement of many people. I would like to thank my parents, Bill and Pat Swaile for their constant love and support throughout my education. Also my inlaws, Harold and Barbara Hanes for all of their help during the past five years. I would like to express my gratitude to Dr. Michael J. Sepaniak for his patience and guidance during the past four years. He has allowed me to follow my own ideas and make my own mistakes but never let flounder for long. Finally, I would like to thank Jim Bowyer, Rod Cole, Craig Powell and all of friends for making graduate school both enjoyable and memorable.

Additionally, I would like to thank the University of Tennessee Department of Chemistry for allowing me to pursue my doctoral degree and financial support in the form of teaching and research assistantships. Financial support from Dr. Sepaniak's research grants are also gratefully acknowledged.

ABSTRACT

Capillary electrokinetic separation methods have become increasing popular in the past decade due to their high efficiency, short analysis times, and ability to analyze minute samples. These advantages are a direct result of performing separations in small diameter capillaries, typically less than 100 μm in internal diameter. These capillaries are able to dissipate heat produced by the passage of current through the electrophoretic medium more effectively than other electrophoretic separation formats, allowing the use of very high electric field strengths. Unfortunately the size of the capillaries employed results in band volumes of less than 10 nL, which often contain less than 1 picomole of analyte, making detection of eluting bands a formidable task. Furthermore, on-column detection is usually required to prevent band broadening.

Laser-based fluorometric detection is one of the most successful detection schemes that has been applied to capillary electrokinetic separation methods. The high power of laser beams result in high sensitively in spite of the short pathlengths created by on-column detection. Furthermore, laser beams are highly collimated, allowing them to be easily focused into the flow channel of the capillary. The major limitation of this method is the lack of available fluorophores. To increase the applicability of this method, fluorescent labels are often attached to the analyte prior to detection. However, this can require either time consuming sample preparation or the use of a post column reactor.

A more desirable situation would involve the labeling reaction occurring during the separation process. Presented herein are two labeling methods that allow the reaction to be performed concurrent to separation. The detection of proteins and surfactants is performed using fluorescent hydrophobic probes. Similarly, the detection of metal ions is accomplished using fluorescent chelating agents.

The detection of fluorescently labeled species can usually be performed at a single wavelength; however, a mixture of native fluorophores may require monitoring several different wavelengths to maximize sensitivity. This is most conveniently accomplished using a multichannel detector such as a diode array. Multichannel detection permits the optimization of emission wavelength and bandpass to enhance sensitivity and detector selectivity. Described herein is the characterization of a fluorometric photodiode array detection scheme for capillary electrokinetic separation methods. Analytical figures of merit and a discussion of the ability of multichannel detection to improve analytical selectivity will be presented.

TABLE OF CONTENTS

Chapter		Page
1.	INTRODUCTION	1
	Brief Historical Perspective	1
	Electrophoretic Mobility and Electroosmosis	8
	Separation In CZE and MECC	11
	Statement of Problem	16
2.	GENERAL EXPERIMENTAL APPARATUS, CONSIDERATIONS AND PROCEDURES	22
	Capillary Parameters	22
	Buffer Parameters	26
	Applied Electric Field Strength	30
	Injection Parameters	31
	Detection Parameters	35
3.	LASER-BASED FLUOROMETRIC DETECTION SCHEMES FOR THE ANALYSIS OF PROTEINS BY CAPILLARY ZONE ELECTROPHORESIS	39
	Experimental	41
	Considerations for Separation Efficiency	44
	Native Fluorescence Detection	50
	Pre-Column Covalent Labeling	52
	On-Column Labeling With Hydrophobic Probes	55
4.	SEPARATION OF ANIONIC SURFACTANTS BY CZE USING ON-COLUMN LABELING WITH 2-P-TOLUIDNYLNAPHTHALENE-6-SULFONATE	63
	Experimental	67
	Separation of Anionic Surfactants	68
	Quantitation of Sodium Dodecyl Sulfate	71
5.	DETERMINATION OF METAL IONS BY CAPILLARY ZONE ELECTROPHORESIS WITH ON-COLUMN CHELATION USING 8-HYDROXYQUINOLINE-5-SULFONIC ACID	78
	Theory	80
	Experimental	81

Detection 83
Manipulation and Prediction of
Electrophoretic Mobility 89
Band Broadening 96

6. FLUOROMETRIC PHOTODIODE ARRAY DETECTION IN
CAPILLARY ELECTROKINETIC SEPARATIONS 101
Experimental 104
Results and Discussion 106

7. CONCLUSIONS 114

LITERATURE CITED 117

VITA 128

LIST OF TABLES

TABLE		PAGE
1.	Experimental parameters which affect separation in CZE and MECC	23
2.	Effects of experimental parameters on peak efficiency for conalbumin	49
3.	Minimum detectable concentrations of conalbumin	52
4.	Minimum injectable amounts of protein for ANS and TNS	62
5.	Calibration data for high purity sodium dodecyl sulfate	74
6.	Limits of detection of calcium, magnisium and zinc	86
7.	Calculated and experimental mobilities of Ca(II) and Mg(II) peaks and band components	95

LIST OF FIGURES

FIGURE		Page
1.	Depiction of parabolic and plug-like flow profiles ..	10
2.	Depiction of the elution range in MECC	15
3.	Depiction of general experimental apparatus	24
4.	Depiction of capillary holders for spectrophotometric and laser-based fluorometric detection	38
5.	Peak profiles of conalbumin in untreated and Clect H-1 capillaries	45
6.	Separations of myoglobin, conalbumin and beta lactoglobin B and A using different pH buffers	47
7.	Peak profiles for conalbumin using native fluorescence detection and pre-column labeling with FITC	54
8.	Effects of TNS concentration on signal and signal to noise ratio for conalbumin	57
9.	Effects of buffer pH on fluorescence signal of TNS in conalbumin	58
10.	Separation of conalbumin, beta lactoglobin B, beta lactoglobin A, and bovine serum albumin	60
11.	Electropherograms of high purity and technical grade sodium dodecyl sulfate	69
12.	Electropherograms of sodium cholate and high purity SDS (A) and commercial soap product (B)	72
13.	Calibration curves for high purity SDS	73
14.	Graph of the effects of sodium dodecyl sulfate	

concentration on electrophoretic mobility 76

15. Separation of test metals under various electrophoretic buffer conditions 85

16. Injection of blood serum with an equal volume of electrophoretic buffer 88

17. Effects of HQS^- concentration on the observed mobility of Ca(II), Mg(II), and Zn(II) 90

18. Graph of the effects of buffer pH on the observed mobility of Ca(II), Mg(II), and Zn(II) 93

19. Depiction of laser-based fluorometric diode array detection scheme 105

20. Calibration curves for sodium fluorescein 107

21. Wavelength/intensity/time chromatogram for sodium fluorescein, Coumarin 102, and DCM 109

22. Signal to noise ratio and noise for sodium fluorescein peak in Figure 21 as a function of bandpass 110

23. Selected spectral region chromatograms of sodium fluorescein, Coumarin 102, and DCM 112

CHAPTER 1

INTRODUCTION

Brief Historical Perspective

Electrokinetic separation methods have greatly increased in popularity in the past decade. Techniques such as zone electrophoresis and isoelectric focusing in gels have been extensively used in the biotechnology field for many years (1). This is a direct result of the strong resolving power of these methods for samples such as proteins and polynucleotides. However, they have not been used as extensively in other fields as have high performance liquid chromatography (HPLC) and gas chromatography, probably due to the laborious nature and relatively long analysis times of the electrophoretic methods. In the late 1970's, the first capillary electrophoretic separations were performed. This innovation (i.e. the use of narrow bore capillaries to confine the electrophoretic medium) allowed the use of much higher electric field strengths to reduce analysis time and permitted the development of automated instrumentation, making these methods comparable to other separation methods.

Electrophoresis was born in 1809 when Reuss observed the movement of clay particles under the application of an electric field (2). It did not become an analytical separation method, however, until 1937 when Tiselius demonstrated the separation of proteins using moving boundary electrophoresis (3). In this early paper,

proteins were placed in a large zone at the bottom of a U shaped tube. Upon application of an electrical field the proteins moved with velocities determined by their electrophoretic mobilities. However, the large size of the sample plug prevented complete separation of sample components, with only the fastest and slowest migrating species being purified. Due to this inherent limitation of moving boundary electrophoresis, it was quickly replaced by zone electrophoresis. This method employs a much smaller sample plug, permitting the separation of sample components into narrow bands or "zones" of high purity.

Along with the growth of zone electrophoresis, other electrokinetic separation techniques such as isoelectric focusing, isotachophoresis, and gel sieving have been developed to enhance separation selectivity (4, 5). Isoelectric focusing separates amphoteric species based upon differences in isoelectric point. This method is often applied to the analysis of proteins and has been shown to separate species that differ in isoelectric points (pI) by as little as 0.001 pH units (1). In isotachophoresis, compounds are separated between relatively concentrated buffers of very high and low mobility under conditions of constant electrophoretic current. Once an equilibrium condition is achieved, the constant current causes all the solutes to move at the same velocity, therefore forcing solutes into bands of similar mobility to prevent the formation of gaps in the solution (1, 5). This method is often used for the analysis of inorganic ions. Gel sieving electrophoresis separates macromolecules based on size, after denaturation, by

performing zone electrophoresis in a porous gel. In this method, migration rates are determined by the mobility of the species and solute size in relation to the size of the pores in the gel (6). Small components easily pass through the pores, while large species are retained. Moreover, these techniques are sometimes combined to improve the peak capacity and resolving power of both methods. For example, gel sieving is sometimes performed after isoelectric focusing to produce a two-dimensional separation method.

One of the major problems of electrokinetic separation methods is the dissipation of heat produced by the passage of current through the electrophoretic buffer. Tiselius's first experiments were performed in free solution. Heat produced in these experiments created temperature gradients in the tube, which created density gradients and convective flow. This undesirable flow caused mixing of the sample zones, which degraded resolution. To prevent convection, several types of stabilizers have been employed such as vertical density gradients and solid supports (4). Generally, convection is reduced by performing the electrophoretic separation in a porous solid support. Paper, cloth, granulated starch gels, and most commonly polyacrylimide gels have been used as solid supports (6). An additional advantage of this method is that the porosity of the stabilizer can be varied to permit size sieving (as discussed above). However, the tortuous path the solute must travel can result in band broadening (often referred to as eddy migration) and inaccurate measurement of electrophoretic mobility.

Furthermore, adsorption of the solute to the stabilizer can result in band broadening.

In 1977, Verheggen *et al.* performed isotachophoretic separations in narrow bore capillaries to prevent convection (7). Narrow bore capillaries reduce turbulent flow, produce less heat than other electrophoretic formats, and more easily dissipate the heat that is produced. The small cross section of narrow bore capillaries prevents the formation of eddy currents, so laminar flow occurs. Also the reduced cross section decreases ion flow between the anode and cathode; consequently the electrophoretic current and amount of heat produced are reduced. Moreover the high external surface area to volume ratio of these capillaries permits the dissipation of heat created by the electrophoretic process, thereby decreasing the temperature gradient in the flow channel of the capillary and convection. Verheggen and coworkers were not the first to use small capillaries for isotachophoresis; 400 - 600 μm inner diameter (i.d.) capillaries were commonly used at that time. However, they were the first to directly compare the heat and temperature gradient produced by different diameter capillaries. Their work demonstrated that a 100 μm i.d. capillary resulted in a lower absolute temperature increase and smaller temperature gradient, for a given current density, than a 400 μm i.d. capillary. Additionally, improved resolution and reduced analysis times were observed when the smaller capillary was employed.

Two years later, this same group reported the first zone electrophoretic separations in 100 μm diameter capillaries (8).

They reported that the shape of the eluting zone was dependent on sample concentration. High sample concentrations resulted in fronted or tailed peaks due to distortions in the electric field. If the conductivity of the band was significantly higher or lower than the surrounding buffer, the electric field strength in the vicinity of the band was increased or decreased according to Ohm's Law. However, low sample concentrations resulted in symmetric peaks because the conductivity in the vicinity of the eluting zone was determined by the buffer. To demonstrate the high efficiency of this method the authors showed the separation of 16 ions in approximately 9 minutes. In fact, several components in their test mixture achieved plate heights of less than 10 μm.

The true potential of capillary zone electrophoresis (CZE) as an analytical method, was not evident until Jorgenson and Lukacs published a landmark paper in 1981 describing electrophoretic separations in glass capillaries (9). They discussed the requirements for achieving high efficiency, the advantages of electroosmosis, and derived equations describing the separation process. They employed higher ionic strength buffers and smaller bore capillaries (75 μm i.d.) than the previous study to reduce band broadening due to distortions in the electric field. Furthermore, by performing sensitive on-column fluorometric detection, they were able to detect lower sample concentrations than Verheggen *et al.*, which further reduced electric field distortions. These modifications resulted in symmetric peaks with plate numbers near 400,000.

Jorgenson and Lukacs were also the first to discuss the advantages of electroosmosis in these separation methods (9, 10). Strong electroosmotic flow caused both anions and cations to move in the same direction so detection could be conveniently performed at a single point on the capillary. Electroosmosis also reduced analysis time and, thereby, band broadening due to axial diffusion. Moreover, the plug-like flow profile of electroosmosis (see later discussion) minimized "resistance to mass transfer" contributions to band broadening. To account for the effects of electroosmosis on the separation process, the authors derived equations for efficiency and resolution. From these equations they determined that efficiency was theoretically limited by molecular diffusion, independent of capillary length, and should be maximized by the use of very narrow short capillaries and high electric field strengths.

In addition to the discussion of the merits of CZE, Jorgenson and Lukacs described advances needed to enhance the utility of CZE; such as more sensitive detection schemes, improved injection techniques, and the development of inert capillary materials (9). During the next decade, approaches to achieving these goals were addressed by numerous research groups, thereby greatly advancing the technology associated with CZE. The development of laser-based fluorometric (11-17), electrochemical (18- 21), and mass spectrometric detection (22, 23) schemes have greatly improved limits of detection. Automated injection systems and the use of internal standards have improved reproducibility of peak height and area to near 1% (24, 25). Furthermore, the development of inert

capillary coatings has greatly reduced solute-wall interactions, permitting the analysis of strongly adsorbing compounds such as proteins (26,-29). Accompanying the development of new instrumentation for performing CZE, other electrokinetic methods have been adapted to a capillary format. These include isoelectric focusing (30) and gel sieving (31, 32), as well as several electrokinetic chromatographic methods (33-35).

The high resolving power of these methods as well as their ability to analyze small sample volumes has resulted in their application to a variety of different samples. Although, the majority of reports in the literature involve the separation of biological samples such as proteins (27, 28, 36- 40) and polynucleotides (38, 41), these techniques have made inroads into other areas. Separations of small organic molecules (35, 42-44), chiral species (45-51), inorganic ions (52-55), and polymers (56) have been reported. The vast interest in these methods is evidenced by the large number of reviews in the recent literature (1, 21, 38, 40, 57-60) and the inclusion of these methods in the fundamental reviews of *Analytical Chemistry* (61). Furthermore, the development of commercial instrumentation for these methods also illustrates their increased use.

The development of capillary electrokinetic separation methods for neutral species is of particular interest, as these compounds cannot be effectively separated by conventional electrophoretic methods. The separation of neutral species is difficult because they have mobilities near zero and separation in

electrophoresis is based on differences in electrophoretic mobility. To address the separation of neutral compounds, Terabe *et al.* added charged surfactants to the electrophoretic buffer above the critical micelle concentration (CMC) of the surfactant, thereby creating a two phase system involving both aqueous and micellar phases (35, 44, 62). As the micellar phase is charged, it has an electrophoretic mobility that affects its velocity. Thus, upon application of an electric field, the two phases move through the capillary with different velocities and separation can occur based on differential partitioning between the two phases. This technique has been christened micellar electrokinetic capillary chromatography (MECC) by Sepaniak *et al* (15, 17, 34, 42, 43, 63,-75).

Plate numbers as high as 500,000 and separation selectivity similar to reverse phase chromatography make MECC an attractive alternative to open tubular chromatography. Furthermore, the interactions of some micellar systems with solutes can result in unique chromatographic selectivity such as those involving chiral separation (45-51). However, MECC suffers from a limited elution range, which reduces peak capacity and hampers the separation of very hydrophobic compounds.

Electrophoretic Mobility and Electroosmosis

The velocity of a solute in an electric field is equal to the force applied to the solute (field strength multiplied by total charge) divided by a friction factor (determined by size of the solute and the viscosity of the surrounding solution). These parameters are

described as the solute's electrophoretic mobility (μ_{eo}), which is the velocity of a solute in a electric field of unit strength and is generally expressed in units of (cm^2/skV). This simple model is complicated by the existence of two counter velocity effects, electrophoretic relaxation and field relaxation (76). Both effects result from the accumulation of counter charges around the solute to maintain the electroneutrality of the solution. The electrophoretic relaxation effect results from counter charges near the solute moving in the opposite direction to the solute. These counter charges reduce the velocity of the solute by physically restricting ("colliding with") movement of the solute and causing solvent near the solute to flow in the opposite direction. This effect can reduce the solute's electrophoretic mobility by more than an order of magnitude. Field relaxation results from the reduction of the electric field by the surrounding counter ions. This effect is usually smaller than electrophoretic relaxation, but can significantly alter the solute's mobility.

Electroosmosis is the flow of solution over an immobile charged species due to the application of a tangential electric field (76, 77). On the wall of fused silica capillaries are a large number of acidic silanol groups (Si-OH groups), which are partially deprotonated under normal buffer conditions in CZE and MECC. The negative sites on the wall attract cations from the buffer which form an electric double layer that can be described by the Stern-Gouy-Chapman model (78). The layer of cations consists of two regions, an inner layer of tightly bound immobile ions and a diffuse

outer layer of somewhat more mobile ions. Upon application of a tangential electric field, ions in the bulk solution and to a lesser degree in the diffuse layer migrate, dragging along solvent and resulting in bulk flow. Unlike flow resulting from a conventional pump which has a parabolic flow profile, electroosmotic flow has a plug-like flow profile (Figure 1). Plug-like flow reduces the velocity gradient across the flow channel of the capillary, thus reducing band broadening due to slow mass transfer across the velocity gradient (77). This allows these methods to be performed in capillaries larger than can be effectively employed in open tubular chromatography.

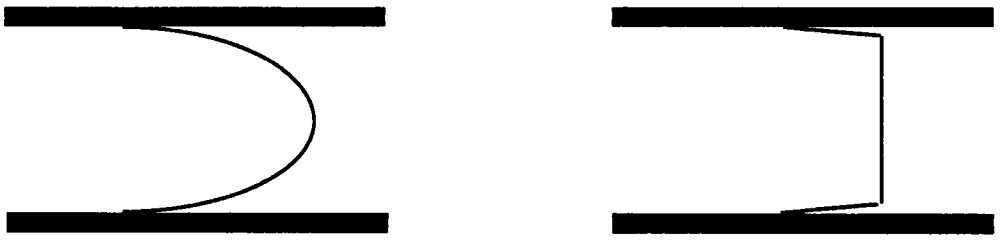

Figure 1. Depiction of parabolic and plug-like flow profiles.

The velocity of electroosmotic flow (v_{eo}) can be determined from the equation:

$$v_{eo} = \left(\frac{\varepsilon}{4\pi\eta} \zeta \right) E \qquad [1]$$

where ε is the dielectric constant of the buffer, η is the buffer viscosity, E is the applied field strength, and ζ is the zeta or double layer potential (77). Often the parenthetical factor in this equation is expressed as the electroosmotic mobility (μ_{eo}) of the buffer/capillary system. Variation in buffer and capillary parameters will affect electroosmotic velocity. For example, the addition of organic solvents to the buffer will lower the dielectric constant and disrupt the double layer by interacting with the capillary wall, resulting in a decrease in velocity (71, 79). Moreover, a reduction in charge density on the capillary wall will reduce the zeta potential and flow rate (80). Therefore, stringent control of buffer conditions is required to assure reproducible flow rates. Changes in flow rate affect migration times and peak areas and hence affect the analytical characteristics of these methods.

Separation in CZE and MECC

In CZE separation is based on the different migration velocities of solutes in an electric field (9). The velocity (v_{sol}) of a solute is determined by its electrophoretic velocity (v_{ep}) and the electroosmotic velocity (v_{eo}) of the electrophoretic buffer, as shown by the equation:

$$v_{sol} = v_{ep} + v_{eo} = (\mu_{ep} + \mu_{eo})E \qquad [2]$$

For all the cases discussed herein, electroosmotic flow is in the same direction as the electrophoretic mobility of cations (toward the negative electrode). This results in cations having a velocity greater than that due to electroosmosis. Although anions have a μ_{ep} in the opposite direction to electroosmosis, their electrophoretic velocity is generally smaller than the electroosmotic velocity of the buffer and they elute in the same direction as cations. Their net velocity through the capillary, however, is less than electroosmosis.

Bandwidths in CZE are theoretically limited by axial diffusion. Since CZE is a single phase separation method and is performed in an open tube, there should be no contributions to plate height from resistance to mass transfer between phases or eddy migration. Combining these advantages with the advantages of electroosmosis discussed previously, make CZE a very efficient separation method. The number of theoretical plates that can be achieved by a solute is given by the equation:

$$N = \frac{(\mu_{ep} + \mu_{eo})V}{2D} \qquad [3]$$

with V being the applied voltage and D the diffusion coefficient for the solute (9). It should be noted here that efficiency is not dependent upon capillary length, but rather on applied voltage. The applied voltage determines the analysis time for a given capillary length and therefore the time axial diffusion can occur. Therefore, short analysis times, resulting from high voltages, should provide

high numbers of theoretical plates. Unfortunately, axial diffusion is usually not the only source of band broadening. Solute/wall interactions, temperature gradients and extra-column effects increase bandwidth, resulting in less than theoretical efficiencies. These other sources of band broadening will be considered in chapter 2.

The resolution (Rs) of two solutes in CZE is given by the equation:

$$Rs = 0.177(\mu_1-\mu_2)\left[\frac{V}{D(\mu_{ave} + \mu_{eo})}\right]^{1/2} \qquad [4]$$

where μ_1 and μ_2 are the mobilities of the solutes and μ_{ave} is their average mobility (9). Although equation 3 predicts the highest efficiency for samples with a large mobility in the same direction as electroosmosis, those conditions are not optimum for resolution. In fact, equation 4 shows that resolution will be maximized when the electroosmotic mobility is equal and opposite in direction to the average electrophoretic mobility of the solutes. However, since this would result in an infinite analysis time, it is not a realistic situation.

MECC, unlike CZE, is based on differential partitioning in a two phase buffer system. The primary phase is an electroosmotically driven aqueous phase, moving at a velocity determined by equation 1. The secondary phase, the micellar phase, is moving at a velocity determined by the electrophoretic mobility of the micelle and

electroosmosis, as shown by equation 2. In all cases to date, the electrophoretic mobility of the micelle has been in the opposite direction to electroosmosis. Therefore, the velocity of the micellar phase is less than the electroosmotic velocity, yet in the same direction. The velocity of a solute ($v_{MECC\ sol}$) that is partitioning between the two phases will then be intermediate (see Figure 2) to the two velocities and can be described by the equation:

$$v_{MECC\ sol} = (\mu_{ep\ mic} + \mu_{eo})E + R(\mu_{ep\ sol} - \mu_{ep\ mic})E \qquad [5]$$

where $\mu_{ep\ mic}$ is the electrophoretic mobility of the micelle, $\mu_{ep\ sol}$ is the mobility of the solute, and R is the retention ratio of the solute (concentration of solute in aqueous phase/total solute concentration) (43). This equation shows the hybrid nature of MECC. The velocity of the solute is dependent on the electrophoretic behavior of the solute, micellar phase, and the aqueous buffer (as reflected in μ), and the chromatographic partitioning between the two phases (as reflected in R).

Since the micellar phase has a net velocity in the same direction as electroosmosis, it will eventually elute from the capillary. This results in a limited elution range for neutral solutes, between the void volume of the column (t_o) and the elution time of the micellar phase (t_m). The limited elution range has two major implications in the implementation of MECC; it results in a limited peak capacity and an optimal range of k' values. Typically, the

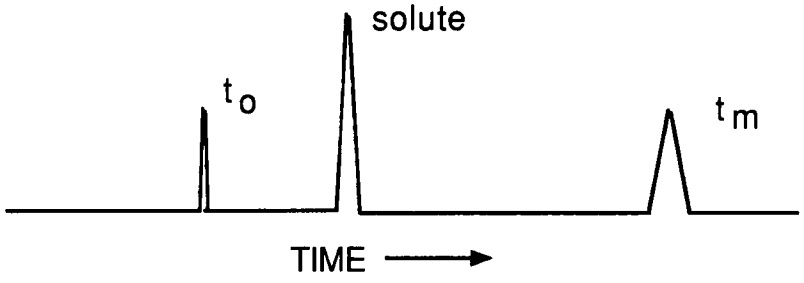

Figure 2. Depiction of the elution range in MECC.

elution window is ten to fifteen minutes in duration for a 75 cm long capillary with an electric field strength of 300 V/cm (t_o/t_m approximately 0.3). Since all neutral solutes will elute during this period, the number (n) of solutes that can be resolved is limited and can be determined from the equation (44, 73):

$$n = 1 + \frac{N^{1/2}}{4} \ln\frac{t_m}{t_o} \qquad [6]$$

Even with the high efficiency of MECC the peak capacity is much lower than techniques with an infinite elution range. For example the peak capacity for t_o/t_m = 0.3 is 96 if an average plate number of 100,000 is achieved.

The effects of the limited elution range on separation are shown by the resolution equation for MECC:

$$Rs = \frac{N^{1/2}}{4}\left(\frac{\alpha-1}{\alpha}\right)\left(\frac{k'_2}{1+k'_2}\right)\left(\frac{1-t_o/t_m}{1+(t_o/t_m)k'_1}\right) \qquad [7]$$

where α is the selectivity factor for the two solutes (k'_2/k'_1), and k'_1 and k'_2 are the capacity factors of the two solutes (44). The effect of the limited elution range is accounted for in the last factor in this equation. This term decreases at large values of k', thus maximizing resolution when k' is between 1 and 5. Consequently, very hydrophobic compounds, which have large k' values, are poorly resolved by this method.

From equations 6 and 7 it is obvious that increasing the elution range (decreasing t_o/t_m) will increase the peak capacity of this method and improve the resolution of solutes with large k' values (75). This is often accomplished by the addition of organic solvents to the buffer which has the effect of reducing electroosmosis. Additionally, organic solvents reduce the partition coefficient of most solutes, resulting in more desirable k' values for hydrophobic compounds. Unfortunately, high organic solvent concentrations can result in extremely long analysis and reduced efficiency. Further discussion of organic modifiers in MECC will be presented in Chapter 2.

Statement of Problem

Since the first paper by Jorgenson and Lukacs, the need for improved detection schemes for capillary electrokinetic separation methods has been evident. Even though a large number of research groups have developed new detectors, the minimum detectable concentration in these methods is higher than is generally observed for gas chromatography and HPLC detectors. The difficulties of

detection in these methods is a direct result of performing the separation in narrow bore capillaries. The minute band volumes created by these capillaries usually require on-column detection, short detection zones, and rapid detector response times to prevent band broadening (see further discussion in Chapter 2). To meet the challenges of detection in CZE and MECC a variety of detection schemes have been development based on optical (11-14, 53, 69, 81-86), electrochemical (18, 19, 87), radiochemical(88), and mass spectrometric methods (22, 23). The most frequently used detection methods are optically based, with absorption spectrophotometry (82-86) and fluorescence (11, 13-15, 69, 81, 85) being the most common.

Spectrophotometric detection monitors the reduction in optical intensity of a light source due to absorption of light by the analyte. The amount of light absorbed can be related to analyte concentration by Beer's law:

$$A = \varepsilon bc \qquad [8]$$

where A is the absorbance (AU), ε is the molar absorptivity of the solute (L m^{-1} cm^{-1}), b is the optical pathlength (cm), and c is the analyte concentration (M) (89). When on-column detection is performed, light is usually passed through the capillary perpendicular to the flow channel. Therefore, the pathlength is the internal diameter of the capillary. Since the capillaries used are typically less than 100 μm in diameter, very small absorbance

values are usually observed (less than 0.01 AU). To maximize sensitivity, detection is usually performed at wavelengths less than 280 nm where many compounds have large molar absorptivities. This necessitates the use of UV transparent fused silica capillaries and, adversely, reduces detector selectivity. Spectrophotometric detection is further complicated by large amounts of stray light, which reduces the linearity of this method. A typical limit of detection with this method is 8 μM for isoquinoline (ε = 18,000) in a 50 μm i.d. capillary (67). Capillaries with inner diameters less than 50 μm are usually not compatible with this detection method due to extremely short pathlengths and high amounts of stray light.

Laser-based fluorometric detection can solve many of the problems associated with spectrophotometric detection. High sensitivity can be achieved in spite of the short pathlengths due to the "fluorescence advantage." Furthermore, because fluorescence is measured against a black background the uncertainty of small signals is reduced. Lasers provide very high average excitation powers, typically between 2 and 20 mW (CW power levels) is employed but up to 1 watt has been reported (11). The advantage of employing very high excitation powers (the fluorescence advantage) is shown by the fluorescence equation:

$$P_f = P_{ex}\Phi k\varepsilon bc \qquad [9]$$

where P_f is the fluorescence power, P_{ex} is the excitation power, Φ is the quantum efficiency of the fluorophore, and k is the fraction of

fluorescence detected (89). Since P_f is directly proportional to P_{ex}, higher powers will result in larger signals. Laser beams are also well collimated; this allows the beam to be easily focused into the narrow flow channel of the capillary. Moreover, this collimation reduces specular scatter from the capillary wall and often results in a scatter pattern that can be discriminated against spatially. Finally since lasers can be focused to very small spot sizes, they produce very short detection zones (usually less than 50 μm) so detector related band broadening is reduced.

The major limitation of fluorometric detection is the lack of available fluorophores. Although many compounds will absorb light in the ultraviolet or visible wavelength regions, very few have fluorescence quantum efficiencies high enough for effective fluorometric detection. The use of laser excitation sources further reduces the number of detectable fluorophores, due to the limited number of easily accessible excitation wavelengths. While virtually any wavelength can be accessed with lasers, using dye lasers and nonlinear optical methods, the expense and complexity of these systems often precludes their use. Therefore, relatively simple laser systems such as low power argon ion and helium cadmium lasers are usually employed.

The applicability of laser-based fluorometric detection can be increased by the use of fluorescent labeling agents and multichannel detection. The attachment of fluorescent labels to solutes prior to (pre-column derivatization) or after (post-column derivatization) separation permits the fluorometric detection of nonfluorescing

species. Moreover, the label can be chosen such that its spectroscopic characteristics coincide with available laser wavelengths. For example, fluoroscein isothiocyanate is a commonly used label with an excitation maxima near 490 nm. This label can be excited by the 488 nm line of an argon ion laser and has been used to detect pre-column derivatized amino acids at picomolar concentration levels (11). Although attaching fluorescent labels to analytes can increase the applicability of fluorometric detection, it is not an ideal detection method. In fact, pre-column labeling can require time consuming sample preparation, and in some cases complicate the separation (see discussion in Chapter 3). Post-column labeling solves many of the problems associated with pre-column labeling but requires a reactor be placed at the outlet of the capillary (12, 81). This significantly complicates the relatively simple experimental apparatus of these methods. Furthermore, the post column reactor can result in detector related band broadening if flow conditions in the reactor are not optimal.

One goal of this work is to increase the applicability of laser-based fluorometric detection by developing novel labeling methods. By performing the labeling reaction during the separation process sample treatment and post-column reactors become unnecessary. Moreover by employing non-covalent chemical interactions for the labeling process, it is possible to avoid or control changes in the electrophoretic mobility of a solute resulting from the labeling process. Changes in the electrophoretic mobility can have deleterious effects on resolution, peak shape, and detectability.

A second goal of this research is to study the utility of multichannel detection for capillary electrokinetic separation methods. Single channel detection requires that emission intensity be monitored at a wavelength where all the solutes in the mixture fluoresce. This often results in the detection of one or more compounds at less than optimal emission wavelengths, thus reducing sensitivity. By monitoring a large range of wavelengths, the emission maximum for each compound in a mixture can be employed for quantitation. Furthermore, the observed bandpass can be chosen to increase the S/N for a given solute. Finally, collection of the entire fluorescence spectra will permit peak identification and allow discrimination of overlapping bands.

CHAPTER 2

GENERAL EXPERIMENTAL APPARATUS, CONSIDERATIONS, AND PROCEDURES

Table 1 lists the experimental parameters that must be controlled to successfully use CZE and MECC as analytical methods. This chapter will discuss each of these parameters and their effects on efficiency, resolution, and detectability. Furthermore, the interplay between the various parameters will be described. The goal of this chapter is to familiarize the reader with many of the idiosyncrasies associated with the performance of these methods and provide general experimental information.

Capillary Parameters

Figure 3 depicts the general experimental apparatus employed throughout this work. Separations were performed in fused silica capillaries that are suspended between two buffer reservoirs. Capillaries are typically less than 100 μm in inner diameter and 10 to 100 cm in length. The ends of the capillary are maintained at equal height to prevent hydrodynamic flow through the capillary. Buffer was introduced into the capillary by affixing a luer lock needle with epoxy to one end of the capillary so that it could be attached to a luer lock syringe. To prevent interference with sample injection, the needle was positioned such that 1 to 2 cm of the capillary protruded from the locking section of the needle.

TABLE 1

EXPERIMENTAL PARAMETERS WHICH AFFECT SEPARATION IN CZE AND MECC

1) Capillary Parameters
   a) Dimensions
   b) Material/Surface Modification
   c) Washing Procedures

2) Buffer parameters
   a) Composition and Concentration
   b) pH

3) Applied Electric Field Strength

4) Injection Parameters
   a) Plug length
   b) Method

5) Detection Parameters
   a) Detection Zone Length
   b) Detector Time Constant
   b) Method

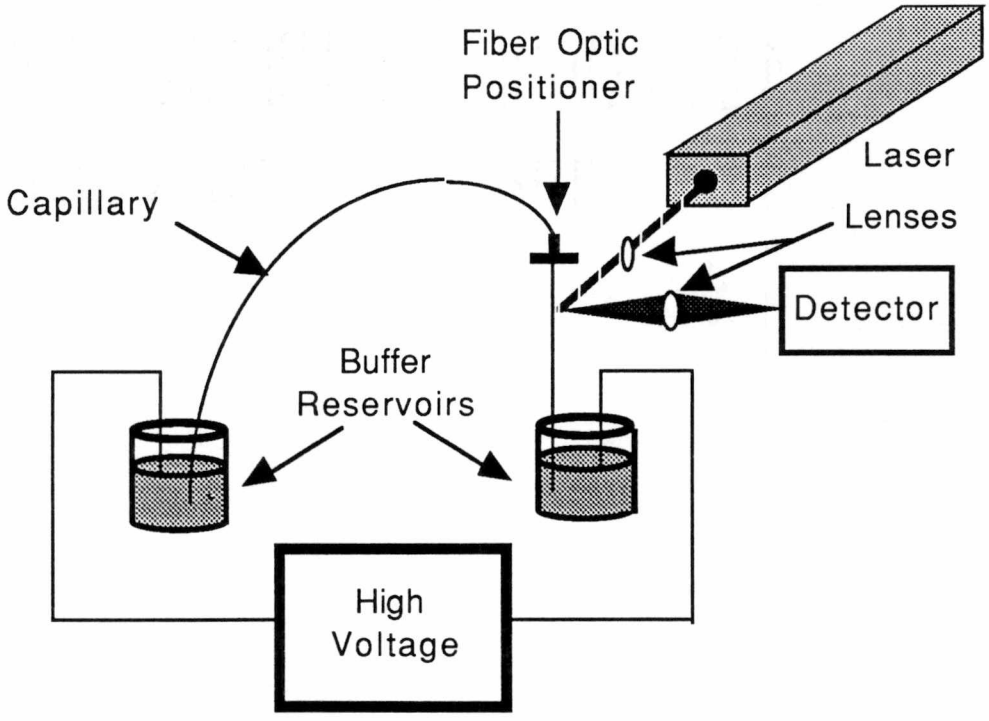

Figure 3. Depiction of general experimental apparatus.

As stated previously, the ability to use high electric field strengths in these methods is largely due to the high external surface area to volume ratio of the capillaries. This allows the capillary to dissipate heat that is produced by the electrophoretic process. Since the surface area to volume ratio of the capillary varies inversely with diameter, smaller i.d. capillaries are able to more easily dissipate heat. Furthermore, the amount of joule heat produced varies inversely with the square of the capillary diameter (7, 8). Therefore, as small a diameter capillary as possible should be used to prevent band broadening due to temperature gradients. Unfortunately, very small diameter capillaries increase the

difficulty of detection, so often larger diameter capillaries (50 to 100 μm i.d.) must be employed. The effects of capillary diameter on the efficiency and detectability of proteins will be discussed in Chapter 3.

Since efficiency in these methods, as discussed in Chapter 1, is dependent on applied electric field strength, rather than capillary length, the length of the capillary is not a critical parameter (9). However short capillaries are desirable, as band broadening due to longitudinal diffusion increases with analysis time and very large applied voltages are difficult to achieve. Therefore, short small diameter capillaries should result in the most efficient separations. Unfortunately, very short capillaries require short injection plugs and detection zones, which complicate these separation procedures.

In most electrokinetic separations, fused silica capillaries with a polyimide coating are employed. Fused silica capillaries are commercially available and are optically transparent in the ultraviolet and visible wavelength regions. The latter of these characteristics permits on-column optical detection to be performed at wavelengths less than 300 nm. Other materials have been used to alter electroosmosis and reduce analyte/wall interactions; however, they usually do not permit on-column optical detection (90). An alternative method of altering flow and reducing wall interactions, is to derivatize the wall of the capillary with a silinating agent. A large variety of silinating reagents have been employed ranging from trimethyl silane to polymeric bonded phases

(26-29). Unfortunately, the stability of these wall coatings is not infinite and changes in wall characteristics can occur with time.

Often CZE and MECC separations are performed in alkaline buffers. Since fused silica is somewhat soluble in alkaline media, etching of the capillary wall can occur. Etching increases the surface area of the capillary wall and the number of exposed silanol groups, which can alter electroosmotic flow and solute/wall interactions. Changes in these parameters can degrade reproducibility in migration time and efficiency. To reduce these effects, the capillary is often washed with a dilute solution of strong base (i.e. 0.1 M NaOH or KOH) prior to initial use and between injections. The initial rinse strongly etches the capillary wall; thereby causing the number of exposed silanol groups to remain more nearly constant during the lifetime of the capillary. Rinsing between runs prevents migration time drift due to the slow acid base equilibrium kinetics of the silanol groups (80). Additionally, rinsing with base removes solutes that were adsorbed to the wall of the capillary. Adsorbed materials can alter the double layer at the capillary wall and effect electroosmosis. This method has been shown to improve the reproducibility of protein separations by Lauer and McManigill (39).

Buffer Parameters

Generally, the role of the electrophoretic buffer in CZE is to provide a continuous level of conductivity in the capillary, be a source of ions to produce electroosmosis, and control the ionization

of acid or base functionalities on solutes. A continuous level of conductivity is required to prevent distortions in the electric field, which can result in poor peak shape (8, 9). This is assured by maintaining the ionic strength of the buffer well above that of injected solutes. If the concentration of the analyte affects the conductivity in the band, it will alter the electric field strength in the vicinity of the band. For example, a high concentration of a compound with a lower electrophoretic mobility than the buffer component of the same charge will decrease the conductivity in the center of band, thereby increasing the electric field strength in the center of the band as compared to its edges. Therefore, the center of the band will have a different migration velocity (as determined by equation 2 and the reduced field strength) than the sides. In this case, the center of the band will have a larger electrophoretic velocity than the sides of the band and cause the band concentration to be skewed forward or appear "tailed". Conversely, compounds with a greater mobility than buffer components will appear fronted. Usually, buffer to analyte concentration ratios of 200 or higher will prevent this from occurring and result in gaussian peak shapes (39).

It should be noted however, that the buffer concentration determines the strength of the electric field that can be applied. Very high buffer concentrations (i.e. > 0.1 M) can produce more heat than the capillary can dissipate if high electric field strengths are employed (36). Low conductivity zwitterionic buffers have been used to reduce this problem; nevertheless, high buffer

concentrations usually require the use of lower electric field strengths (36, 39, 40).

Since electroosmosis is a result of buffer ion/wall interactions, the composition of the buffer will affect flow rates. Since the wall of the capillary is negatively charged, cations in the buffer will interact with it most strongly. Buffers with small metal cations (i.e. Na^+ and K^+) are most commonly used and result in flow toward the negative electrode. However, buffers containing certain quaternary ammonium salts demonstrate flow toward the positive electrode, due to a reversal in the zeta potential (73, 91, 92). Flow rate can also be altered by the addition of compounds to the buffer that interact with the wall or change the dielectric constant of the buffer. Solutes such as putrecene (39) and Triton-X (93) will adsorb to the wall of the capillary, disrupting the double layer and reducing electroosmosis. Also, the addition of organic solvents will reduce flow rates by reducing the dielectric constant and interacting with the capillary wall (34, 42, 71, 72, 75, 79, 94).

The pH of the electrophoretic buffer can be used to control the electrophoretic mobility of solutes, solute/wall interactions, and electroosmosis. Buffer pH controls the state of the acid or base functionalities of a solute, hence the charge and mobility. Careful control of buffer pH can permit separation of very similar compounds. For example, isotopically substituted benzoic acids have been separated using this method (95). In addition buffer pH can be used to reduce solute/wall interactions. Buffer conditions that cause a solute to have a negative charge will result in it being

repelled by the negative sites on the wall, thus reducing wall interactions (39). Additionally, very acidic buffers can be employed to titrate the silanol groups on the capillary wall, thereby reducing the surface charge and coulombic interactions (27). Electroosmosis is also affected by buffer pH due to its dependence on the charge of the capillary wall. Since acidic buffers reduce surface charge, they result in slower electroosmotic flow rates than alkaline buffers (80). As the buffer pH affects more than one separation parameter, predicting the effects of altering the pH can often be difficult and require the evaluation of a large amount of experimental data.

In MECC analyte-micelle interactions are mainly responsible for separation, so stringent control of buffer components must be maintained. Variation of parameters that can alter the phase ratio of the system, the partition coefficient, or the electrophoretic behavior of the micelle or buffer can degrade reproducibility and resolution. Two parameters that must be controlled include surfactant concentration and percent organic modifier in MECC. Experimentally, the major difference between CZE and MECC is the addition of surfactant to the buffer. Low surfactant concentrations (near the CMC) have been shown to result in poor efficiency, therefore concentrations much higher than the CMC need to be employed (usually 5 to 10 times the CMC) (75). This increases the conductivity of the buffer and can often reduce the maximum field strength that can be employed when compared to CZE. The majority of MECC separations have used sodium dodecyl sulfate (SDS) at concentrations near 0.05 M (15, 34, 35, 42, 62, 73, 75, 96- 101).

To reduce the effects of the limited elution range in MECC, organic solvents are often added to the buffer. Organic solvents reduce electroosmotic flow and k', but can greatly increase analysis time (75). Solvents such as methanol and isopropanol extend the elution range greatly, while acetonitrile has less of an effect. This is possibly a result of weaker interactions between acetonitrile and the capillary wall. The relative reduction in k' for a solvent can be roughly estimated from the strength of the solvent as a reverse phase eluent. Typical solvent concentrations are between 5 and 20 % (v/v). Higher concentrations destroy the micellar phase and degrade efficiency. The use of organic solvents in MECC has been extensively investigated by Sepaniak *et al.* (34, 42, 64, 67, 68, 71, 75).

Applied Electric Field Strength

The driving force in capillary electrokinetic separation methods is the application of a strong electric field parallel to the flow channel of the capillary. Although capillaries permit the use of much higher field strengths than conventional electrophoretic methods, very high field strengths can produce more heat than the capillary is able to dissipate. Excessive heat results in a radial temperature gradient in the flow channel of the capillary. The temperature gradient causes a radial viscosity gradient. Since electroosmosis and electrophoretic mobility are dependent on viscosity, temperature gradients can adversely affect these parameters. The plug-like flow profile of electroosmosis (discussed in Chapter 1) requires a constant viscosity; when a viscosity

gradient occurs a range of velocities across the flow channel results and a more parabolic flow profile is observed. This result is band broadening due to resistance to mass transfer across the flow profile. Likewise, a viscosity gradient will result in a range of mobilities for a single species and band broadening (9). Grushka and Jones determined that temperature gradients resulting from large electric field strengths had a parabolic profile (102). Using calculations based on a parabolic temperature gradient, Grushka *et al.* showed that the reduction in efficiency due to these effects was worse for slowly diffusing molecules (i.e. macromolecules) than for more rapidly diffusing species (103). In addition, the use of larger diameter capillaries (greater than 50 μm) exacerbated these effects. Thus, the strength of the electric field that can be applied to achieve maximum efficiency and shortest analysis time is dependent on several variables: capillary diameter, buffer conductivity, and the diffusion coefficient of the analyte.

Injection Parameters

Ideally, solutes would enter the capillary in an infinitely narrow band (i.e. a delta function). However, since solutes are injected in a plug of finite length, the contribution of the plug length to overall bandwidth must be considered. The peak variance due to the length of the injection plug (σ_{inj}) can be determined from the equation:

$$\sigma^2_{inj} = \frac{L^2_{inj}}{12} \qquad [10]$$

where L_{inj} is the length of the injection plug (104). Short injection plugs result in guassian peaks, whose variance is determined by band broadening mechanisms that occur as the solute transverses the capillary. Long injection plugs, however, result in nonguassian peaks whose dimension are greatly determined by the injection process (74, 91). In fact, Huang *et al.* determined that, when the injection plug length was longer than 4 times the diffusion length for a solute (as determined from the Einstein equation and the migration time of the solute), the width of the eluted band will be determined solely by the injection plug length. Consequently, all hydrodynamically injected solutes should have the same bandwidth, provided that all other sources of band broadening are negligible (91).

The maximum injection plug length that can be employed is dependent on the number of theoretical plates necessary for separation and the capillary length. In an excellent treatment of the extra-column parameters that affect efficiency in these methods, Otsuka and Terabe determined that an injection plug of 0.39 mm would contribute only 5% to the overall band variance if 10^6 theoretical plates were achieved in a 50 μm i.d. x 50 cm capillary (104). However, if the capillary was shortened to 10 cm an injection plug of 78 μm or less would be required to achieve this efficiency. The use of very short injection plugs is often difficult

and not reproducible. For example, Grushka and McCormick have shown that merely placing the capillary inlet in the sample can result in extraneous sample injection, which can be longer than the desired injection plug length (105) .

Injection in both CZE and MECC is usually performed on-column by hydrodynamic or electroinjection, although several other injection system have been described in the literature (20, 106, 107). Hydrodynamic injection (or syphoning) is preformed by placing the inlet of the capillary in the sample and creating a pressure difference between the two ends of the capillary. The pressure difference can be created by increasing the pressure at the inlet of the capillary, by drawing a vacuum on the outlet of the capillary, or by simply raising the inlet of the capillary above the outlet while in the sample. The length of the injection plug is controlled by varying the duration and magnitude of the pressure difference. The length of the injection plug can be determined, experimentally, by a continuous injection method. This requires that the inlet of the capillary be placed in the sample and the injection process continued until the sample reaches the detection zone (assuming the injected sample has the same hydrodynamic properties as the mobile phase). The injection rate and consequent injection volumes can be determined from the length of the capillary to the detection zone and the time necessary for the sample to reach the detection zone. This very simple injection method provides uniform injection of all solutes. In one reported comparison between automated and manual

hydrodynamic injection systems variations of approximately 1% and 10%, respectively, were observed(24).

Electroinjection is the direct electromigration of solutes into the capillary. This is performed by placing the inlet of the capillary in the sample and applying an electric field. Solutes are injected at a rate based on electroosmosis and their electrophoretic mobility. Therefore, solutes with large negative electrophoretic mobilities will be injected at a slower rate than those with more positive electrophoretic mobilities. This biases injection toward early eluting compounds (108). The amount of solute injected is also dependent on the conductivity of the sample solution. If the sample conductivity is much lower than the buffer conductivity, the sample will be concentrated in the injection plug. Although this can be used to enhance detectability, it can confuse quantitation if the conductivity of standard solutions and samples differ (108). Furthermore, since the injection plug length is dependent on the electrophoretic mobility of the sample components, the plug length will be different for each sample component. Therefore, injection conditions must be determined based on the mobility of the compound of interest and solutes with more positive electrophoretic mobilities could exhibit injection related band broadening. Recently, Guiochon and Dose determined that by employing two internal standards the effects of injection bias could be corrected and the reproducibility of electroinjection improved (25). Electroinjection is often employed in automated systems as it is often mechanically simpler than hydrodynamic injection schemes.

Detector Parameters

The narrow capillaries employed in these methods result in more stringent detector requirements than other separation techniques. Minute band volumes usually preclude the use of post-column detectors, since the fittings used to connect the capillary to the detector usually result in band broadening. Therefore, on-column detection is generally employed. Nevertheless, detector related band broadening can occur if the length of the detection zone or the detector time constant is too large. The maximum length of the detection zone, like the length of the injection plug, is determined by the peak variance and the length of the capillary. Wang *et al.* used computer simulation to show that the detection zone length should be less than or equal to one standard deviation of the peak to prevent distortion of the bandwidth (109). In a similar study, Otsuka and Terabe determined that a somewhat shorter zone (0.7σ) should be employed to minimize detector related band broadening (104). Using the more rigid of these two criteria requires detection zones of 0.39 mm and 78 μm to prevent detector related band broadening for a peak with 10^6 theoretical plates in 50 and 10 cm long capillaries, respectively. Since, as stated above, laser-based fluorometric detection results in very short detection zones, this source of band broadening is usually not significant.

As the residence time of a band in the detection zone is often only a few seconds, the detector response must be fast enough to prevent band broadening. The rate of detector response is established by the time constant of the detector. Short time

constants result in fast response times, but do not discriminate against high frequency detector noise. The maximum time constant employable is determined by the migration time of the zone and its efficiency. For very efficient peaks with short migration times, detector time constants of less than 0.1 seconds should be employed, while for more slowly migrating bands a slower response time can be used to reduce baseline noise (104).

Another consequence of on-column detection is that the time variance of a solute is dependent on its migration velocity. In post column detection, all analytes move through the detector at the same velocity (that of the mobile phase), so bands with equal length variances will have the same time variance. However in CZE and MECC, bands move through the detection zone at different velocities depending upon mobility or partition coefficient. Therefore, late eluting peaks will have a larger time variance than early eluting bands with the same length (80, 91). This affects quantitation by causing slower eluting bands to have larger peak areas than faster eluting bands. Furthermore, small changes in electroosmosis or other parameters that influence velocity will result in irreproducible peak areas. Reproducibility can be improved by multiplying peak area by the inverse of the band's velocity to correct for these effects. Reproducibility can also be improved by the use of an internal standard (25, 98, 110, 111).

On-column optical detection is performed by removing a small section of the capillary's polyimide coating to create on-column flow cells. This allows light to focused through the flow channel

perpendicular to the capillary. The polyimide coating is usually removed using a flame, followed by a methanol wash.

Throughout this work, spectrophotometric detection has been employed to study many of the experimental parameters influencing separation (in fact, much of this data is not presented in this manuscript). The detector employed was a modified LDC Monitor III HPLC detector. The HPLC flow cells were removed and fiber optics used to deliver light from an external flow cell to the photodiodes of the detector. External on-column flow cells were created using a split block capillary holder as shown in Figure 4. A thin spacer separated two metal blocks, creating a slit for light to pass through and a slot to hold the capillary in place. After placing the capillary in the block, it was mounted next to a cadmium pen lamp (229 nm), which was used as the source. The fiber optics were positioned on the opposite side of the block to collect light passing through the capillary. This design resulted in small amounts of stray light and good optical throughput (67).

Figure 3 shows the general experimental apparatus for electrokinetic separations with on-column laser-based fluorometric detection. The capillary was affixed with epoxy to a cylindrical holder (shown in Figure 4), which was held by a fiber optic positioner. Use of the positioner permitted translation of the capillary in three directions to assure passage of the laser beam through the flow channel. The laser beam was focused into the flow channel of the capillary generally using a f/1 fused silica lens. Fluorescence was collected at 90° to excitation generally using a

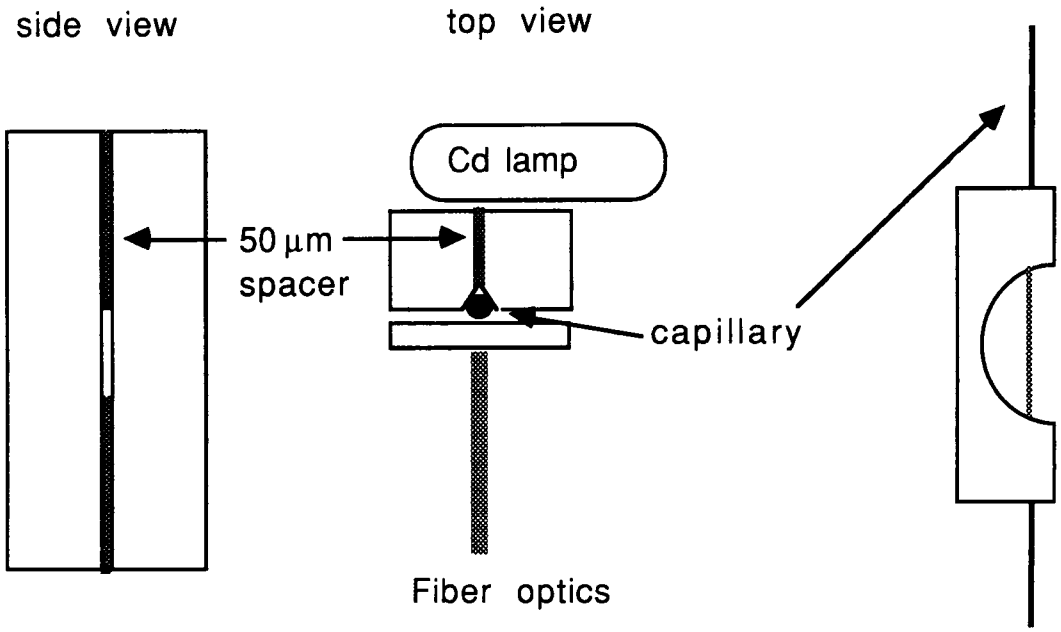

Split Block Capillary Holder

Fluorescence Capillary Holder

Figure 4. Depiction of capillary holders for spectrophotometric and laser-based fluorometric detection.

f/2 lens and isolated using either a filter monochromator combination or dispersed across an array detector using a spectrograph. Single channel detection was performed using a photomultiplier tube and a photometer. Multichannel detection was preformed with a photodiode array. Specifics of each detection system will be presented in later chapters due to the diversity of instrumentation involved.

CHAPTER 3

LASER-BASED FLUOROMETRIC DETECTION SCHEMES FOR THE ANALYSIS OF PROTEINS BY CAPILLARY ZONE ELECTROPHORESIS

Since the inception of electrophoresis as an analytical method, it has been employed for the analysis of proteins. However, conventional methods are labor intensive and time consuming. Also, detection of proteins requires staining after separation. Staining further increases analysis time and can prove difficult for quantitative purposes (1). Therefore, developmental work involving capillary electrophoretic separation methods has been directed toward solving these problems. The high field strength and automated instrumentation employed in CZE greatly reduce analysis time and increase sample throughput. Furthermore, on-line detection removes the need for staining and makes detection more convenient.

The analysis of proteins by CZE is hampered by two problems, adsorption to the wall of the capillary and poor detector sensitivity. The former of these problems has been the subject of several studies, which have resulted in different strategies to reduce adsorption. These include employing very high or low pH buffers and the use of wall coated capillaries (26-28, 39, 40). The detection of proteins has also been studied by several research groups. Detection is usually performed by absorption photometry, at wavelengths less

than 230 nm (82, 84, 86). In this region the aromatic amino acids and peptide groups in the proteins have high molar absorptivities (112). Nevertheless, the short path length associated with on-column detection reduces sensitivity and detectability.

To improve sensitivity and detectability, several fluorometric detection schemes have been investigated using both conventional and laser excitation sources (16, 81, 85, 97). Fluorometric detection of proteins has been performed by employing the native fluorophores of the protein, fluorescent labels, and indirect fluorescence. Green and Jorgenson developed a variable wavelength fluorescence detector using a Hg-Xe lamp and a double monochromator (85). This system was able to detect submicromolar concentrations of protein using their native fluorophores, resulting in minimum injectable amounts (MIA) of approximately 2 femtomoles. To further reduce limits of detection, post-column derivatization schemes have been developed, employing o-phthaldiadehyde as a fluorescent label (81, 97). These detection schemes resulted in MIAs of 22 femtomoles for myoglobin using a conventional excitation source and 44 attomoles for a laser source. However, use of the post column reactor increased the complexity of the experimental apparatus and resulted in band broadening (as much as an order of magnitude reduction in plate number (81)).

An alternative method, indirect fluorescence, has been investigated for the detection of proteins by Yeung and Kuhr (14, 16, 53). This method involves "doping" the electrophoretic buffer with a fluorophore and, in most cases, detecting the reduction in

fluorescence signal after displacement of the dopant. The displacement mechanism most commonly used is ion repulsion. The potential for large charges on proteins suggest that each protein could displace numerous fluorophores, resulting in excellent detectability (16). In fact, the MIA for lysozyme using this method is approximately 100 attomoles. However, the existence of ions other than the fluorophore in the buffer will reduce displacement efficiency. Moreover, when employing a buffer pH near the isoelectric point of the protein (the importance of which is discussed later) the charge of the protein, and consequently sensitivity, will be reduced. These effects can result in undesirable compromises in buffer composition that effect both detectability and separation.

The remainder of this chapter will examine the applicability of three laser-based fluorometric detection schemes to the analysis of proteins by CZE. The use of the native fluorescence of proteins for detection, the difficulties of pre-column labeling, and a novel method of on-column labeling with "hydrophobic protein probes" will be described. Conditions for accomplishing the latter method will be investigated and analytical figures of merit will be presented.

Experimental

Conalbumin (CON), bovine serum albumin (BSA), beta lactoglobin A and B (BLG A and BLG B), fluoroscein isothiocyanate (FITC), 1-anilinonaphthalene-8-sulfonate (ANS), 2-p-toluidinonaphthalene-6-sulfonate (TNS) and 2-[Cyclohexylamino]-

ethanesulfonic acid (CHES) were purchased from Sigma Chemical Company (St. Louis, MO). All other chemicals employed were reagent grade and obtained from Baxter Healthcare (Stone Mountain, GA).

Studies were performed using 25, 50, and 75 μm i.d. untreated capillaries obtained from Polymicro Technologies (Phoenix AZ) and Clect H-1 capillaries from Supelco (Bellefonte PA). Clect H-1 capillaries have a 50 μm i.d. and a moderately hydrophobic wall coating. Untreated capillaries were washed with 1M KOH, 0.1 M KOH, and distilled water prior to initial use. Between injections the capillary was washed for 5 minutes with 0.1 M KOH, water, and buffer. Electrophoretic buffers for detection and efficiency studies were made with HPLC grade water that contained 20 mM CHES and were adjusted to pH 10.2 using KOH. Electrophoretic buffers used in the study of Clect H-1 capillaries were made from HPLC grade water and contained 10 mM Na_2HPO_4 and 6 mM $Na_2B_4O_7$. High voltage was applied across the capillary using a Hipotronics (Brewster, NY) model 840A power supply.

Laser-based native fluorescence detection of proteins was performed using a Coherent (Palo Alto, CA) Inova 100 argon ion laser (514 nm, 7 W CW) that was frequency doubled to produce 257 nm radiation using an InRad (Northvale, NJ) model 527-003 harmonic generator. The excitation power was approximately 9 mW. Detection of FITC labeled proteins was accomplished using a Uniphase Cyonics model 2001SL (San Jose, CA) argon ion laser (488 nm, 10 mW CW) for excitation. Excitation of ANS and TNS was performed using a Liconix 4230NB (Santa Clara, CA) helium-

cadmium laser (325 nm, 15 mW). Fluorescence was isolated with a Instruments SA H-10 (Metuchen, NJ) monochromator. Emission wavelengths were as follows: native fluorescence - 325 nm, FITC-labeling - 520 nm, ANS-labeling - 500 nm, and TNS-labeling - 450 nm. Detection was performed with a Hamamatsu (Bridgewater, NJ) 1P28 photomultiplier tube and photocurrents were processed with a Pacific Precision Photometer model 126 (Concord, CA). Conventional fluorimetry was performed using a SpectroVision (Chelmsford, MA) instrument.

Minimum detectable concentrations (MDC) for native fluorescence and FITC-labeled proteins were determined by filling the capillary with solution and observing the signal under static conditions. MDCs are based on a S/N = 2. Injections were performed hydrodynamically, by raising the inlet of the capillary 15 cm for 10 to 30 seconds. The injection volume was determined by continuous injection of sample. Minimum injectable amounts and linear dynamic ranges were determined using calibration curves. Minimum detectable concentrations for ANS- and TNS- on-column labeling were determined by calculating the concentration at band center for the lowest concentration on the calibration plot (S/N < 6) and extrapolating to S/N = 2.

Conalbumin was labeled with FITC by stirring 2 mg of protein, in 0.02 M sodium borate solution, with the desired amount of label for 24 hours at 4° C. The two ratios of [FITC]/[CON] used in this study were 5 and 10.

Considerations for Separation Efficiency

Under ideal conditions efficiency in CZE is limited by axial diffusion (9). Therefore, very high plate numbers can be achieved in protein separations due to their low diffusion coefficients. However, experimental parameters such as capillary type, pH, buffer conductivity, applied voltage, and capillary diameter must be optimized to achieve high efficiency.

Solute capillary wall interactions must be minimized or prevented to achieve high efficiency. Guiochon and Martin have shown that capacity factors, due to wall interactions, as low as 0.1 can significantly increase plate height (113). Moreover, the contribution to the overall plate height increased with capacity factor. As stated above, protein-wall interactions can be greatly reduced by employing either high or low pH electrophoretic buffers to control the charge on the protein and the capillary (27, 39, 40). Alternately, wall coated capillaries can be employed to reduce interactions (26-28). In this work the use of high pH buffers and coated capillaries has been studied. The utility of these two methods is illustrated in Figure 5. The poor peak shape observed at pH = 8.3 in the untreated capillary presumably results from strong interactions between the amine groups on the protein and the silanol groups on the capillary wall. Raising the pH of the buffer reduces the charge of the amines and the strength of the interaction, so a better peak shape is observed. When a Clect H-1 bonded phase capillary is employed the conalbumin results in a good peak shape, even when the buffer pH is below the isoelectric point (pI) of the

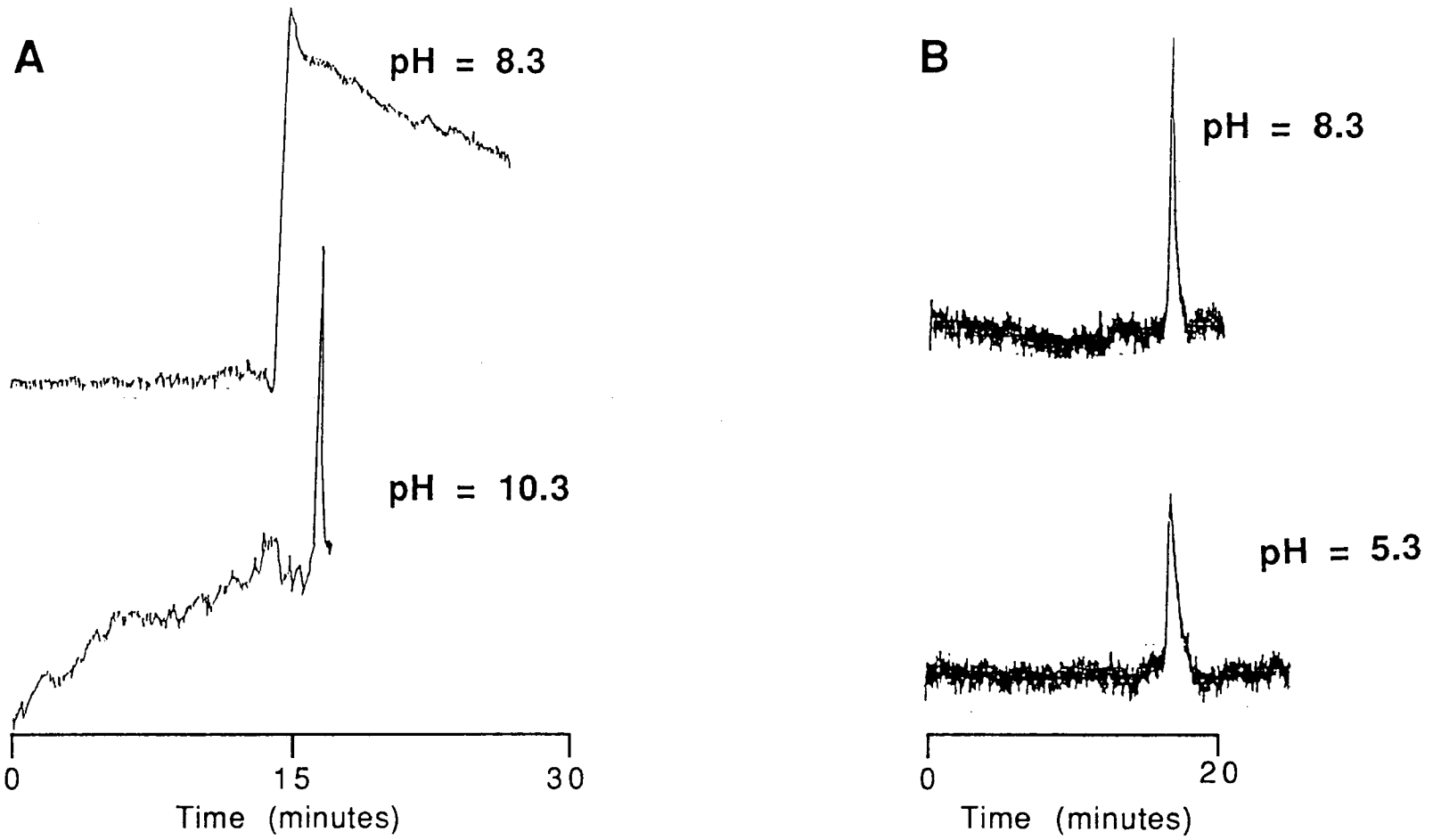

Figure 5. Peak profiles of conalbumin in untreated (A) and Celect H-1 (B) capillaries. Conalbumin concentration 1 mg/mL. Conditions A: 10 mM CHES / 30 mM KCl, 50 µm i.d. x 60 cm, 200 V/cm. Conditions B: 10 mM Na_2HPO_4 / 6 mM $Na_2B_4O_7$, 50 µm i.d. x 60 cm, 200 V/cm. Spectrophotometric detection was employed for both studies.

protein. The polymeric coating of the Clect H1 capillary reduces the number of exposed silanol sites on the capillary wall, thereby reducing the coulombic interactions.

The advantage of coated capillaries in the analysis of proteins is illustrated in Figure 6. By reducing the pH dependence of efficiency, it is possible to use the pH of the buffer to alter the electrophoretic mobility of proteins and enhance separation. Buffers below the pI of a protein will result in a more positive mobility than those above the pI. Reduction of the buffer pH increases the positive charge of myoglobin, thereby increasing its electrophoretic mobility, permitting separation from the conalbumin peak. This could not be accomplished in the untreated capillary due to the poor peak shape of conalbumin in neutral pH buffers. Although coated capillaries are advantageous for many samples, the use of untreated capillaries is still more common due to the increased expense of coated capillaries and the fact that they have only recently been commercially available. For these reasons, untreated capillaries and high pH buffers are employed in the majority of this work.

A major advantage of CZE over traditional electrophoretic techniques is the ability to use high electric field strengths without experiencing detrimental thermal effects (9). As stated previously, the maximum electric field strength that can be employed is determined by the capillary diameter, buffer conductivity and type of solute being analyzed. Table 2 documents the effects of several experimental parameters on the efficiency of conalbumin, obtained

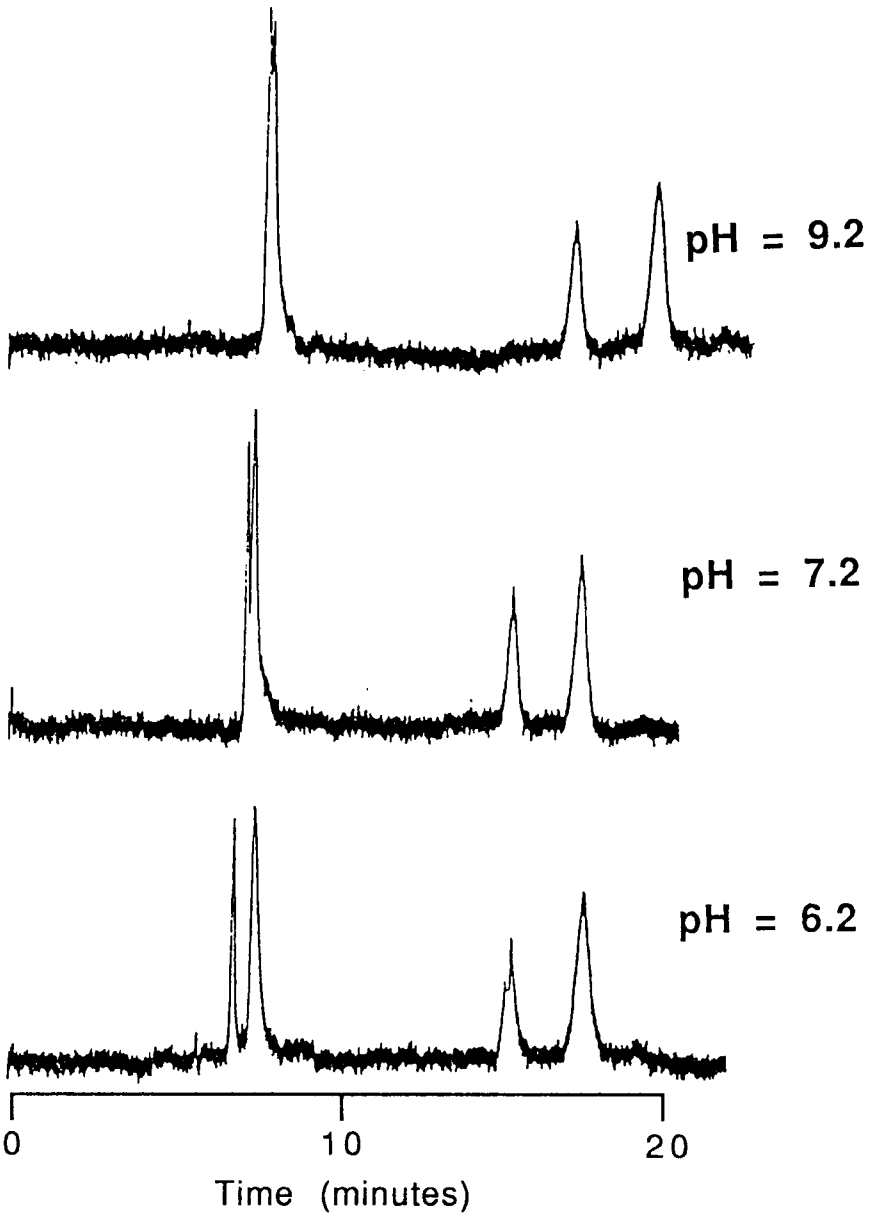

Figure 6. Separations of myoglobin, conalbumin and beta lactoglobin B and A using different pH buffers. Elution order as listed. Conditions: 10 mM Na_2HPO_4 / 6 mM $Na_2B_4O_7$ buffer, 50 µm i.d. x 60 cm Celect H-1 capillary, 200 V/cm. Spectrophotometric detection was employed.

at a pH of 10.2 in untreated capillaries. High buffer concentrations and large diameter capillaries (greater than 50 μm), that result in large electrophoretic currents, can produce more heat than the capillary is capable of dissipating, thereby creating a radial temperature gradient within the capillary. Under these conditions the plug-like flow profile of electroosmotic flow is distorted and band broadening occurs due to slow mass transfer across the flow profile (103). However, it should be noted that if the conductivity of the buffer is significantly lower than the conductivity of the sample, distortion of the band shape will be observed (8, 114, 115). This is the cause of the dramatic increase in efficiency in Table 2 when the KCl concentration was increased from 15 mM to 30 mM (25 μm capillary). The peak in the lower ionic strength buffer exhibits significant "fronting", which reduces the efficiency of the band. Further increasing the KCl concentration (to 45 mM) increases the heat produced and degrades efficiency. Increasing the applied voltage also increases the power that the capillary must dissipate. This results in a decrease in plate number, which is illustrated in the table by the 25 μm i.d./30 mM KCl data at the two different field strengths.

Since the power that can be dissipated by the capillary is determined by the surface to volume ratio of the capillary, the use of smaller diameter capillaries will allow the application of higher electric fields to minimize analysis time and axial diffusion without incurring thermal-related band broadening. This is illustrated by the higher efficiency of the 25 μm i.d./45 mM KCl data

TABLE 2.

EFFECTS OF EXPERIMENTAL PARAMETERS ON PEAK EFFICIENCY FOR CONALBUMIN.

Capillary Diameter	Mobile Phase Concentration of KCl					
	15 mM		30 mM		45 mM	
	N (m^{-1}) / N/time ($m^{-1}min^{-1}$)	Power (Wm^{-1})	N (m^{-1}) / N/time ($m^{-1}min^{-1}$)	Power (Wm^{-1})	N (m^{-1}) / N/time ($m^{-1}min^{-1}$)	Power (Wm^{-1})
25 μm [a]	52,000 / 4,600	0.12	474,000 / 37,600	0.24	230,000 / 17,500	0.40
25 μm [b]			156,000 / 18,300	0.71		
75 μm [c]	52,000 / 2,600	0.30	10,000 / 400	0.53		

a) applied field 235 V/cm
b) applied field 350 V/cm
c) applied field 150 V/cm

Note: Electrophoretic buffer contained 20 mM CHES. Detection was preformed by native fluorescence.

as compared to 75 μm i.d./30 mM KCl case, even though the smaller capillary has a greater "thermal load". Moreover, the smaller diameter capillary results in lower electrophoretic currents, which reduces the power that must be dissipated by the capillary (compare the 30 mM KCl data for the two diameters).

Analysis time is another important consideration. Grushka *et al.* have calculated that band broadening due to temperature gradients is most detrimental for macromolecules when employing high flow rates in large diameter capillaries (103). Therefore, to achieve high efficiency and short analysis times, small capillaries must be employed. This is illustrated by the larger number of theoretical plates per minute achieved when the 25 μm i.d. capillary is employed. The high efficiency is a result of the decrease in thermal-related band broadening and a large increase in electroosmotic flow at the higher field strength.

Native Fluorescence Detection

In order to prevent errors that can occur during the labeling of a sample, it is desirable to base detection on some intrinsic characteristic of the protein. This can be achieved by detecting the UV absorbance (λ between 200 and 230 nm) of the peptide bonds in the protein. Similarly, although somewhat complicated by the lack of "convenient" (i.e., reliable, low cost, and easy to operate) UV laser sources, laser-based detection can be accomplished by exciting the aromatic amino acid residues of the protein. The amino acids tyrosine, tryptophan and phenylalanine have excitation maxima

between 260 and 280 nm and fluoresce (albeit fairly weakly) between 280 and 350 nm, with some band shifts due to their incorporation into the structure of the protein (112). Therefore, the emission spectrum of the protein is the combination of the fluorescence of the three fluorophores and sensitivity is determined by the number of these aromatic amino acids in the protein.

Since there is not a convenient continuous-wave laser that operates between 260 and 280 nm, we employed the frequency doubled 514 nm output of an argon ion laser for excitation. Although not optimum, the wavelength (257 nm) produced by this system can be use to excite the aromatic amino acids. The minimum detectable concentration (MDC) for conalbumin (conalbumin has 61 aromatic amino acids (116)) using this method with different diameter capillaries is presented in Table 3, along with the MDC for pre-and on-column labeling (see later discussion). The increase in MDC with decreasing capillary diameter is expected due to the decrease in pathlength. However, the loss in detectability would be somewhat compensated by the higher efficiency (i.e. higher concentration at band center for a given injected concentration) of the smaller capillary and the possibility of more rapid analysis (see 25 and 75 μm i.d. data in Table 2).

Unfortunately, the utility of native fluorescence detection detection method is reduced by the expense and complexity of the laser instrumentation, which required a 4 hour warm up time and exhibited large changes in power during the course of a day.

TABLE 3

MINIMUM DETECTABLE CONCENTRATIONS OF CONALBUMIN

Detection Method	Capillary Diameter (μm)	Minimum Detectable Concentration (nM)
Native Fluorescence	50	14
	25	25
FITC Labeling	50	0.1
TNS Labeling	25	360
ANS Labeling	25	615

Note: MDC for FITC labeling was determined by static measurement after dialysis and does not account for loss of peak integrity during separation. [FITC]/[CON] = 5.

However, this method could become viable for daily operation if convenient UV lasers are developed in the future.

Pre-column Covalent Labeling

As stated previously, the detection of non-fluorescent species is often performed by labeling the analyte with a fluorescent tag prior to injection. This has been done in CZE separations of small molecules, using FITC (11) which reacts with amine functionalities and can be excited with the 488 nm line of an argon ion laser. Although this method permits the use of a convenient laser, it requires time consuming sample preparation. More significant to this study, the labeling of proteins with FITC destroys the integrity of the CZE band (by producing a complex mixture of derivatives) and renders this method unusable for quantitative analysis of proteins in complex mixtures.

The peak profiles of conalbumin detected by the native fluorescence and pre-column labeling are shown in Figure 7. For native fluorescence a sharp conalbumin peak and a small impurity peak are observed. However, in the case of pre-column labeling, multiple peaks are observed. Furthermore, increasing the derivatization ratio ([FITC]/[conalbumin]) exacerbates this problem and reduces the observed peak height. This same problem has been observed by other researchers (97) and is probably the result of heterogeneous labeling of the protein. Conalbumin has a total of 102 side chain amine groups that can react with FITC (116). Conalbumin

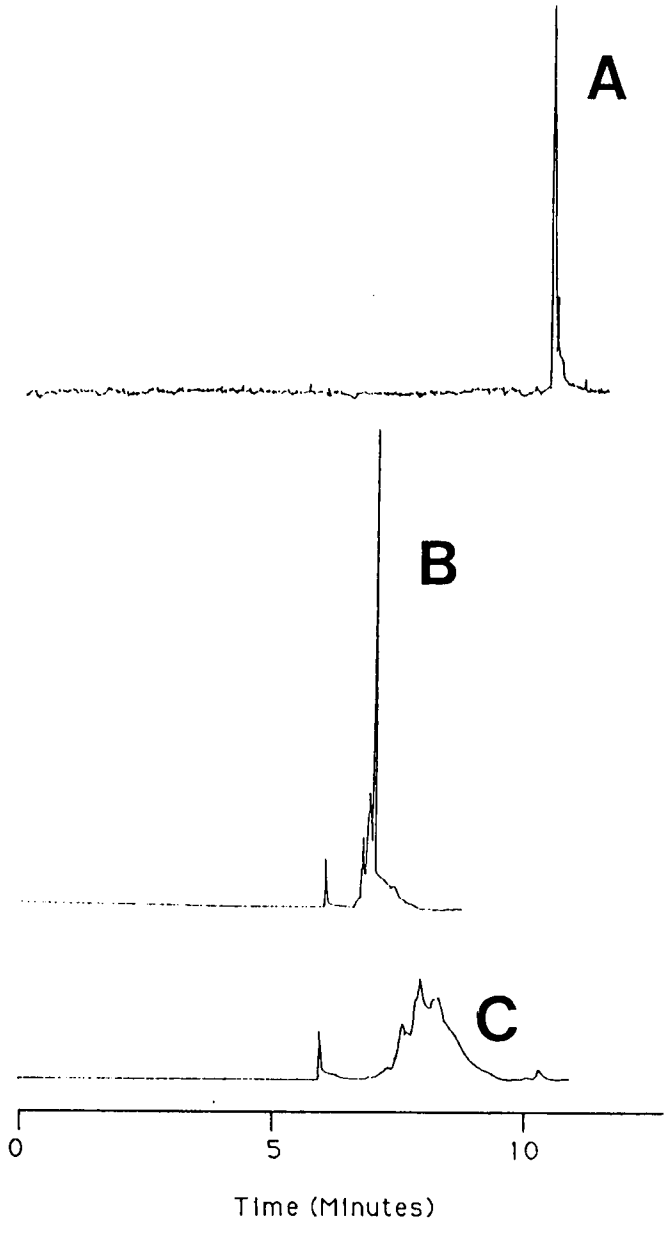

FIGURE 7. Peak profiles for conalbumin using native fluorescence detection and pre-column labeling with FITC. A) Native fluorescence detection, conditions: 25 μm i.d. x 80 cm capillary, 20 mM CHES/ 30 mM KCl buffer, and 1 mg/mL conalbumin. B) FITC labeled detection, conditions: 25 μm i.d. x 60 cm capillary, 5:1 FITC/conalbumin derivatization ratio, same buffer as A, and 0.5 mg/mL conalbumin. C) FITC labeled detection,conditions: 10:1 FITC/conalbumin derivatization ratio, same capillary, buffer and conalbumin concentration as B. Note: B and C are on same scale.

molecules labeled with different numbers of FITC molecules will, hence, possess different mass to charge ratios and different electrophoretic mobilities. This heterogeneous mixture possessing a range of electrophoretic mobilities results in a very broad band.

On-Column Labeling with Hydrophobic Probes

In an attempt to alleviate the aforementioned problems, the use of fluorescent hydrophobic probes to label proteins was investigated. These compounds undergo changes in their fluorescent characteristics as a result of noncovalent interactions with proteins. 1-anilinonaphthalene-8-sulfonate (ANS) and 2-p-toluidinonaphthalene-6-sulfonate (TNS) are two such compounds (117, 118) that have been used to investigate the secondary structure of proteins (118). These compounds intercalate into the hydrophobic regions of proteins with binding constants that range between 10^4 and 10^6 (117). Upon intercalation, the fluorescence quantum efficiency of the probe increases dramatically. Therefore, it should be possible to detect proteins by simply incorporating these compounds into the electrophoretic buffer.

The mechanism for this effect is based on an unusually large increase in dipole moment upon excitation, which causes the fluorescent characteristics of ANS and TNS to be dependent on their environment. In polar solvents (e.g. water) the Franck Condon state produced by solvent interactions results in large Stokes shifts and low quantum efficiencies (generally less than 0.01) (117-122). In viscous or non-polar solutions these effects are not observed and

fluorescence occurs. Under these conditions, quantum efficiencies as high as 0.6 are observed (122). Similarly, when intercalated into the non-polar regions of proteins, the probe is protected from solvent interactions and fluorescence is observed (120).

Since the protein-probe interaction is an equilibrium process, the response factor of this detection scheme will be determined by both the fluorescent characteristics of the probe and experimental parameters that influence the equilibrium. The effects of TNS concentration in the electrophoretic buffer are illustrated in Figure 8. As the concentration of TNS increases the signal (as measured in peak height) increases due to the intercalation of more of the probe into the protein. The signal should continue to increase with concentration until the binding sites on the protein are completely filled. However, the expected increase in detectability with probe concentration is not achieved due to a large increase in the fluorescent background and baseline noise when the TNS concentration exceeds approximately 0.2 mM. Above that concentration there is about a 25 fold increase in the baseline noise, which substantially reduces the S/N for conalbumin. This could be the result of intra-TNS interactions that influence the aforementioned relaxation process and enhance fluorescence.

The effects of pH on the fluorescence signal of TNS in a conalbumin solution are illustrated in Figure 9. Although this study was performed using conventional fluorimetry, it does show that the pH of the solution has an effect on the equilibria. It should be noted

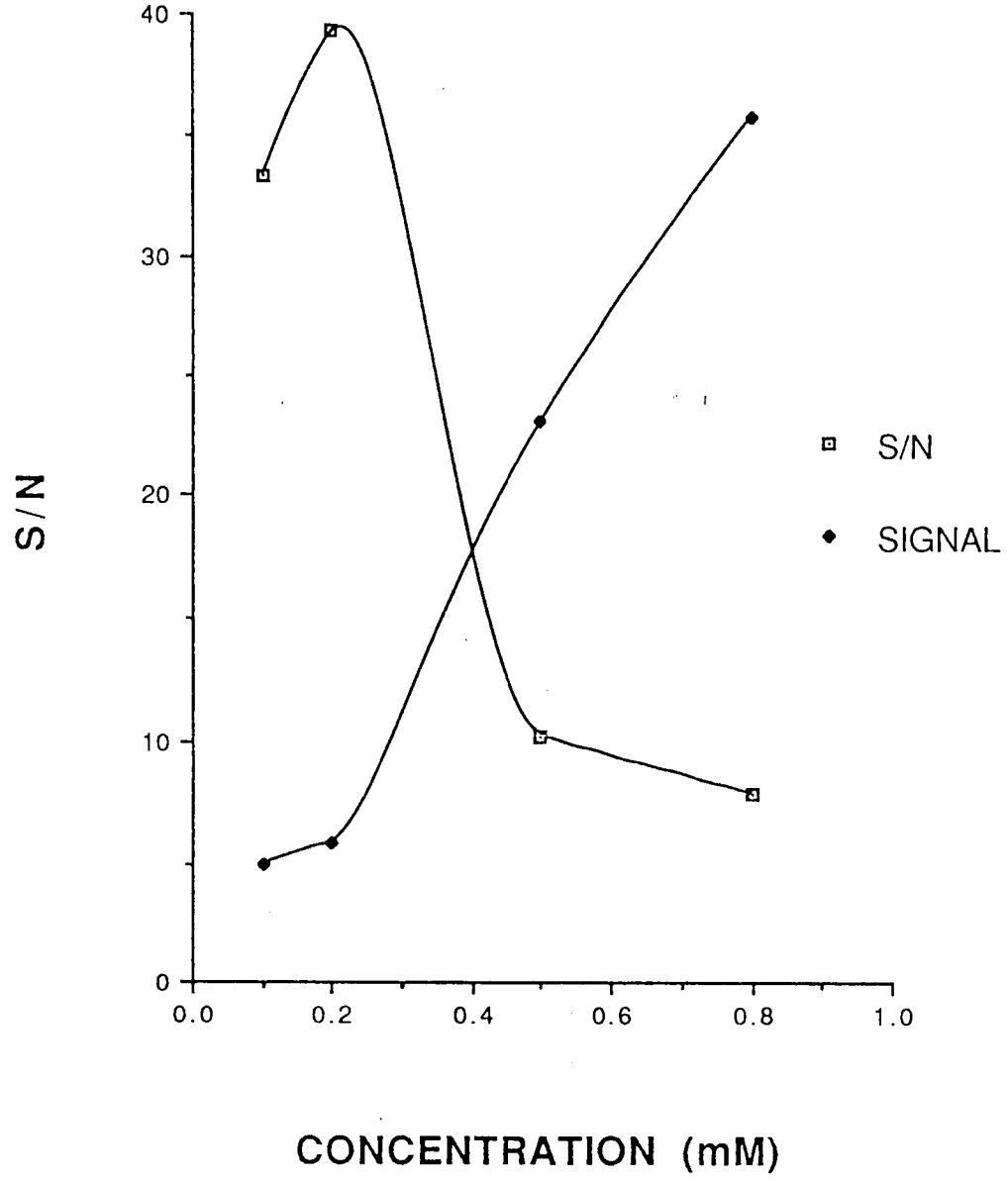

FIGURE 8. Effects of TNS concentration on signal and signal to noise ratio for conalbumin. Conditions: 0.5 mg/mL conalbumin, 25 µm i.d. x 60 cm untreated capillary, 20mM CHES/ 30 mM KCl buffer and 235 V/cm.

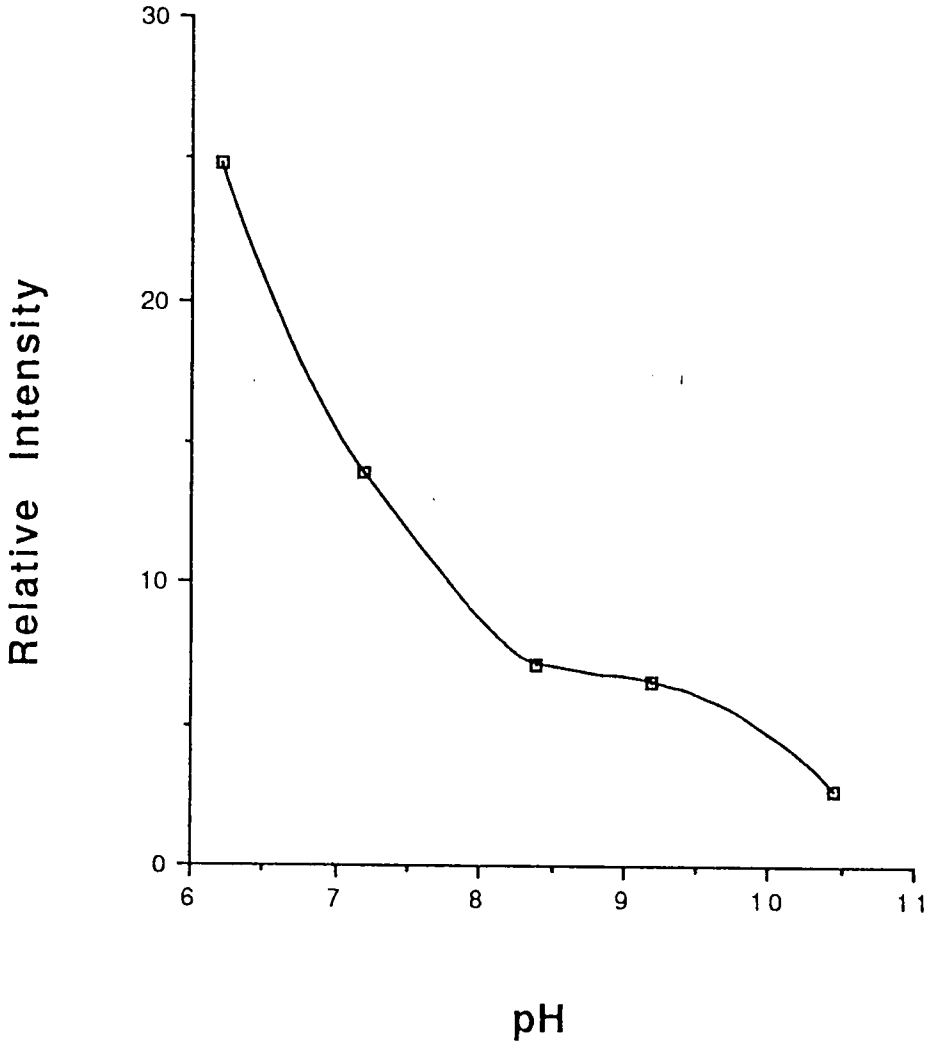

Figure 9. Effects of buffer pH on fluorescence signal of TNS in conalbumin. Conditions: 1 mg/mL conalbumin, 0.2 mM TNS, 20 mM CHES /30 mM KCL buffer, $\lambda_{excitation}$ = 325 nm, and $\lambda_{emission}$ = 450 nm.

that in this particular study, no fluorescence signal was observed at any pH if conalbumin was not present in the solution. The increased signal is probably a result of an increase in positive charge on conalbumin at neutral pH, which would increase the interaction of the anionic probe with the protein. However, as discussed earlier, the use of neutral pH buffers in untreated capillaries can reduce efficiency in CZE. Buffer pH could be optimized if wall coated capillaries were employed to reduce solute-wall interactions. Nevertheless, when the hydrophobic wall coated capillary described above was employed a very large fluorescent background was observed, resulting in increased baseline noise and reduced detectability. This is possibly due to interaction between the hydrophobic probe and the hydrophobic wall coating. Therefore, the detection limits shown in Table 3, determined at pH 10.2 in an untreated capillary, are not at optimum conditions for fluorescence.

The minimum detectable concentrations for ANS and TNS were presented in Table 3. These were determined using the probe concentration that produced the highest signal to noise ratio for conalbumin at a pH 10.2. Although these minimum detectable concentrations are higher than the other fluorescence detection schemes, they represent a significant improvement over conventional spectrophotometric detection, as observed in ourlaboratory. Furthermore, the peak profile for conalbumin and several other proteins are not distorted by the labeling process (see Figure 10). This is probably the result of the dynamic nature of this labeling mechanism established by the moderate binding constant

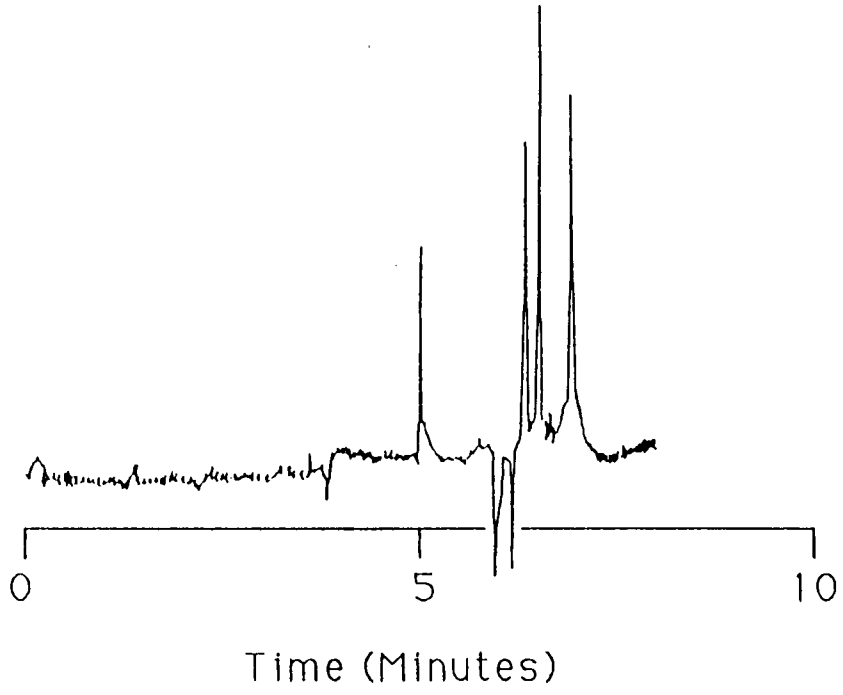

Figure 10. Separation of conalbumin, beta lactoglobin B, beta lactoglobin A, and bovine serum albumin . Elution order as listed Conditions: 25 µm i.d. x 60 cm capillary,1 mg/mL CON, 0.3 mg/ mL BLG B, 0.3 mg/mL,BLG A, 0.25 mg/mL BSA, 20 mM CHES/ 30 mM KCl buffer and 235 V/cm.

with these proteins. Large equilibrium constants can result in band broadening due to slow exchange between different species present in the band (see discussion in chapter 5).

To show the general applicability of this method, the minimum injectable amounts (MIAs) using the two probes, for conalbumin, bovine serum albumin and beta lactoglobin A are given in Table 4. Of particular interest is the difference in detectability of the two different probes. TNS provides lower and more uniform MIAs than ANS. The lower MIAs for TNS probably results from a larger change in dipole moment upon the excitation than ANS, which causes a larger change in quantum yield upon binding (118). The greater uniformity in MIA for TNS could possibly be explained by TNS having a generally higher binding constant for these proteins than ANS. This would force the labeling equilibrium toward completion for each protein and result in similar detectability.

In conclusion, hydrophobic probes can be used to conveniently detect proteins in very small diameter capillaries without degrading efficiency. Future work in this area should include the investigation of other arlyaminonaphthalene-sulfonate derivatives as labeling agents and the use of other wall coated capillaries to optimize buffer pH. Furthermore, it should be possible to reduce the fluorescent background by the use of polarized fluorescence detection to discriminate against the fluorescence from unbound label molecules.

TABLE 4

MINIMUM INJECTABLE AMOUNTS OF PROTEIN FOR ANS AND TNS

Protein	ANS (femtomoles)	TNS (femtomoles)
Conalbumin	15	1
Bovine Serum Albumin	0.6	0.2
Beta Lactoglobin A	not detected	0.4

Note: The linear dynamic range for the proteins shown is 1.5 and 2 orders of magnitude for ANS and TNS, respectively.

CHAPTER 4

SEPARATION OF ANIONIC SURFACTANTS BY CZE USING ON-COLUMN LABELING WITH 2-P-TOLUIDINONAPHTHALENE-6-SULFONATE

Surfactants are compounds which contain both hydrophilic and hydrophobic moieties (123). The hydrophilic region, often called the head group, can be anionic, cationic, zwitterionic, or polar neutral (nonionic). The type of head group is generally used to classify surfactants. The large difference between the water solubility of these two moieties causes these compounds to interact with each other in aqueous solution. At low concentration surfactants exist as free monomers, but as the concentration is increased (to above the critical micelle concentration (CMC)) they associate to form micelles. Normal micelles are aggregates of surfactant molecules positioned such that the hydrophilic region of the compound is pointed toward the center of the micelle with the head group exposed to the surrounding aqueous solution. This creates a more thermodynamically favorable environment for the hydrophobic region and causes the interior of micelles to be very nonpolar in nature. The size and shape of the micelle is dependent on the surfactant type, concentration, and the nature of the surrounding solvent. High salt concentrations and organic solvents will alter the CMC of the the surfactant and the aggregation number of the micelle (123).

Surfactants, due to their ability to solubilize organic compounds in aqueous solutions, have proven to be useful reagents in many scientific applications. As described previously, surfactants are employed as a pseudostationary phase in MECC (35, 44, 73, 75). They are also used in more conventional separation methods such as reverse phase chromatography (124) and liquid extraction methods (125), usually to increase the selectivity of the method. Moreover surfactants are components in a variety of manufactured goods such as detergents (126), cosmetics (127, 128), and pharmaceuticals (129).

Since surfactants and the micelles they form are so commonly used, numerous methods have been developed for their quantitation and the study of their physical and chemical properties. Surfactant systems have been quantitated by a vast array of procedures including spectrophotometry (130), mass spectrometry (131, 132), and chromatography (130-134). The utility of spectrophotometry is limited by the availability of strong chromophores on the surfactant. Because many surfactants do not contain UV active chromophores (i.e. aromatic rings), less sensitive infrared spectroscopy must often be employed. However, the narrow absorption bands of IR spectroscopy can be more useful in the analysis of complex samples than UV absorbance bands (130). Mass spectroscopy can provide both quantitative and qualitative information about the surfactant. However, the low volatility of surfactants usually requires the use of more complex ionization methods such as fast atom bombardment or field desorption (132).

Chromatographic separation of surfactants can be based on interaction with either the hydrophilic or hydrophobic region of the compound. Ion chromatography is often employed for the analysis of charged species, but since separation is based only on interaction with the head group, surfactants with different hydrophobic regions are sometimes not separated (130). This method is often used for the isolation of a single class of surfactants but not for the characterization of homologous mixtures. Gas chromatography and reversed phase HPLC can provide separation based on differences in the hydrophobic region of the surfactant. Surfactant analysis by gas chromatography is hampered by the low volatility of many surfactants. Therefore, to facilitate use of this method the surfactant must be quantitatively converted to a hydrophobic oil prior to analysis (131, 133). Reversed phase HPLC permits the direct analysis of surfactants but detection of surfactants can require derivatization with a compound containing a suitable chromophore or fluorophore (130, 134).

Some of the techniques used to study the physical and chemical properties of micelles include light scattering, fluorescent probes, and NMR. Light scattering can provide information about the size and shape of the micelle (135). Fluorescent probes can be used to determine the CMC of the micelle as well as provide information about the polarity of the micelle's interior (136, 137). Finally NMR can be used to study the molecular orientation of surfactants in micelles and the micelle monomer equilibrium (138, 139).

Although rarely, electrophoresis has also been used for the study of surfactants. Bodenmiller and Latz used conventional gel electrophoresis for the separation of several types of surfactants (140). They added dioxane to the electrophoretic buffer to prevent micelle formation, which permitted the separation of similar compounds. Recently, their have been two reports of capillary electrokinetic separations of surfactants. Ewing *et al.* used MECC for the analysis of linear alkylbenzene sulfonates (141) and Gobel *et al.* used CZE for the separation of alkyl sulfonates (142). These methods employed conventional and indirect (based on ion displacement) spectrophotometric detection. As mentioned above, conventional spectrophotometric detection is unable to detect surfactants that do not contain strongly absorbing chromophores. Indirect detection can be applied to nonabsorbing species but restricts the choice of mobile phase composition. Furthermore, these methods suffer from the aforementioned limitations of spectrophotometric detection (see Chapter 1) in capillary electrokinetic separation methods.

This chapter describes the use of CZE with laser-based fluorometric detection to separate and detect anionic surfactants. Detection is facilitated by the addition of 2-p-toluidinonaphthalene sulfonate (TNS) to the electrophoretic buffer. As with proteins (see chapter 3), the quantum efficiency of TNS is increased when solubilized by micelles. When in the hydrophobic core of the micelle the TNS molecule is protected from the previously discussed solvent cage quenching mechanism and fluoresces more efficiently.

Therefore, eluting zones that contain surfactants above their CMC will result in increased TNS fluorescence and detection of the micellar zone.

Experimental

High purity sodium dodecyl sulfate (99% by weight), technical grade sodium dodecyl sulfate, sodium cholate, sodium deoxycholate, sodium taurocholate, and 2-p-toluidinonaphthalene-6-sulfonate (TNS) were acquired from Sigma Chemical Company (St. Louis, MO). The technical grade sodium dodecyl sulfate contained 67 % sodium dodecyl sulfate, 26 % sodium tetradecyl sulfate, and 5 % sodium hexadecyl sulfate according to the manufacturer's assay. Sodium hexadecyl sulfate was purchased from Aldrich (Milwaukee, WI). All other chemicals employed were reagent grade and obtained from Baxter Healthcare (Stone Mountain, GA). The commercial liquid soap product used in this work was obtained locally.

The experimental apparatus for this study was the same as used for the on-column labeling of proteins. Peak areas and heights were determined using a Varian 4400 integrator (Walnut Creek, CA). A 50 μm i.d. x 60 cm untreated capillary from Polymicro Technologies (Phoenix, AZ) and a field strength of 300 V/cm were employed throughout the study. Electrophoretic buffers contained 0.01 M Na_2HPO_4, 0.006 M $Na_2B_4O_7$ and the appropriate amount of TNS. The commercial liquid soap product was diluted 1 to 10 with electrophoretic buffer prior to injection, to reduce the viscosity of the sample.

Limits of detection were determined by constructing calibration curves. Peak areas were normalized by multiplying by the inverse velocity of the band to correct for changes in solute migration velocity (see Chapter 2). Quantitation by standard addition was performed using an electrophoretic buffer and standard solutions containing 0.1 mM TNS . Observed electrophoretic mobilities ($\mu_{ep\ obs}$) were calculated by the following equation:

$$\mu_{ep\ obs} = \mu_{obs} - \mu_{osm} = \left(\frac{L^2}{t_m} - \frac{L^2}{t_o} \right) / V \qquad [11]$$

where μ_{obs} is the observed mobility, μ_{osm} is the electroosmotic mobility, L is the length of the capillary, t_m is the migration time of the band, t_o is the migration time of water (the electroosmotic velocity). Electroosmotic velocity (t_o) was determined by a system peak resulting from the injection of water.

Separation of Anionic Surfactants

Figure 11 shows electropherograms of 0.05 M high purity sodium dodecyl sulfate (SDS) and 0.05 M technical grade SDS. The negative peak immediately before the large SDS micelle peak, in both electropherograms is due either to the displacement of TNS by SDS monomers or the retention of TNS in the region before the SDS peak by micelles in the eluting band. The latter of these scenarios would result from the TNS having a large partition coefficient into the micelle and the micellar band having a larger capacity for TNS

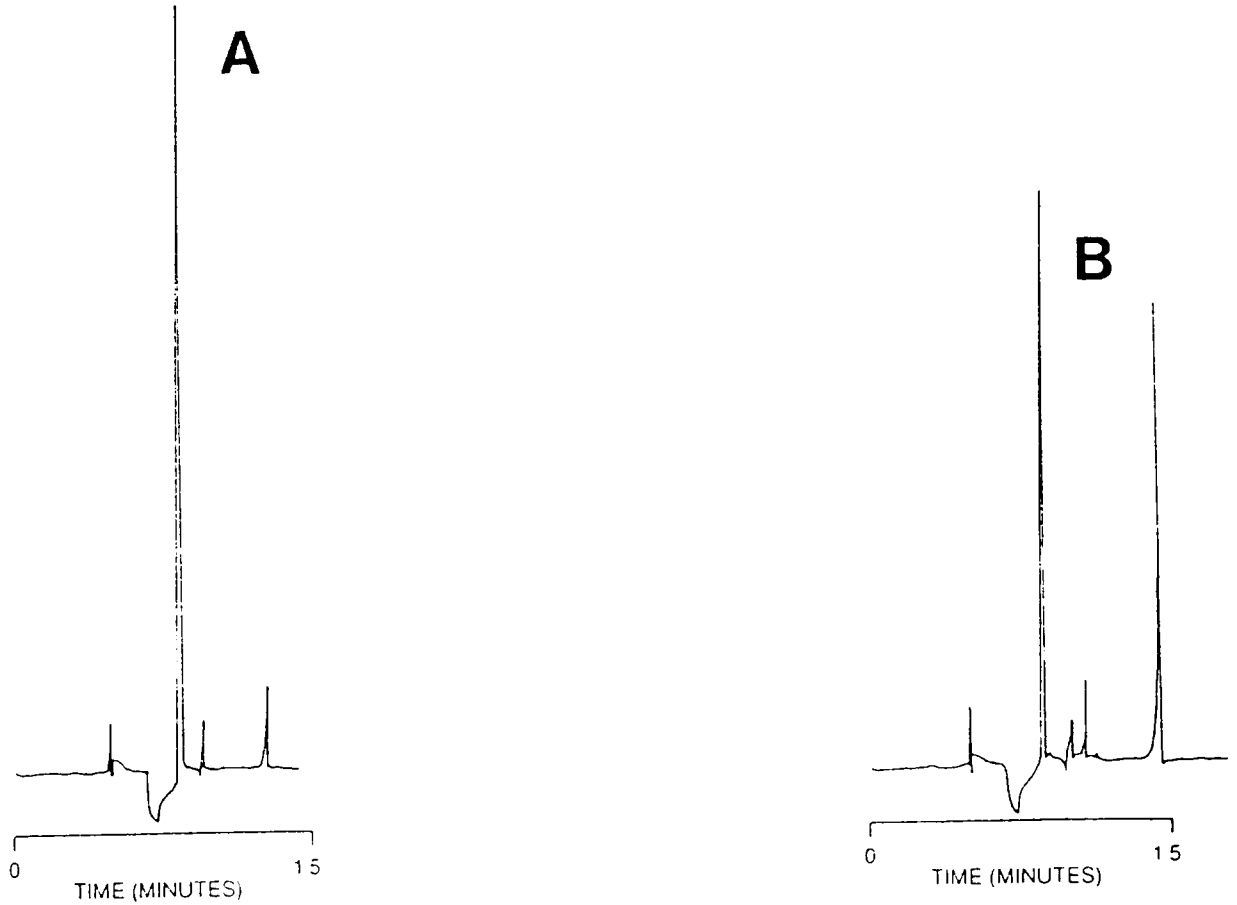

Figure 11. Electropherograms of high purity (A) and technical grade (B) SDS. Conditions: 10 mM Na_2HPO_4 / 6 mM $Na_2B_4O_7$ / 0.1 mM TNS buffer, 50 µm x 60 cm capillary, 300 V/cm.

than can be filled by the TNS concentration in the band. Therefore, as the micellar band moves slowly (relative to the surrounding buffer) though the capillary it could concentrate TNS in the band, at the expense of the region eluting prior to the micelle band. Either of these situations would result in a decrease in the fluorescence background and a negative peak.

It is evident from these electropherograms that both samples contain more than one component. This was expected for the technical grade sample because based on the manufacturer's assay all three components should be present above their CMC. Injection of the same concentration of sodium hexadecyl sulfate (SHS) as in the technical grade SDS sample (based on manufacturer's assay) resulted in the detection of a very small peak with a similar migration time to last peak in Figure 11B. Because of the large discrepancy in peak height, it is assumed that the hexadecyl sulfate is coeluting with the tetradecyl sulfate (STS) (which is present at a much higher concentration). Moreover, addition of SHS to the technical grade SDS sample resulted in a increase in the size of the last peak. The coelution of STS and SHS micelles could be the result either of the two compounds having similar electrophoretic mobilities or the formation of a mixed micelle that is sufficiently stable so as not to dissociate during the electrophoretic process. Since the addition of SHS to the technical grade sample did not result in the formation of a new peak by altering the mobility of SHS band (see later discussion), it is probable that coelution is due to the formation of a stable mixed micelle. The formation of mixed micelles resulted in

unusual retention orders in the work of Bodenmiller and Latz. However, use of large concentrations of organic solvent to prevent micelle formation (as performed by Bodenmiller and Latz) is precluded in this method, as that would destroy the detection mechanism which requires micelle formation.

Figure 12 shows two other surfactant separations. The separation of the micelles of the bile salt sodium cholate (NaC) from SDS is illustrated in Figure 12A. Separation of other bile salt micelles from NaC was not achieved. Separate injections of sodium cholate, sodium deoxycholate and sodium taurocholate showed these bile salt micelles to have similar electrophoretic mobilities which prevented their separation. The selectivity of this detection scheme is illustrated by the electropherogram of a commercial soap product in Figure 12B. The commercial soap product contains 26 ingredients (according to the label), most of which are not observed in the electropherograms. Although not identified with standards, the second peak in the electropherogram is expected to be due to the major components in the sample, sodium C14-C16 olefin sulfonate.

Quantitation of Sodium Dodecyl Sulfate

Calibration curves and data for high purity SDS using peak area and height are shown in Figure 13 and Table 5 for two TNS concentrations. The higher TNS concentration resulted in greater sensitivity and a lower limit of detection. The greater sensitivity is probably due the partitioning of more TNS into the micelle at a given surfactant concentration. The limits of detection determined

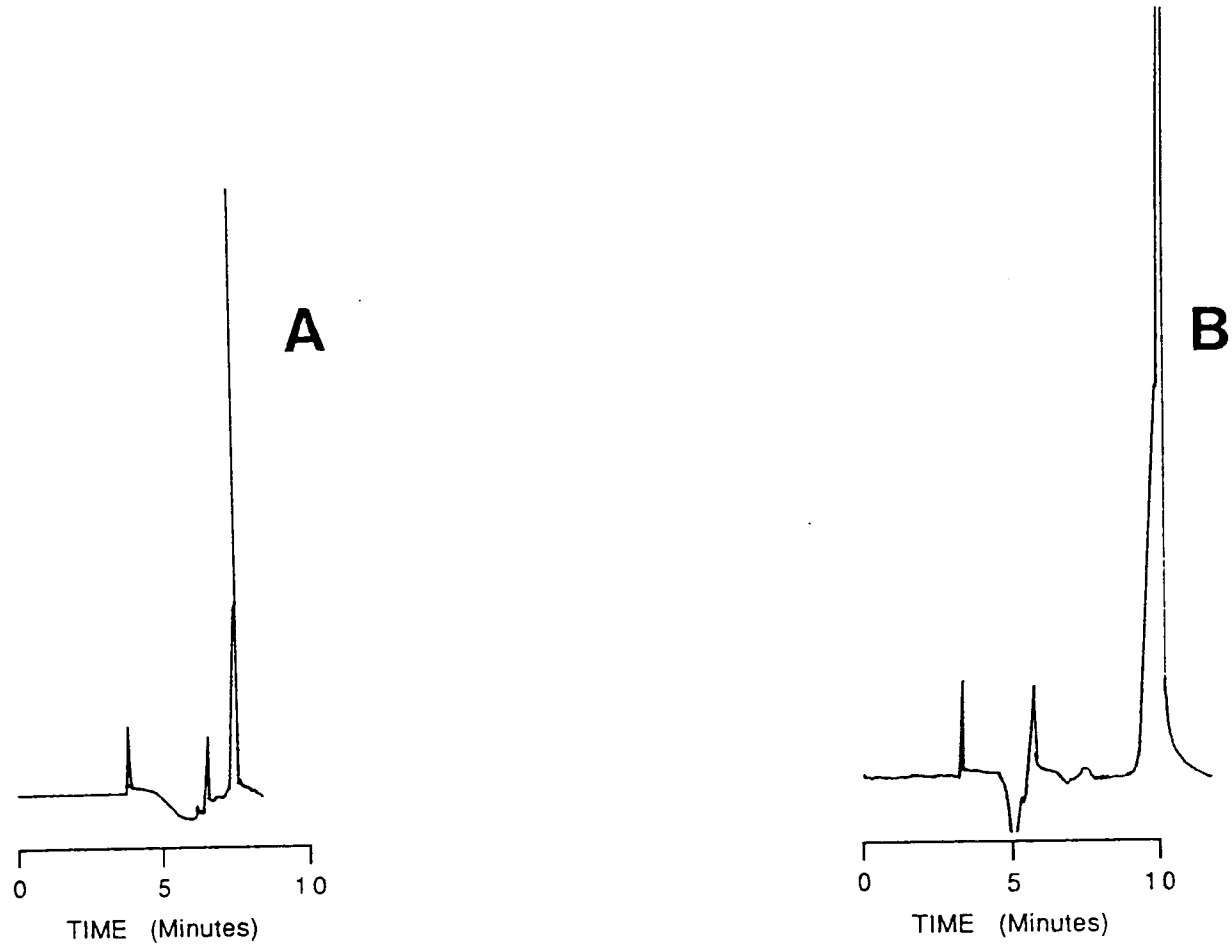

Figure 12. Electropherograms of sodium cholate and high purity SDS (A) and commercial soap product (B). Elution orders: (A) water (t_o) 3.6 minutes, sodium cholate 6.3 minutes, sodium dodecyl sulfate 7.3 minutes; (B) water (t_o) 3.7minutes, sodium dodecyl sulfate 5.6 minutes, C14-16 olefine sulfonate 9.7 minutes. Same conditions as Figure 11.

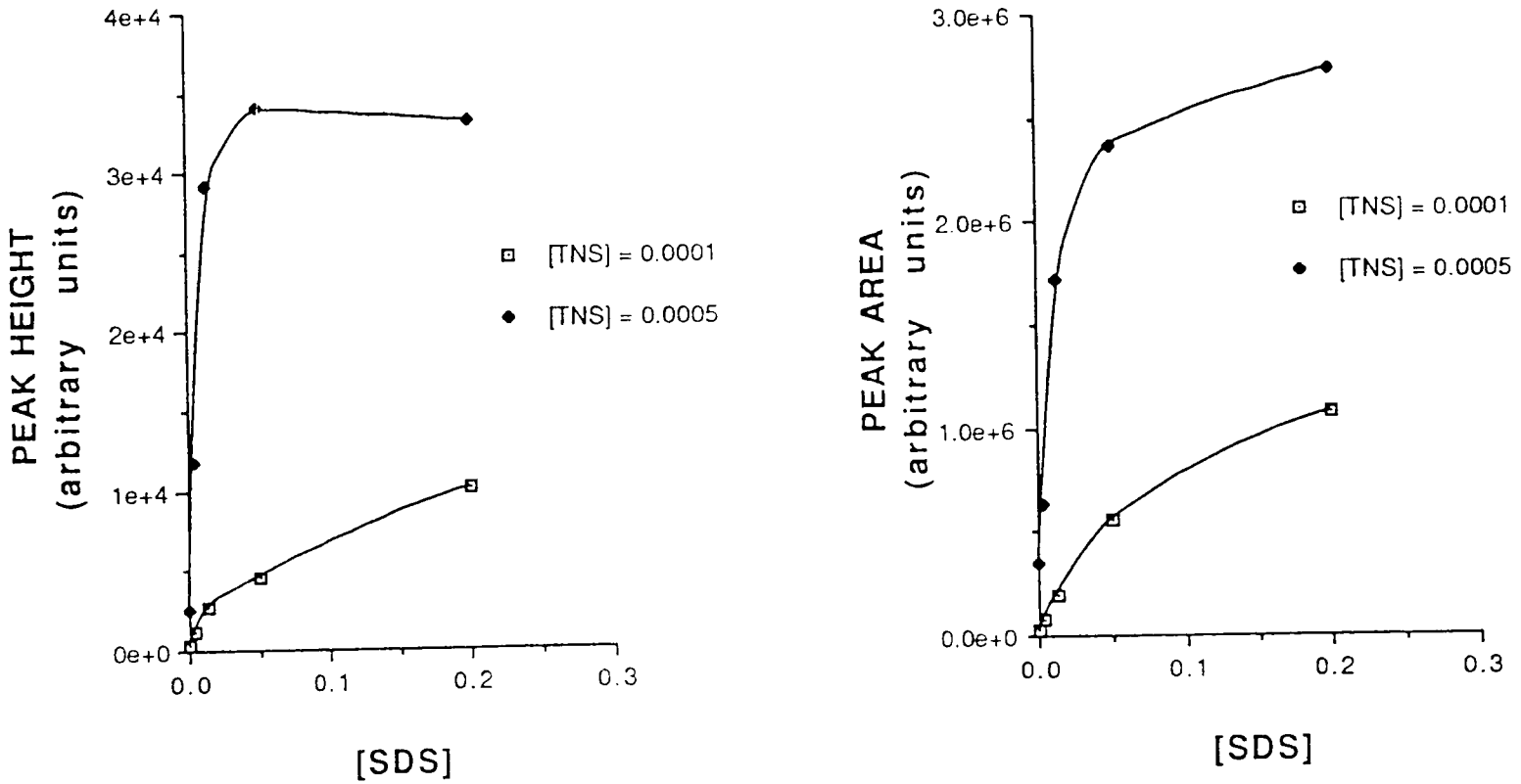

Figure 13. Calibration curves for high purity SDS. Conditions: 10 mM Na_2HPO_4 / 6 mM $Na_2B_4O_7$ buffer, 50 µm x 60 cm capillary, 300 V/cm.

TABLE 5

CALIBRATION DATA FOR HIGH PURITY SODIUM DODECYL SULFATE

	PEAK HEIGHT		PEAK AREA	
TNS Concentration	0.1 mM	0.5 mM	0.1 mM	0.5 mM
Linear Dynamic Range	LOD to 0.0125 M	LOD to 0.0125 M	LOD to 0.05 M	LOD to 0.0125 M
Limit of Detection	0.4 mM	0.1 mM	0.4 mM	0.1 mM
RSD_{pooled}	6.63 %	31.67 %	6.08 %	10.49 %

were below the CMC of SDS in pure water, however, since the exact nature of the surfactant/probe adduct at low surfactant concentrations is unknown, it is possible that detection could occur below the CMC of the surfactant. Detection below the CMC could occur based on the same mechanism that resulted in the large background increase observed at high TNS concentrations in Chapter 3. Furthermore, the relatively high ionic strength of the electrophoretic buffer could reduce the CMC dramatically and allow micelle formation at these low concentrations (123). Both TNS concentrations resulted in a linear region from the limit of detection to near 0.0125 M. Above that concentration the calibration curve demonstrated a dramatic negative deviation from linearity,

possibly due to insufficient TNS to saturate all of the micelles in the eluting band. The use of an internal standard could have improved the relatively poor reproducibility of both peak height and area (see table 5). Attempts to use the fluorescent dye Coumarin 120 as an internal standard were unsuccessful because of a very poor peak shape at high SDS concentrations, possibly due to association with the SDS micelle in the injected band during the early minutes of the separation. This hypothesis is feasible based on the large k' observed for Coumarin derivatives in MECC experiments using SDS (34, 75).

Quantitation and peak identification in this method are complicated by a dependence of electrophoretic mobility on sample concentration. The dependence of mobility on concentration for the data used to generate Figure 13 is plotted in Figure 14. Electrophoretic mobility becomes more negative as the injected SDS concentration is increased. This is possibly due to the change in mole fraction of TNS in the micelle across this concentration range. At low mole fractions (high SDS concentrations), the change in mobility with concentration is small as evidenced by the reduced slope of the mobility plot at high SDS concentrations. Therefore, it may be possible to reduce this adverse affect by using very low TNS concentrations; however, that would greatly reduce detectability.

Quantitation can be performed, nevertheless, by using standard addition. Furthermore the standard addition method permits peak identification, as the peak height is increased by the addition of the standard. Moreover since the mobility of a band is concentration

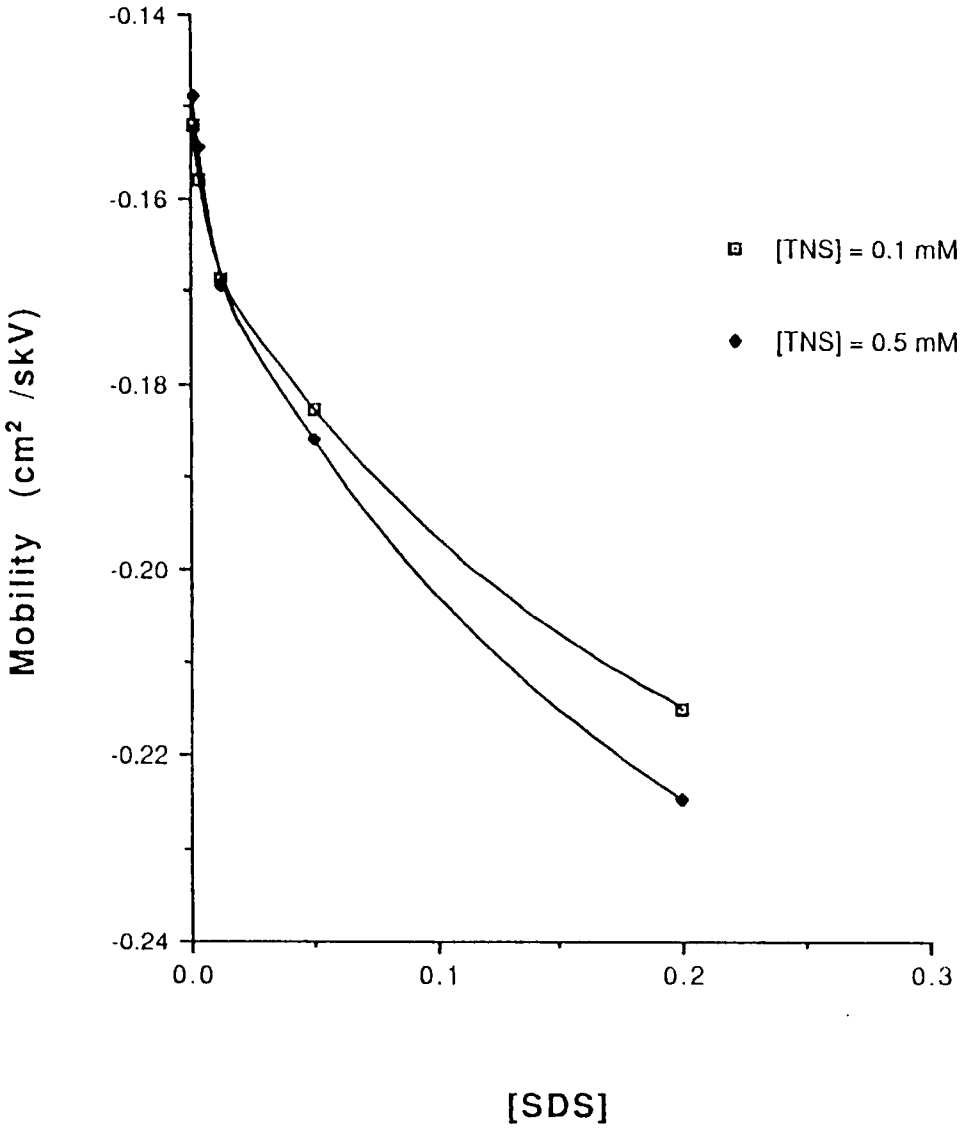

Figure 14. Graph of the effects of sodium dodecyl sulfate concentration on electrophoretic mobility. Data from calibration curves in Figure 13.

dependent, the addition of standard could determine if coelution was occurring by altering the mobility of the compound of interest and permitting separation. The addition of 25 ml of 0.0780 M high purity SDS to 1 mL of 0.0088 M technical grade SDS (concentration based on the molecular weight of SDS) showed the SDS sample to be 75% SDS by weight using corrected peak areas. The manufacturer's assay showed the sample to be 67% by weight. The determined concentration is higher than the manufacturer's assay; however the difference could be due to the relatively poor reproducibility of this method or an erroneous report by the manufacturer. The use of an automated injection system or an internal standard (if an acceptable compound can be found) could reduce the difference between these two numbers.

In conclusion, the addition of hydrophobic probes in electrophoretic buffers will allow the detection of surfactants separated by CZE. Despite some difficulties, quantitation of surfactants is possible using this method. Perhaps a more important application of this method in the future will be the investigation of the electrophoretic mobility of micelles using very low TNS concentrations. This will facilitate study of the electrical double layer around the surfactant and other physical characteristics of the micelle (i.e. size and shape).

CHAPTER 5

DETERMINATION OF METAL IONS BY CAPILLARY ZONE ELECTROPHORESIS WITH ON-COLUMN CHELATION USING 8-HYDROXYQUINOLINE-5-SULFONIC ACID

The majority of CZE applications have involved the separation of biological macromolecules; however, the technique is amenable to the separation of any ionic species. Metal ion analysis by CZE has been virtually ignored, probably due to the unavailability of a simple, sensitive, and selective detection scheme. The few reports of metal ion separations by CZE to date have employed conductivity, spectrophotometry, and indirect fluorimetry for detection (52, 54, 55, 71). Although, the conductivity detection scheme described in the literature provided good sensitivity, it required that minute holes be drilled in the capillary wall so that electrodes could be placed in the flow channel. Boring of these holes required the use of a computer controlled CO_2 laser and was difficult to perform (143). Due to small metal ion absorption bandwidths, complex-formation is necessary, if spectrophotometric detection is to be performed (52, 54, 55). Recently, indirect fluorescence has been employed for the separation of several group I and II metal ions (53). This mode of detection provides better sensitivity and is universal for all cations. However, indirect fluorescence does not provide the specificity of a chemical reaction and consequently may not always be applicable to the analysis of complex samples. Metal analysis by CZE is also

hampered by coulombic interactions of the metal cation with the surface of the fused silica capillaries commonly employed in CZE. These interactions can result in band broadening, which reduces both detectability and resolution.

In this chapter, the detection and separation of some metal ions via their interaction with a common chelating agent, 8-hydroxyquinoline-5-sulfonic acid (HQSH) will be described. HQSH exists in anionic form (HQS^-) in aqueous solutions and exhibits virtually no native fluorescence but forms fluorescent complexes with a large number of metal ions. Dasgupta and coworkers have reported the spectroscopic characteristics of 42 different metal HQS^- complexes, as well as the use of these complexes for detection in ion chromatography (53, 144, 145). The formation of these complexes can be used to sensitively detect metal ions separated by CZE using laser-based fluorimetry. It is possible to create the fluorescent species within the capillary by merely adding HQS^- to the electrophoretic buffer. In addition to allowing the detection of these ions, interaction with this chelating agent tends to impart a negative charge to the metal ion which reduces interactions with the wall of the capillary. Furthermore, by manipulating electrophoretic buffer parameters such as HQS^- concentration and pH, it is possible to affect the electrophoretic mobility of the metal ion and optimize the separation.

Theory

The interaction between the metal ion and HQS^- is described by the following equilibrium expression

$$K' = \frac{[M(HQS^-)n]}{[M][HQS]^n} \qquad [12]$$

where K' is the overall conditional formation coefficient for that metal ion and n is the number of ligands. Although this equation describes the overall reaction of the metal with HQS^-, the reaction generally occurs in a stepwise fashion. Therefore, several different metal HQS^- complexes can exist simultaneously. As the HQS^- to metal ratio increases, the charge of the complex becomes effectively more negative and mobility decreases. Thus, the net mobility of the resulting CZE band is determined by the distribution between the various possible forms of the metal complex. The effect of electrophoretic buffer pH on K' is described by equation 13

$$K' = \alpha^n K_f \qquad [13]$$

where K_f is the overall formation constant for the metal at infinite dilution and α is the degree of protonation of the amine and phenolic functionalities on the HQS^- chelate.

The observed electrophoretic mobility of the metal ion ($\mu_{ep\ obs}$) can be assumed to be a combination of the mobility of the free metal and various complexes, which can be described by

$$\mu_{ep\ obs} = X_M\mu_M + X_{ML}\mu_{ML} + X_{ML_2}\mu_{ML_2} + \ldots \qquad [14]$$

where μ_M, μ_{ML}, and μ_{ML_2} are the mobilities of the free metal ion, 1:1 HQS^- complex, and 1:2 complex and X_M, X_{ML}, and X_{ML_2} are the mole fractions of each species in the capillary. These mole fractions are a function of electrophoretic buffer parameters, which affect the above equilibrium equation. The remainder of this chapter will consider the effects of varying experimental parameters on detectability, observed mobility of calcium, magnesium and zinc ions, and band broadening.

Experimental

8-Hydroxyquinoline-5-sulfonic acid was purchased from Sigma Chemical Company (St. Louis, MO). Sodium phosphate dibasic, sodium borate, magnesium sulfate, calcium sulfate and zinc sulfate were obtained from Baxter Healthcare Corporation (Stone Mountain, GA). Coumarin 120 was acquired from Eastman Kodak Company (Rochester, NY) . Blood serum was obtained in house and not treated with an anticoagulant.

Separations were performed in untreated fused silica capillaries 45 to 60 cm in length and 50 μm id, obtained from Polymicro Technologies (Phoenix, AZ). Fluorescence excitation was performed using either the Coherent Inova 100 argon ion laser or the Liconix 4230NB helium-cadmium laser described in Chapter 3. Emission was isolated at 505 nm (bandpass approximately 10 nm)

with a 425 nm high pass filter and an Instruments SA H-10 monochromator.

Electrophoretic buffers were 10 mM Na_2HPO_4, 6 mM $Na_2B_4O_7$ and the appropriate concentration of HQS^- in triply distilled, deionized water. The pH of the electrophoretic buffer was adjusted using HCl or NaOH. Standard metal solutions were injected on-column, by siphoning, from aqueous solutions. Injected volumes were determined by continuous injection. Calibration plots were constructed using Coumarin 120 as an internal standard, to normalize for imprecision in the injection method and variation in electroosmosis. Electroosmotic velocity (t_0) was determined by a system peak resulting from the injection of water. Blood serum was diluted with a equal volume of electrophoretic buffer prior to injection.

Observed electrophoretic mobilities were calculated using equation 11. Equilibrium mole fractions were determined from the equilibrium expressions and mass balance equations for each metal. These calculations only considered the formation of complexes for which formation and protonation constants are reported in references 146 and 147. The formation of higher HQS^- to metal ratio complexes is possible but should represent a very small fraction of the species present in the band and, therefore, not significantly affect the mobility of the band. The mobilities of the various species in the calcium and magnesium band were calculated by simultaneously solving equation 13 for various electrophoretic buffer conditions. These calculations were performed using an

Apple Macintosh SE (Cupertino, CA) with MathCAD software from Mathsoft Inc (Cambridge, MA). This software solves an equation or set of equations, given a set of boundary conditions and a reasonable approximation for the solution.

Detection

Fluorescence spectra of the three metal-HQS^- complexes studied herein exhibited broad maxima near 400 and 505 nm for excitation and emission, respectively. This suggests the use of the UV output of an argon ion laser for excitation. Employing an argon laser, operating in an all lines UV mode (total power = 50 mW, several lines between 330 and 365 nm) resulted in a minimum detectable injected concentration near 1 μM for magnesium. However, this laser damaged the fused silica after a short time at high power and exhibited poor baseline stability at low power. These factors combined with the expense and complexity of the Inova 100 argon ion laser prohibited its general use. Therefore, a low power helium-cadmium laser (λ = 325 nm) was employed as an excitation source for most of this study.

Electrophoretic buffer parameters which affect the complexation reaction will affect both detectability and CZE efficiency. Increasing the HQS^- concentration will shift the metal HQS^- complex toward the formation of complex and increase the fluorescence signal. However, if high HQS^- concentrations are used to control the complexation reaction, an increase in the fluorescence background (presumably due to impurities in the electrophoretic

buffer) and large electrophoretic currents (which can degrade efficiency) will be observed, both of which effect detectability. The effects of varying HQS^- concentration on CZE peak profiles are illustrated in Figure 15A. The Ca(II) and Mg(II) peaks follow the expected trend, showing greater peak heights at higher HQS^- concentrations. The broad and asymmetric Zn(II) peak, however, exhibits a maximum peak height when the [HQS^-] is 2.5 mM. Above that concentration, the Zn peak becomes very broad and peak height is reduced (see later discussion).

The pH of the electrophoretic buffer must also be chosen carefully to maximize detectability. Since the pH of the electrophoretic buffer effects K', it will influence the concentration of fluorophore in the band and the efficiency of the band (see later discussion). Reducing the pH decreases α (see equation 12) and the concentration of complex resulting in reduced peak area (see Ca(II) and Mg(II) peaks of electropherograms in Figure 15B). Although high pH electrophoretic buffers create larger concentrations of fluorophore, large increases in detectability (as measured using peak height) are not always realized, due to a loss of efficiency (see Zn(II) peak in Figure 15B and later discussion of band broadening). Therefore, it is suggested that a slightly alkaline electrophoretic buffer containing 1-5 mM concentrations of HQS^- will result in optimal detectability for the ions studied in this work.

Minimum detectable injected concentrations and amounts for Ca(II), Mg(II) and Zn(II), based on a peak height of twice the baseline noise, are compiled in Table 6 for an electrophoretic buffer

Figure 15. Separation of test metals under various electrophoretic buffer conditions. A) Electrophoretic buffer pH = 8, applied voltage = 20 kV, capillary length = 50 cm and laser intensity = 1.5 mW. Elution order is Ca(II), Mg(II), Zn(II). All metal ions were 0.3 mM. The arrow denotes a Ca(II) peak with S/N = 2. B) Electrophoretic buffer contained 2.5 mM HQS-, applied voltage = 20 kV, capillary length= 45 cm and laser intensity = 2.5 mW. Same elution order as in (A). Metal concentrations were Ca(II) = 0.63 mM, Mg(II) = 0.08 mM, and Zn(II) = 0.15 mM.

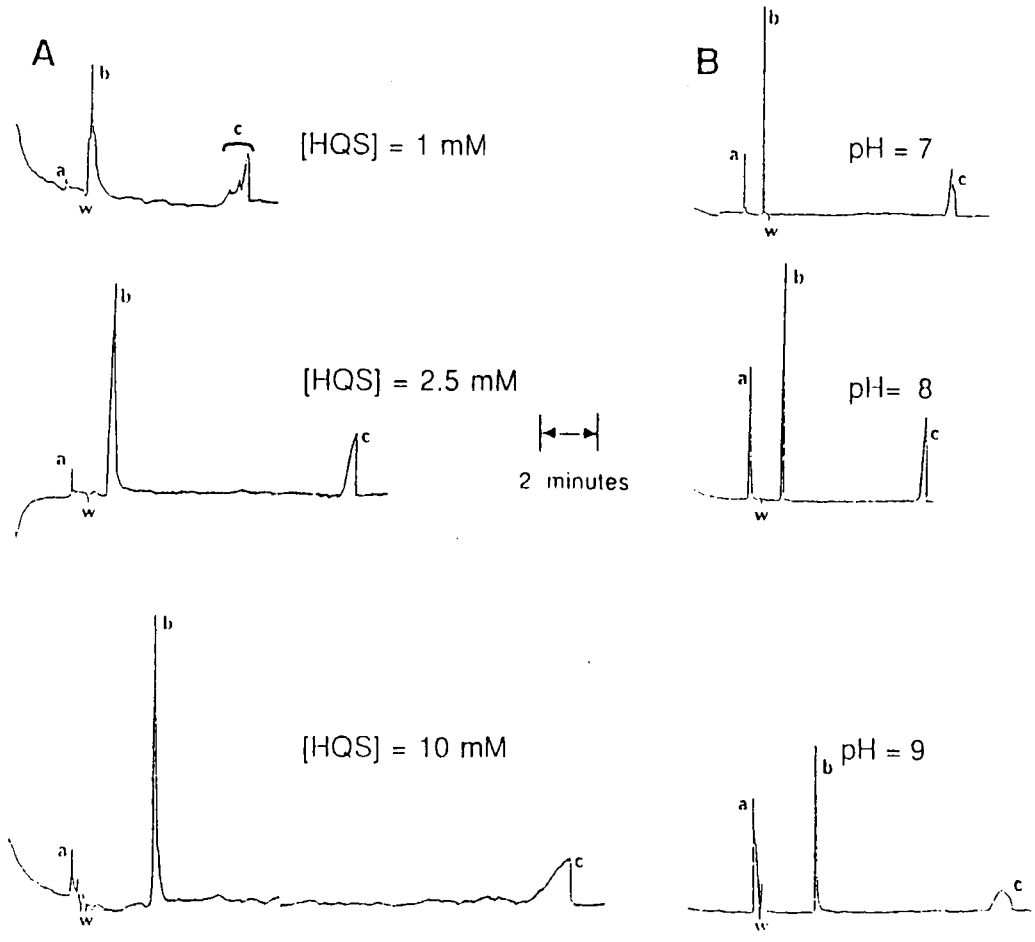

Figure 15. Separation of test metals under various electrophoretic buffer conditions. A) Electrophoretic buffer pH = 8, applied voltage = 20 kV, capillary length = 50 cm and laser intensity = 1.5 mW. Elution order is Ca(II), Mg(II), Zn(II). All metal ions were 0.3 mM. The arrow denotes a Ca(II) peak with S/N = 2. B) Electrophoretic buffer contained 2.5 mM HQS-, applied voltage = 20 kV, capillary length= 45 cm and laser intensity = 2.5 mW. Same elution order as in (A). Metal concentrations were Ca(II) = 0.63 mM, Mg(II) = 0.08 mM, and Zn(II) = 0.15 mM.

TABLE 6.

LIMITS OF DETECTION FOR CALCIUM, MAGNESIUM AND ZINC IONS

Metal Ion	Minimum Detectable Concentration		Minimum Detectable Amount		Correlation Coefficient
	molar	ppb	femtomoles	picograms	
Ca(II)	1.5×10^{-5}	613	105	4.2	0.9952
Mg(II)	2.0×10^{-6}	46	14	0.3	0.9992
Zn(II)	3.1×10^{-6}	205	21	1.4	0.9989

Electrophoretic buffer contained 2.5 mM HQS^- and was adjusted to pH =8. Limits of detection are based on a S/N= 2 and a 7 nL injection volume. Correlation coefficients are for a 2 order of magnitude concentration range above the limit of detection. RSD for peak height = 10%.

containing 2.5 mM HQS^- at pH = 8. Minimum injectable amounts are based on a 7 nL injection volume. The existence of a strong fluorescence background (approximately 200 nA), probably resulting from metal impurities in the electrophoretic buffer, limits the detectability of this method. Therefore, the use of a stabilized laser or ultra pure water should improve the detectability of this method.

The RSD in peak height for each metal ion was less than 10% (N=5) and the linear dynamic range (LDR) was two orders of magnitude above the limit of detection ($R > 0.995$). The LDR is limited at high concentrations by a loss of efficiency and a reduction in the mole fraction of complexed metal. Although changes in the concentration of injected metal ion shift equilibria and thereby alter $\mu_{ep\ obs}$ (see equation 13), retention times over the 100 fold LDR were reasonably reproducible (RSD $\leq$ 3 %, $N > 10$).

The potential application of this technique to the analysis of metal ions in complex matrices is illustrated with the electropherogram in Figure 16. Blood serum was diluted with electrophoretic buffer prior to injection to reduce the effects of metal binding to proteins in the serum. Without the dilution, the eluted bands exhibited greater negative mobilities and were very broad. A peak for Zn(II) is not observed. This was attributed to its high binding constant to proteins which prevented its interaction with HQS^- (148). The use of a digestion method prior to injection could possibly solve this problem.

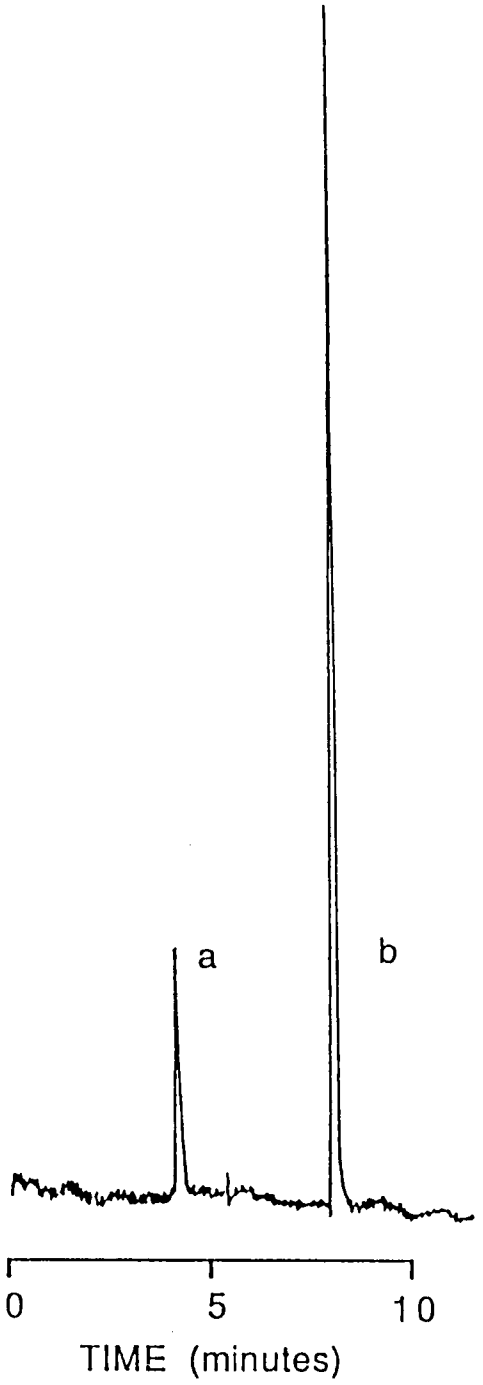

Figure 16. Injection of blood serum diluted with an equal volume of electrophoretic buffer. Electrophoretic buffer contained 2.5 mM HQS^- at pH = 8, applied voltage = 20 kV and capillary length = 60 cm. Peak a is calcium and b is magnesium.

Manipulation and Prediction of Electrophoretic Mobility

Although the use of selective detection schemes can facilitate the elucidation of a specific compound in a complex mixture, it is often necessary to manipulate electrophoretic mobility to optimize resolution. As shown in equation 4 resolution in CZE is dependent on differences in the electrophoretic mobilities of solutes. Equation 14 predicts that the observed mobility of a band will be a function of the concentrations of the various forms of the metal in the capillary. Therefore, by controlling electrophoretic buffer parameters, which effect the mole fractions of these forms, it should be possible to manipulate the observed electrophoretic mobility ($\mu_{ep\ obs}$) of the band and influence the resolution of any separation.

Equation 12 indicates that increasing the concentration of HQS^- in the electrophoretic buffer will cause the formation of more metal complex. This reduces $\mu_{ep\ obs}$ by tending to impart a negative charge to a divalent metal ion. Figure 17 shows the effects of HQS^- concentration on the observed mobility of the three test metals. The trends in these curves can be qualitatively understood by considering the formation constants, changes in the distribution between the various forms of the metal, and the mobilities of those forms. The positive sign and small reduction in $\mu_{ep\ obs}$ for Ca(II) is consistent with the formation of a nearly neutral 1:1 Ca-HQS^- complex (the expected neutral 1:1 complex will be positively charged, if protonation of the amine functionality on the HQS^- ligand occurs). The formation of complexes with higher HQS^- to metal

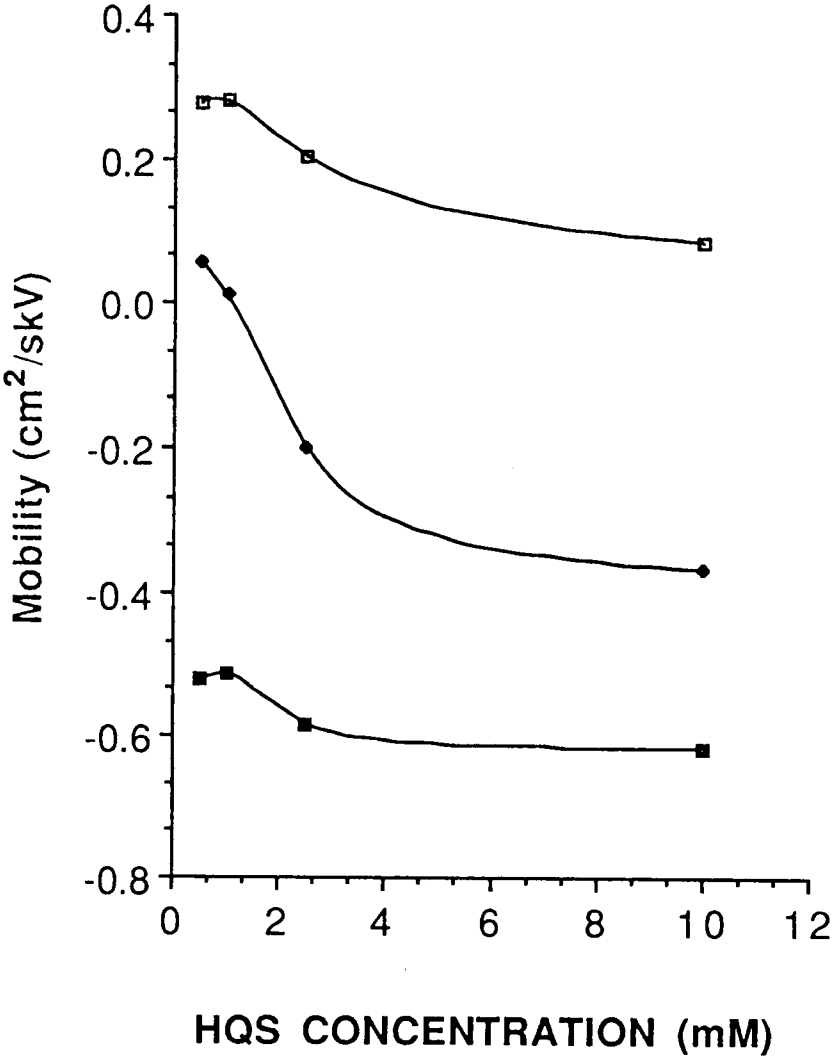

Figure 17. Effects of electrophoretic buffer HQS^- concentration on the mobility of Ca(II), Mg(II) and Zn(II). Conditions the same as in Figure 15A. Symbols: Ca(II) (□), Mg(II) (◆), and Zn(II) (■).

ratios, in significant concentrations, should result in a negative observed electrophoretic mobility for this peak. Likewise, the slow decline in the mobility curve would be appropriate for the relatively low formation constant of the Ca(II) complex ($K_f = 10^{3.4}$), which would require a high HQS^- concentration to force the complexation reaction to completion. Magnesium reacts with HQS^- to form both a nearly neutral 1:1 complex and a negatively charged 1:2 complex. An increase in concentration of the 1:2 complex would explain the change in sign of the observed electrophoretic mobility for Mg(II) in the figure. Furthermore, the higher overall formation constant of Mg(II) ($K_f = 10^{8.2}$) would allow the formation of the 1:2 complex at relatively low HQS^- concentrations, which explains the sharp initial decline in the Mg curve. At higher HQS^- concentrations the growth rate of the 1:2 complex is reduced. Between 0.5 and 2.5 mM HQS^-, the mole fraction of 1:2 complex increases at a rate of 24% per mM increase in ligand concentration, while between 2.5 and 10 mM HQS^- the rate is only 4%. The very high overall formation constant for Zn(II) can explain the greater negative mobility and slow decline of its mobility. Zn(II) probably exists predominantly in the 1:2 complex due to its very high overall formation constant ($K_f = 10^{16}$). This results in the more negative mobility of this band. The slow decline of this curve is the conversion of any remaining 1:1 complex to 1:2 complex.

Mobilities can also be manipulated by changing the electrophoretic buffer pH. As the pH is increased from 6 to 9, α (shown in equation 13) increases from 0.0037 to 0.79. By increasing

the conditional formation constant, the fraction of free metal ion present in the band and the observed mobility are decreased. The effects of varying pH on the mobility of the three test metal ions are illustrated in Figure 18. Using similar arguments as above it is possible to understand these curves. The low slope of the Ca(II) curve again is consistent with a slow change in the predominant species in the band, from free metal ion to a nearly neutral 1:1 complex. The large negative slope and change in mobility of the Mg(II) curve results from the increased concentration of the negatively charged $Mg(HQS^-)_2$ complex, which occurs at higher conditional formation constants. The low slope of the Zn(II) curve can again be explained by the large formation constant of the Zn(II) 1:2 complex, which is not affected enough by the pH change to dramatically change the mole fraction of the complex species, and thereby the observed mobility of the band.

It should be noted at this point that detectability can be degraded by steps taken to improve electrophoretic resolution (see earlier discussion of detection and Figure 15). Also, the reader is warned against predicting optimum separation conditions strictly from mobility data. As electrophoretic buffer conditions are changed the electroosmotic flow also changes and this can confuse predictions concerning resolution (see equation 4). Moreover, since small changes in electrophoretic buffer parameters can greatly affect efficiency, electrophoretic mobility and electroosmotic flow, stringent control of experimental conditions is required to achieve reproducible results.

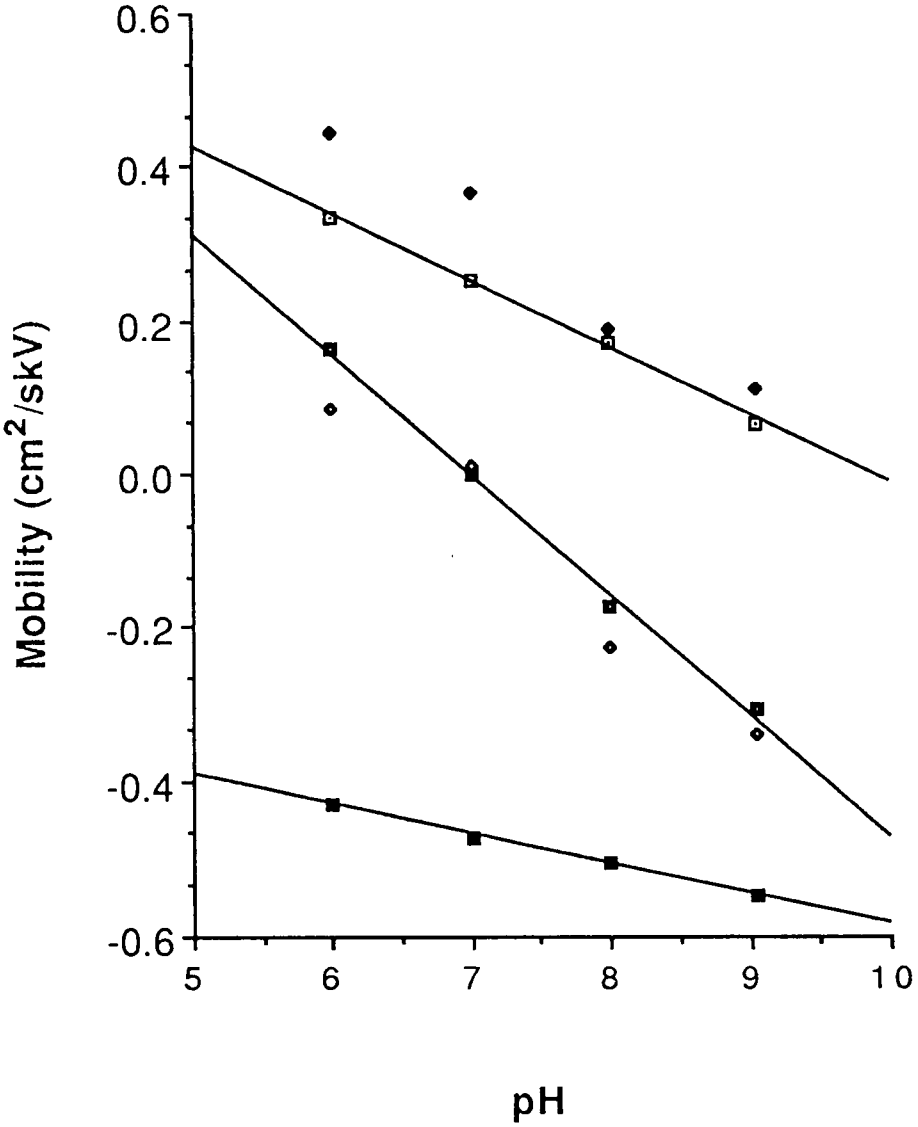

Figure 18. Effects of electrophoretic buffer pH on the mobility of Ca(II), Mg(II), and Zn(II) and calculated mobilities for Mg(II) and Ca(II). Conditions the same as Figure 15B. Symbols: Ca(II) $_{exp}$ (⊡), Ca(II) $_{cal}$ (◆), Mg(II) $_{exp}$ (◇), Mg(II) $_{cal}$ (□), and Zn(II) (■).

If equation 14 is a valid description of electrophoretic mobility for this method, then it should be possible to predict mobilities from basic equilibrium equations and a minimum of experimental data. This will allow the adjustment of conditions to optimize separation conditions. By invoking several assumptions, the individual mobilities of the components of the metal-ligand bands can be indirectly determined. First, the injected plug of sample is assumed to instantaneously reach equilibrium with the surrounding electrophoretic buffer. Second, while the distribution between the various forms of the metal influences peak shape and efficiency, the overall mobility of the band can be determined by the retention time of the peak's maximum. Third, the observed mobility of the band is only a function of the metal and metal-HQS^- complexes (i.e. other equilibria are insignificant). Finally, the mole fraction of the metal ion in the band is equal to the mole fraction of each component under equilibrium conditions for a given pH and HQS^- concentration.

Using these assumptions, the equilibrium expression for each metal, mass balance equations, and the data in Figure 17, it is possible to calculate the mobility of each of the components of the band. This was done by simultaneously solving equation 14 for each of the data points on the Ca(II) and Mg(II) curves of Figure 17. Zn(II) cannot be similarly treated due to its high formation constant, which is not compatible with our iterative calculation method. The mobilities of the differing components of the Mg(II) and Ca(II) band are shown in Table 7, as well as the calculated mobilities for each

TABLE 7.

EXPERIMENTAL AND CALCULATED MOBILITIES OF Ca(II) AND Mg(II) BANDS IN FIGURE 17 AND MOBILITIES OF BAND COMPONENTS

[HQS^-] (mM)	$\mu_{Ca(II)\ exp}$ (cm^2/skV)	$\mu_{Ca(II)\ cal}$ (cm^2/skV)	$\mu_{Mg(II)\ exp}$ (cm^2/skV)	$\mu_{Mg(II)\ cal}$ (cm^2/skV)
0.5	0.28	0.36	0.06	0.07
1.0	0.28	0.29	0.01	-0.01
2.5	0.20	0.19	-0.20	-0.19
10.0	0.08	0.09	-0.37	-0.36
		$\mu_{Ca(II)\ free} = 0.455$		$\mu_{Mg(II)\ free} = 0.09$
		$\mu_{Ca(HQS)} = 0.045$		$\mu_{Mg(HQS)} = 0.08$
				$\mu_{Mg(HQS)_2} = -0.436$

Separation conditions are the same as in Figure 1A. Experimental mobilities were calculated using equation 4. Calculated mobilites of the various components of each band and the overall mobility were determined using using equations 1, 2 and 3 and formation constants from references 13 and 14.

HQS^- concentration. These mobilities agree well with the qualitative description of Figures 17 and 18.

In order to illustrate the prediction capabilities of this treatment, the mobilities of the various species were used to calculate the Ca(II) and Mg(II) band mobilities at the various electrophoretic buffer pH values discussed above. Calculated mobilities are shown in Figure 18 and represent a reasonable approximation of the experimental data. The relatively poor fit of the data points at pH 6 and 7 on the Ca(II) curve are probably a result of interactions of Ca(II) with other components in the electrophoretic buffer. At these pH values the conditional formation constant for the $Ca(HQS^-)$ complex is very low while the formation constant for $CaHPO_4$ is reasonably large (147). The formation of these complexes would reduce the mole fraction of free Ca(II) in the band and thereby the electrophoretic mobility of the band.

Band Broadening

Since quantitative measurements in this work were performed using peak height, and resolution is a function of efficiency, the issue of peak efficiency needs to be addressed. As stated previously, band broadening in CZE results from molecular diffusion, temperature gradients, wall-solute interactions and injection and detection effects. In this method, the existence of various species in a single band which have different mobilities and the concomitant possibility of nonequilibrium conditions, can also result in band broadening. While molecular diffusion is not strongly dependent on

equilibrium conditions, the other sources of band broadening can be significantly reduced if the proper electrophoretic buffer conditions are employed. The Mg(II) peaks shown in Figure 15 will be used to illustrate the influences of certain electrophoretic buffer parameters on efficiency. It should be noted that the two studies in this figure were performed with different metal concentrations, lengths of capillary, and laser intensities.

Considering first the effect of HQS^- concentration in the electrophoretic buffer, a general increase in plate number is observed with increasing concentration. This is probably a result of two effects. High HQS^- to metal ion ratios force the complexation reaction toward completion, thereby reducing the mole fractions of free metal ion and partially complexed metal. Also high HQS^- concentrations quickly force the sample plug into equilibrium with the surrounding buffer so nonequilibrium band broadening is reduced. At 0.5 mM the equilibrium mole fractions of Mg(II) and its complexes are 0.36, 0.60 and 0.04 for the free metal ion, 1:1 and 1:2 complexes, respectively, while at 10 mM the fractions of free metal ion and 1:1 complex are greatly reduced (to 10^{-4} and 0.14) and the 1:2 complex is predominant (0.86). Therefore, band broadening from the existence of species within the band that possess different mobilities is reduced. As stated above, the high concentration of HQS^- in the electrophoretic buffer facilitates the rapid establishment of equilibrium following sample injection. This prevents the band from containing regions of differing HQS^- concentration during the early moments of the experiment. If these

regions exist, then each will have a different overall mobility, as determined by equations 11 and 13, and band broadening will result. Although high concentrations result in good equilibrium conditions, the current passed through the capillary is greatly increased, which can result in band broadening.

Control of the pH of the electrophoretic buffer can also improve the efficiency of eluting bands. In Figure 15B there is a decrease in efficiency as the pH of the electrophoretic buffer is increased. Again this is a result of more than one effect; the existence of differing species in the band and slow exchange kinetics between forms. At neutral pH the 1:1 complex of Mg(II) predominates (X_{ML} = 0.71), while the other two forms exist in much lower quantities, so band broadening due to differing species is reduced. Also, the low α value at this pH reduces the conditional formation constants for the various complex forms and increases the kinetics of exchange between forms. If the conditional formation constant is considered to be proportional to the ratio of formation to disassociation reaction rates, then as the constant is reduced the difference between these rates becomes smaller, the exchange between the various forms occurs more frequently and nonequilibrium band broadening is reduced (149). Increasing the pH to 8 results in the existence of both the 1:1 and 1:2 complexes of Mg(II) in appreciable amounts (X_{ML} =0.38, X_{ML_2} = 0.60) and the rate of exchange between the various forms is reduced, so plate height is increased. For example, the plate number for Mg(II) is reduced from 108,000 to 86,000 per meter when the pH is increased from 7 to 8.

By further increasing the pH, the mole fraction of the 1:1 complex is reduced but still remains significant (0.18) and is still fairly broad (N = 86,000 per meter).

Since the existence of multiple species within each band is probably the greatest source of band broadening, it should be examined in greater detail. Along with the formation of metal HQS-complexes, other electrophoretic buffer components or sample components can interact with the metal ion. As stated previously, the phosphate ions in the electrophoretic buffer can form complexes with Ca(II) or the other test metals. Furthermore, under the alkaline conditions employed in this work the formation of metal hydroxides is also likely. The formation of mixed complexes will exacerbate this problem by creating a larger number of possible complexes. The poor efficiency of the Zn(II) peak at pH = 9 in Figure 15B is probably a result of the formation of numerous complexes due the the high formation constant for hydroxide complexes at this pH. Also, if the sample contains strong chelating agents, it is possible that they will compete with the HQS^- for the metal ion or prevent its interaction (see earlier discussion Zn(II) in blood serum). This would affect both the observed mobility of the peak and its fluorescence signal.

In conclusion on-column chelation reactions can be used for the detection and separation of metal ions in CZE. This method provides good detectability, two modes of mobility manipulation, and can be easily understood by examining basic stoichiometric and equilibrium relationships. In the future, the investigation of other

possible fluorescent chelation agents could improve the utility of this methods. For example, lanthanide metals could be detected using beta diketone derivatives as chelating agents. Furthermore the ability of this method to manipulate electrophoretic mobility could be used in conjunction with other detection schemes to improve resolution. One possible application could the use of on-column chelation to improve separation of radioactive metals ions in conjunction with radiochemical detection.

CHAPTER 6

FLUOROMETRIC PHOTODIODE ARRAY DETECTION IN CAPILLARY ELECTROKINETIC SEPARATIONS

The minute band volumes of CZE and MECC require a detection scheme with very high mass sensitivity. As shown in the previous chapters laser-based fluorometric detection combined with the use of fluorescent labels can provide the necessary sensitivity. However, the detection of a mixture of native fluorophores can be somewhat more complicated. Sensitivity in fluorometric detection is maximized when optimum excitation and emission wavelengths are employed. In laser-based fluorometric detection the choice of excitation wavelength is often limited by available lasers. This is not a problem when fluorescent labels are employed, as the label can be chosen such that its absorption bands match available laser wavelengths. Choice of laser wavelength for the detection of several native fluorophores can be more difficult, since each component in the mixture will have different excitation spectra. Therefore, excitation must be performed at a wavelength that results in the maximum overall sensitivity for the entire mixture. This often results in the excitation of one or more components in the mixture at nonoptimum wavelengths. Nevertheless, the high power of laser beams can result in high sensitivity even when excitation is performed at nonoptimum wavelengths.

Likewise when detection is performed at a single wavelength, choice of emission wavelength must be made to maximize sensitivity for the entire mixture. Therefore, not all components in the mixture are detected at their emission maxima. Again, this problem is reduced when fluorescent labels are employed, since labeled compounds tend to emit in a relatively small wavelength range. However, the detection of native fluorophores can require detection at several different wavelengths to maximize detectability for every compound. In addition, the emission maxima of many compounds are dependent on experiment parameters, such as pH and solvent polarity (89). So changes in experimental parameters to improve separation can have deleterious effects on detection by causing a compound to shift its fluorescence maximum away from the detection wavelength.

One way to correct for these problems is to collect the entire fluorescence spectrum for each eluting compound. This allows the detection of each species at its emission maxima. Furthermore, the emission bandpass can be controlled to enhance sensitivity. Finally, by proper choice of emission wavelength and band pass, it can be possible to discriminate against compounds that are coeluting with the compound of interest.

Fluorescence spectra can be collected using a high speed scanning monochromator with a single detector or a multichannel detection scheme. Lee *et al.* modified a commercial fluorimeter to repeatedly scan emission from the eluent of a super critical fluid column (150). As the scan rate must very high to prevent detector

related band broadening, this method can be difficult to apply to separation methods with very narrow bands (recall from Chapter 2 that detector time constants in these methods should be approximately 0.1 seconds). Multichannel detectors, such as photodiode arrays and charge coupled devices, are more capable of rapidly recording fluorescence spectra. Furthermore, since multichannel detectors observe all wavelengths simultaneously, the time that each wavelength is observed is increased, as compared to a scanning system, without resulting in detector related band broadening (89). This increases fluorescence S/N, as it varies with the square root of the observation time. Charge coupled devices (CCD) are very efficient multichannel detectors with low readout noise levels; however, in the one report in the literature using a CCD a very slow scan rate (6 seconds per scan) had to be employed (151). This resulted in only a few data points per peak which can result in improper visualization of the separation (152, 153).

Photodiode arrays can be scanned more rapidly so this problem is avoided. Novotony *et al.* used a linear intensified photodiode array to monitor the emission spectra of polyaromatic hydrocarbons eluting from a slurry packed capillary column (154). They employed a conventional light source and illustrated the advantages of multichannel detection in the separation of complex samples. The remainder of this chapter describes a simple laser-based fluorescence photodiode array detector for capillary electrokinetic separations. This detector permits the collection of three dimensional (wavelength/intensity/time), total fluorescence, or

selected spectral region(s) chromatograms. The ability of this detector to enhance detectability and selectivity in electrokinetic separations is demonstrated. In particular, the simultaneous collection of a series of limited spectral region chromatograms can improve selectivity relative to a total fluorescence chromatogram because of the spectral information available. Furthermore, the ability of this detector to improve the analysis of very hydrophobic compounds in MECC is discussed.

Experimental

Separations were performed in an untreated 50 μm i.d. x 39 cm untreated fused silica capillary from Polymicro Technologies (Phoenix, AZ) that was flushed with mobile phase for 30 minutes before the first injection. Samples were injected hydrodynamically and injection volumes were determined by continuous injection. Excitation was performed using the Liconix 4230NB helium-cadmium laser described previously, operating at 442 nm (30 mW). Emission was collected at a 90° angle from excitation and collimated by a 4 cm diameter, f/1 quartz lens, then focused by 4 cm diameter, f/3 quartz lens, onto the entrance slits of a Spex 1681 spectrometer (Spex Industries, Edison, NJ) that dispersed the emission across the diode array (Figure 19). The entrance slit of the spectrometer was set at 1 mm, which prevented specular scatter from reaching the photodiodes.

Detection was accomplished using a Tracor Northern TN 6100 photodiode array (Middleton, WI). Photocurrents were processed by a

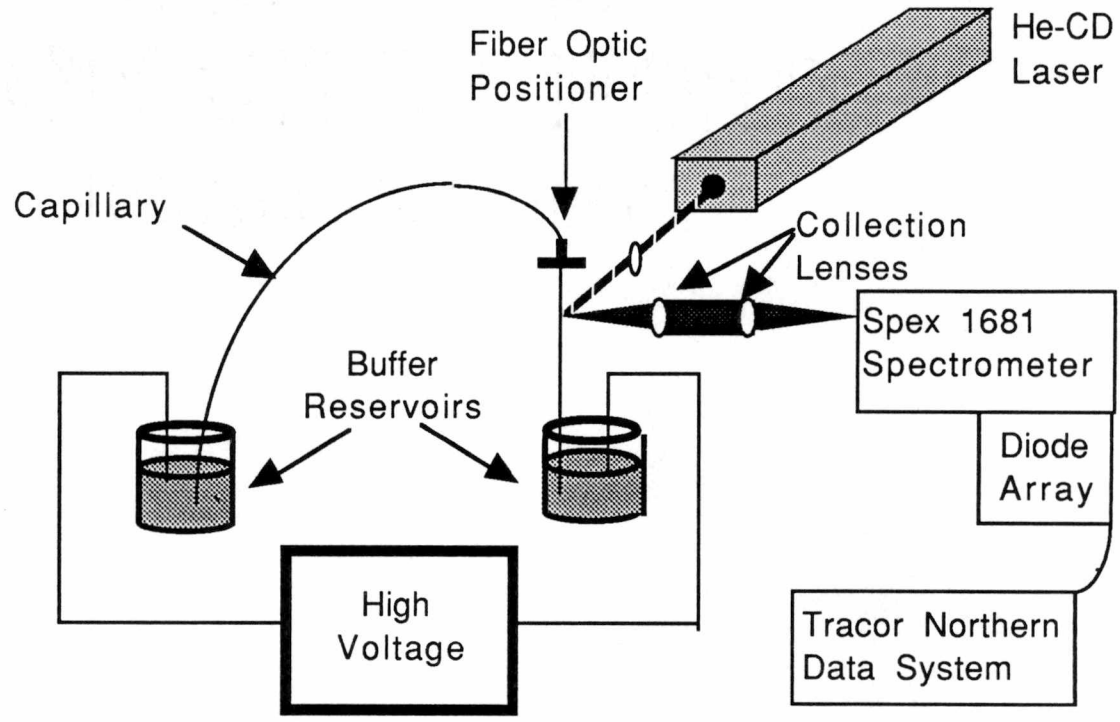

Figure 19. Depiction of laser-based fluorometric diode array detection scheme.

TN 6500 Controller/Analyzer. The unintensified 1024 diode array was operated at the lowest possible resolution (16 diodes per channel) to reduce memory requirements, which resulted in a spectral resolution of approximately 4 nm per channel. The spectral region observed by the diode array was approximately 460 to 715 nm. Calibration data was collected in the histogram mode to further reduce memory requirements. This mode of operation integrates over previously declared spectral regions and displays the integral versus time resulting in a selected spectral-region chromatogram. Data for selectivity and bandpass studies were collected as a series

of fluorescence spectra, one scan every 0.2 seconds, from which selected spectral region chromatograms were later produced.

Peak areas were determined using the net integration mode of the TN 6500 after manually declaring the boundaries of the peak. Peak heights and baseline noise were found by digitizing a 5 second section of the histogram before and after the peak. The peak height was the maximum peak intensity minus the average of the baseline. The noise was the standard deviation of the digitized background.

Mobile phases were 0.05 M sodium dodecyl sulfate (Sigma Chemical Co., St. Louis, MO), 10 mM Na_2HPO_4, 6 mM $Na_2B_4O_7$ in triply distilled deionized water. Separations were performed on a mixture composed of a charged solute, sodium fluorescein, and two neutral laser dyes, Coumarin 102 and 4-(Dicyanomethylene)-2-methyl-6-(p-dimethylaminostyryl)-4H-pyran (DCM) from Eastman Kodak Company (Kingsport, TN).

Results and Discussion

Calibration curves (Figure 20) for sodium fluorescein were constructed using both peak area and peak height. A scan time of 0.1 second was used to prevent detector time constant related band broadening. This resulted in a minimum of 15 data points per peak. These calibration curves exhibit good linearity from 1.23×10^{-7} M to 1.23×10^{-4} M, with correlation coefficients of 0.997 and 0.984 for peak area and peak height, respectively. The poor fit of the lowest concentration peak height data point is a result of a large increase in peak efficiency. Tailing, which occurs at concentrations

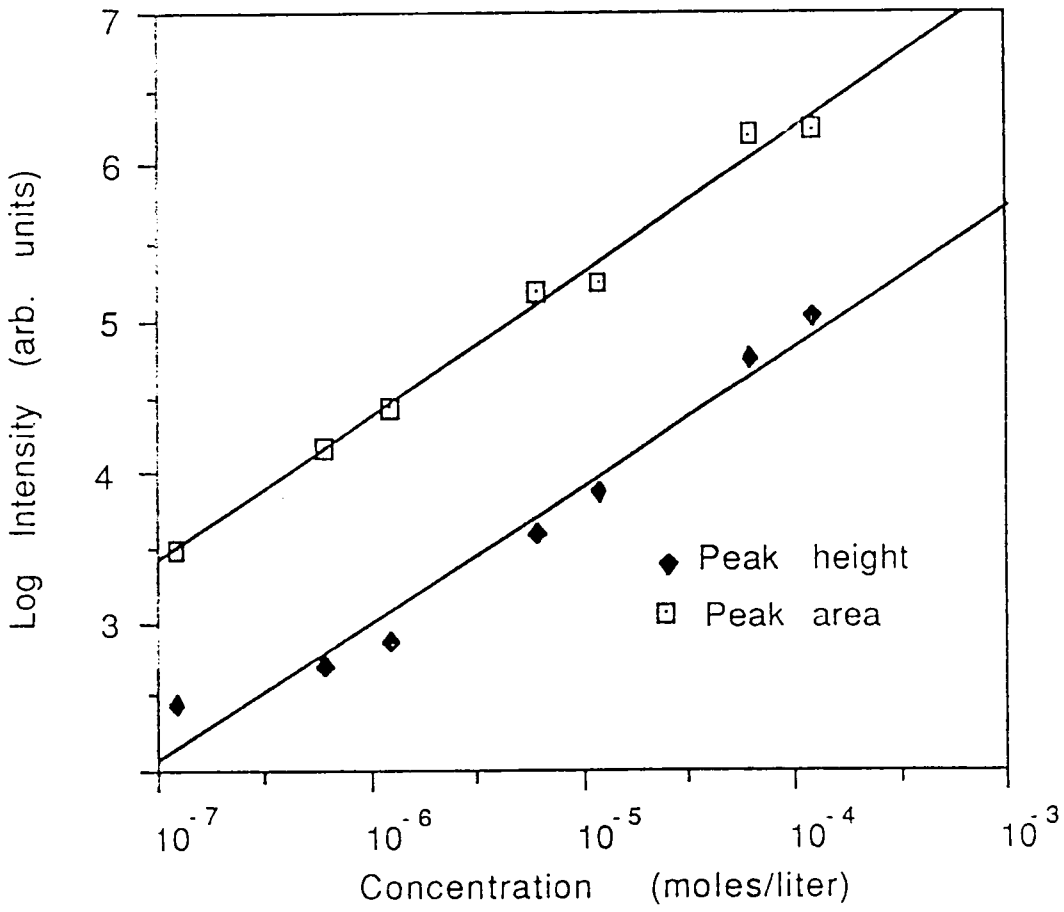

Figure 20. Calibration curves for sodium fluorescein. Conditions: 10 mM Na_2HPO_4 / 6 mM Na_2B4O_7 buffer, 50 mM SDS, 50 µm i.d. x 39 cm capillary, 512 V/cm.

higher than 5 x 10^{-7} M (possibly because of interactions with the wall of the capillary or local distortions in the electric field), is no longer observed and the number of theoretical plates per meter increased dramatically from 50,000 to 125,000. The relatively poor efficiency is caused primarily by the large injection volume. The injection volume was made large to illustrate the selectivity advantage of multichannel detection (see later discussion).

The injection volume employed was 3.4 nL (a 1.7 mm injection length). This resulted in a minimum injectable amount (S/N = 2) of less than 60 femtograms (159 attomoles) of sodium fluorescein. This compares favorably to the LOD reported for the intensified photodiode array detection scheme mentioned above; however it is higher than the LOD of the aforementioned CCD detection scheme (4 attomoles of sodium fluorescein). Significant reductions in minimum detectable amount would be expected if an intensified photodiode array. Typically, intensified arrays have a gain that is 10^3 to 10^4 greater than standard arrays (89).

Careful designation of spectral bandpass can be used to maximize S/N ratio. Integrating the wavelength/intensity/time chromatogram in Figure 21 over a series of bandwiths centered at 514 nm results in a maximum S/N ratio for the sodium fluoroscein peak when a bandpass of 40 nm is used (see Figure 22). This value is approximately the full width at half maximum of the fluorescence emission spectrum of sodium fluoroscein. This suggests that in separating a mixture with a limited memory instrument, a series of optimized bandpass chromatograms collected simultaneously across

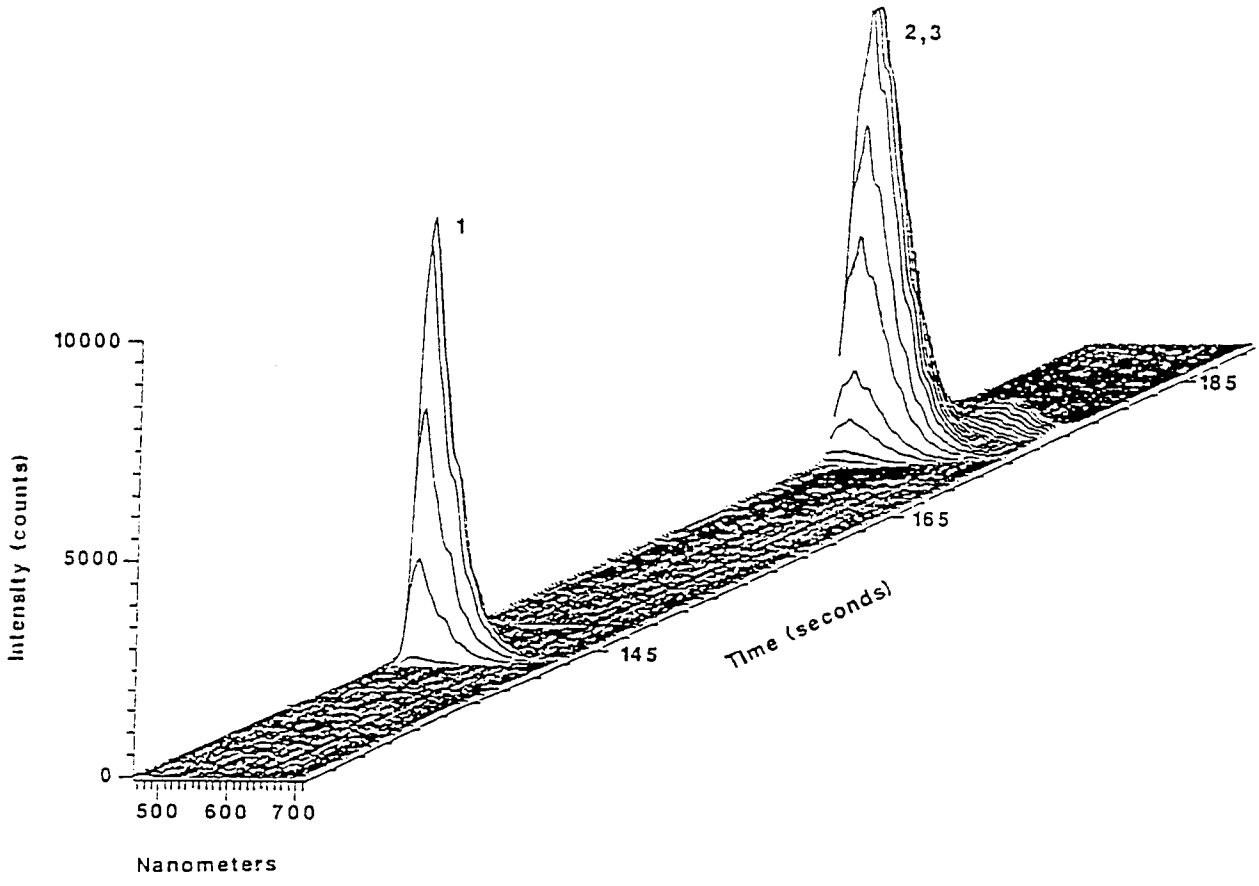

Figure 21. Wavelength/intensity/time chromatogram for: 1. sodium fluorescein, 2. Coumarin 102, and 3. DCM. Same conditions as Figure 20.

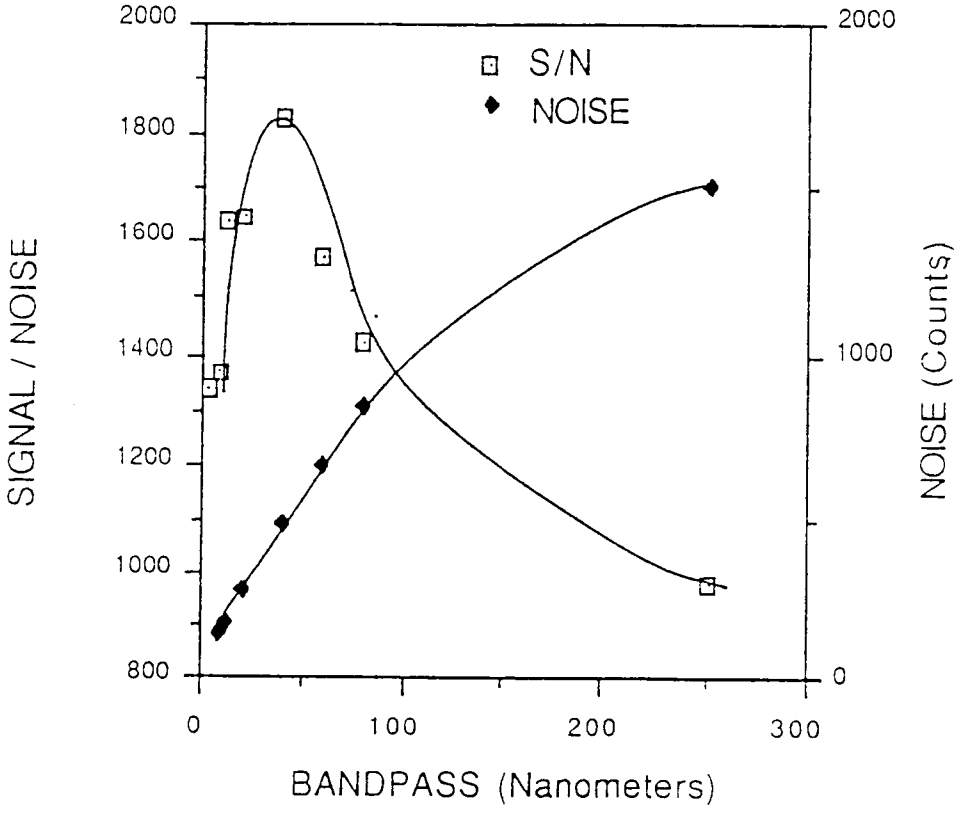

Figure 22. Signal to noise ratio and noise for the sodium fluorescein peak in Figure 21 as a function of bandpass.

the entire spectral range would result in a greater S/N ratio for every solute in a mixture than a total fluorescence chromatogram.

Hydrophobic compounds (i.e. compounds with large capacity factors, *k*'s) are not resolved easily by MECC without extending the elution range by adding organic solvents to the buffer. However, in most cases, addition of organic solvents greatly increases analysis time by reducing electroosmotic flow. If these compounds could be resolved spectrally, the need for organic solvents could be reduced or eliminated. Certain spectral regions of the wavelength/intensity/time chromatogram in Figure 21 can be integrated to produce selected spectral region chromatograms. If these regions are chosen correctly, both resolution and S/N ratio can be maximized. Figure 23a is the total fluorescence chromatogram of sodium fluorescein, Coumarin 102, and DCM. The Coumarin 102 and DCM coelute at the retention time of the micellar phase, t_m (34, 75). Using a 20 nm bandpass centered at 496 nm, a chromatogram is obtained (Figure 23b) that exhibits a good signal to noise for sodium fluorescein and Coumarin 102 without any interference from the DCM. Conversely, DCM can be determined by using a 20 nm region of integration at 685 nm without interference from Coumarin 102 (Figure 23c). From these two selected bandpass chromatograms it can be seen that the Coumarin 102 and DCM do not exactly coelute, but differ in retention time by 5 seconds. Due to the limited memory of this experimental apparatus, separations with long elution ranges preclude the storage of wavelength/intensity/time chromatograms. The same selectivity advantages can be achieved, however, by the

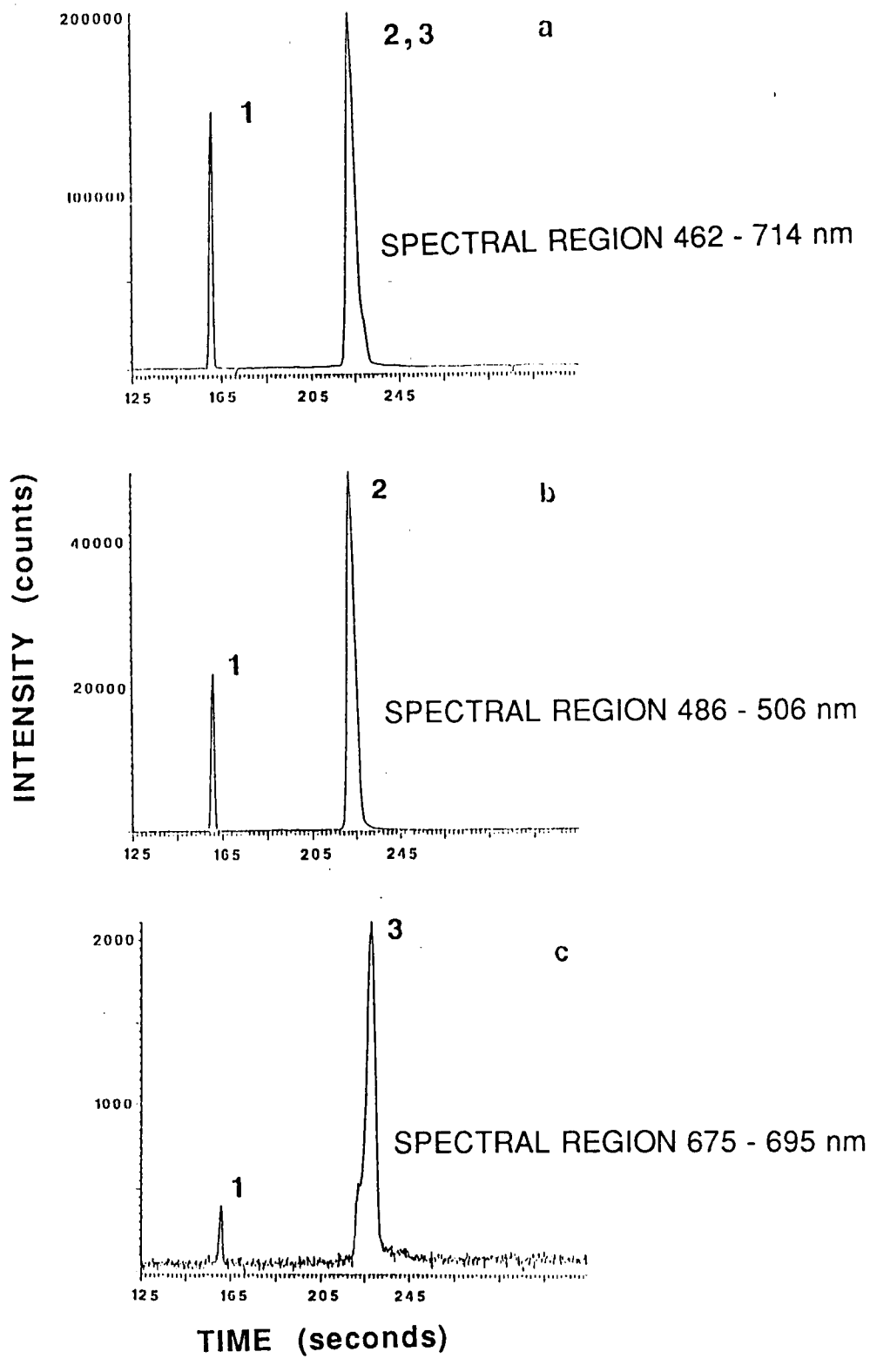

Figure 23. Selected spectral region chromatograms for the compounds in Figure 21.

simultaneous collection of a series of small bandpass histograms that cover the entire spectral range.

In conclusion the ability to optimize emission wavelength and bandpass using multichannel detection can improve detectability and the resolving power of capillary electrokinetic separation methods. Future work should include the investigation of intensified diode arrays and fast scanning CCDs to improve detectability. Furthermore, the ability of this detection method to improve the analysis of very hydrophobic compounds in complex mixtures by MECC, such as polyaromatic hydrocarbons in shale oil, should be examined.

CHAPTER 7

CONCLUSIONS

Although specific conclusions were presented in each chapter there are several general conclusions that can be reached from this work. Laser-based fluorescence is one of the most sensitive detection schemes that has been applied to capillary electrokinetic separation methods. However, the application of this method is limited by available fluorophores and convenient laser systems. Presented in this dissertation were three detection schemes that improve the applicability of this method. The use of fluorescent labels can improve the utility of this method as they permit the detection of nonfluorescent species and can be chosen to match available lasers. However, the use of covalent labeling reactions can increase the complexity of electropherograms due to inhomogeneous labeling of sample components. The use of noncovalent labeling reactions can reduce these effects. Furthermore if the labeling reaction produces a fluorescent compound from relatively nonfluorescent reactants, the labeling reaction can be performed during the separation process. Finally, on-column labeling does not require time consuming sample preparation or the use of a post-column reactor.

Sensitivity and detectability in on-column labeling methods are dependent on the extent of the reaction, the increase in quantum efficiency upon reaction, and the fluorescence background of

unreacted label. Although labeling reactions with large forward rate constants result in large fluorescent signals, band broadening can occur due to slow kinetics in the labeling reaction. Since sensitivity is determined by the change in fluorescent signal due to the labeling reaction, large changes (i.e. from completely nonfluorescent to a quantum efficiency near unity) are desirable. The use of large concentrations of labeling reagents, to enhance the labeling reaction, can result in a large fluorescence background due to a small inherent quantum efficiency or labeling of impurities in the buffer. Large fluorescence backgrounds are undesirable as they increase the baseline noise and reduce detectability.

In this work on-column labeling methods have been used for the detection of proteins, surfactants, and metal ions. In the case of proteins, on-column labeling permits fluorometric detection without degrading the integrity of the band and is compatible with the use of very small diameter capillaries. Likewise on-column labeling permitted the detection of surfactants that do not possess strong chromophores. Finally, by employing a chelation reaction which produced a fluorescent species, the analysis of metal ions was be performed by CZE. Furthermore, since the chelation reaction altered the electrophoretic mobility of the metal, a model for predicting mobility was presented.

Multichannel detection can also improve the applicability of laser-based fluorometric detection. Collection of the entire fluorescence spectrum for eluting compounds permits the optimization of emission wavelength and bandpass for both

sensitivity and detector selectivity. Moreover if the collection of the entire fluorescence spectrum is precluded by a limited memory instrument, sensitivity can be improved by the collection of a series of optimum bandpass electropherograms. Finally the added selectivity of multichannel detection can be used to enhance the selectivity ofthese methods and permit the quantitation of coeluting species. Although this work employed a relatively simple sample, the utility of multichannel detection for these separation methods has been demonstrated. In the future, multichannel detection will surely improve the applicability of MECC and CZE for the analysis of extremely complex samples.

LITERATURE CITED

LITERATURE CITED

(1) Jorgenson, J. *Overview of Electrophoresis* in New Directions in Electrophoretic Methods; Jorgenson, J. W. , Marsha, P. Eds.; American Chemical Society: Washington D.C., Vol. 335, 1987, p 275.

(2) Reuss, F. F. *Memoires de la Societe Imperiale des Naturalistes de Moscou* **1809**, *2*, 324.

(3) Tiselius, A. *Trans. Faraday Soc.* **1937**, *33*, 524.

(4) Righetti, P.; Oss, C. V.; Vanderhoff, J.*Introduction - Brief Historical Survey* in Electrokinetic Separation Methods; Righetti, P., Oss, C. V. , Vanderhoff, J. Eds.; Elsevier/North-Holland Biomedical Press: Amsterdam, 1979, p vii-xiii.

(5) Vesterberg, O. *J. Chromatogr.* **1989**, *480*, 3.

(6) Dunn, M. J. *Electrophoresis in Polyacrylamide Gels* in New Directions in Electrophoretic Methods; Jorgenson, J. W. , Marsha, P. Eds.; American Chemical Society: Washington D. C., Vol. 335, 1987, p 275.

(7) Verheggen, T.; Mikkers, F.; Everaerts, F. *J. Chromatogr.* **1977**, *132*, 205.

(8) Mikkers, F.; Everaerts, F.; Verheggen, T. *J. Chromatogr.* **1979**, *169*, 11.

(9) Jorgenson, J.; Lukas, K. *Anal. Chem.* **1981**, *53*, 1298.

(10) Jorgenson, J.; Lukacs, K. *J. Chromatogr.* **1981**, *218*, 209.

(11) Wu, S.; Dovichi, N. *J. Chromatogr.* **1989**, *480*, 1441.

(12) Zare, R. N.; Burgi, D. S.; Haung, X.; Pentoney, S. L. *Anal. Chem.* **1988**, *60*, 2625.

(13) Yeung, E. S.; Christensen, P. L. *Anal. Chem.* **1989**, *61*, 1344.

(14) Yeung, E. S.; Kuhr, W. G. *Anal. Chem.* **1988**, *60*, 2642.

(15) Burton, D. E.; Sepaniak, M. J.; Maskarinec, M. P. *J. Chromatogr. Sci.* **1986**, *24*, 347.

(16) Kuhr, W. G.; Yeung, E. S. *Anal. Chem.* **1988**, *60*, 2642.

(17) Sepaniak, M. J.; Swaile, D. F. *J. Microcol. Sep.* **1989**, *1*, 155.

(18) Wallingford, R. A.; Ewing, A. G. *J. Chromatogr.* **1988**, *441*, 299.

(19) Wallingford, R. A.; Curry, P. D.; Ewing, A. G. *J. Microcol. Sep.* **1989**, *1*, 23.

(20) Wallingford, R. A.; Ewing, A. G. *Anal. Chem.* **1988**, *60*, 1972.

(21) Wallingford, R. A.; Ewing, A. G. *Capillary Electrophoresis* in Advances in Chromatography; Giddings, J. C., Gruska, E. , Brown, P. Eds.; Marcel Dekker Inc.: New York and Basel, Vol. 29, 1989, p 1.

(22) Smith, R.; Loo, J.; Barinaga, C.; Edmonds, C.; Udseth, H. *J. Chromatogr.* **1989**, *480*, 211.

(23) Caprioli, R.; Moore, W.; Martin, M.; DaGue, B.; Wilson, K.; Moring, S. *J. Chromatogr.* **1989**, *480*, 247.

(24) Rose, D.; Jorgenson, J. *Anal. Chem.* **1988**, *60*, 642.

(25) Dose, E.; Guiochon, G. *Anal. Chem.* **1991**, *63*, 1157.

(26) Hjerten, S. *J. Chromatogr.* **1985**, *347*, 191.

(27) McCormick, R. M. *Anal. Chem.* **1988**, *60*, 2322.

(28) Poppe, H.; Bruin, G. J. M.; Chang, J. P.; Kuhlman, R. H.; Zegers, K. *J. Chromatogr.* **1989**, *471*, 429.

(29) Dougherty, A. M.; Woolley, C. L.; Williams, D. L.; Swaile, D. F.; Cole, R. O.; Sepaniak, M. J. *J. Liq. Chromatogr.* **1991**,*14*, 907.

(30) Hjerten, S.; Elenbring, K.; Kilar, F.; Liao, J.-L.; Chen, A. J. C.; Siebert, C. J. *J. Chromatogr.* **1987**, *403*, 47.

(31) Cohen, A.; Nagarian, D.; Smith, J.; Karger, B. *J. Chromatogr.* **1988**, *458*, 323.

(32) Cohen, A.; Karger, B. *J. Chromatogr.* **1987**, *397*, 409.

(33) Terabe, S.; Isemura, T. *Anal. Chem.* **1990**, *62*, 650.

(34) Balchunas, A. T.; Sepaniak, M. J. *Anal. Chem.* **1988**, *60*, 617.

(35) Terabe, S.; Otsuka, K.; Ichikawa, K.; Tsuchiya, A.; Ando, T. *Anal. Chem.* **1984**, *56*, 111.

(36) Bushey, M.; Jorgenson, J. *J. Chromatogr.* **1989**, *480*, 301.

(37) Hjerten, S.; Valtcheva, L.; Elenering, K.; Eaker, D. *J. Liq. Chromatogr.* **1989**, *12*, 2471.

(38) Karger, B.; Cohen, A.; Guttman, A. *J. Chromatogr.* **1989**, *492*, 585.

(39) Lauer, H. H.; McManigill, D. *Anal. Chem.* **1986**, *58*, 166.

(40) Grossman, P. D.; Colburn, J. C.; Lauer, H. H.; Nielsen, R. G.; Riggin, R., M.; Sittampalm, G. S.; Rickard, E. C. *Anal. Chem.* **1989**, *61*, 1186.

(41) Cohen, A. S.; Terabe, S.; Smith, J. A.; Karger, B. L. *Anal. Chem.* **1987**, *59*, 1021.

(42) Balchunas, A. T.; Swaile, D. F.; Powell, A. C.; Sepaniak, M. J. *Sep. Sci. Technol.* **1988**, *23*, 1891.

(43) Swaile, D. S.; Burton, D. E.; Balchunas, A. T.; Sepaniak, M. J. *J. Chromatogr. Sci.* **1988**, *26*, 406.

(44) Terabe, S.; Otsuka, K.; Ando, T. *Anal. Chem.* **1985**, *57*, 834.

(45) Dobashi, A.; Ono, T.; Hara, S.; Yamaguchi, J. *J. Chromatogr.* **1989**, *480*, 413.

(46) Dobashi, A.; Ono, T.; Hara, S.; Yamaguchi, J. *Anal. Chem.* **1989**, *61*, 1984.

(47) Gassmann, E.; Kou, J.; Zare, R. *Science* **1985**, *230*, 813.

(48) Nishi, H.; Fukuyama, T.; Matsuo, M.; Terabe, S. *J. Microcol. Sep.* **1989**, *1*, 234.

(49) Nishi, H.; Fukuyama, T.; Matsuo, M.; Terabe, S. *J. Chromatogr.* **1990**, *515*, 233.

(50) Otsuka, K.; Terabe, S. *J. Chromatogr.* **1990**, *515*, 221.

(51) Terabe, S.; Shibata, M.; Miyashita, Y. *J. Chromatogr.* **1989**, *480*, 403.

(52) Aguilar, M.; Huang, X.; Zare, R. N. *J. Chromatogr.* **1989**, *480*, 427.

(53) Gross, L.; Yeung, E. *Anal. Chem.* **1990**, *62*, 427.

(54) Saitoh, T.; Hoshino, H.; Yotsuyanagi, T. *J. Chromatogr.* **1989**, *469*, 175.

(55) Tsuda, T.; Nomura, K.; Nakagawa, G. *J. Chromatogr.* **1983**, *264*, 385.

(56) Amanka, L.; Scholl, J.; Kuhr, W. *Anal. Chem.* **1990**, *62*, 2189.

(57) Ewing, A.; Wallingford, R.; Olefirowicz, T. *Anal. Chem.* **1989**, *61*, 292.

(58) Knox, J.; Grant, I. *Chromatographia* **1987**, *24*, 135.

(59) Kirkland, J. J.; McCormick, R. M. *Chromatographia* **1987**, *24*, 58.

(60) Knox, J. H.; McCormack, K. A. *J. Liq. Chromatogr.* **1989**, *12*, 2435.

(61) Kuhr, W. G. *Anal. Chem.* **1990**, *62*, 403.

(62) Terabe, S.; Otsuka, K.; Ando, T. *J. Chromatogr.* **1985**, *332*, 219.

(63) Powell, A. C.; Sepaniak, M. J. *Paper 698* Pittsburgh Conference Atlanta, GA., 1989.

(64) Powell, A. C.; Sepaniak, M. J. *J. Microcol. Sep.* **1990**, *2*, 278.

(65) Sepaniak, M. J.; Burton, D. E.; Maskarinec, M. P. *Micellar Electrokinetic Capillary Chromatography* in Ordered Media in Chemical Separations; Hinze, W. L. , Armstrong, D. W. Eds.; American Chemical Society: Washington, D.C., Vol. 342, 1987, p 142.

(66) Sepaniak, M. J.; Cole, R. O. *Anal. Chem.* **1987**, *59*, 472.

(67) Sepaniak, M. J.; Swaile, D. F.; Powell, A. C. *J. Chromatogr.* **1989**, *480*, 185.

(68) Sepaniak, M. J.; Swaile, D. F.; Powell, A. C.; Cole, R. O. *JHRC & CC* **1990,** *13,* 679.

(69) Swaile, D. F.; Sepaniak, M. J. *J. Microcol. Sep.* **1989**, *1*, 155.

(70) Hoyt, A.; Sepaniak, M. *Anal. Lett.* **1989**, *22*, 861.

(71) Gorse, J.; Balchunas, A. T.; Swaile, D. F.; Sepaniak, M. J. *JHRC & CC* **1988**, *11*, 554.

(72) Cole, R. O.; Sepaniak, M. J.; Hinze, W. L. *JHRC & CC* **1990**,*13*, 579.

(73) Burton, D. E.; Sepaniak, M. J.; Maskarinec, M. P. *J. Chromatogr. Sci.* **1987**, *25*, 514.

(74) Burton, D. E.; Sepaniak, M. J.; Maskarinec, M. P. *Chromatographia* **1986**, *21*, 583.

(75) Balchunas, A. T.; Sepaniak, M. J. *Anal. Chem.* **1987**, *59*, 1466.

(76) Overbeek, J.; Bijsterbosch, B. *The Electrical Double Layer and the Theory of Electrophoresis* in Electrokinetic Separation Methods; Righetti, P., Oss, C. V. , Vanderhoff, J. Eds.; Elsevier/North-Holland Biomedical Press: Amsterdam, 1979, p 1.

(77) Pretorius, V.; Hopkins, B.; Schieke, J. *J. Chromatogr.* **1974**, *99*, 23.

(78) Bard, A. J.; Faulkner, L. R. *Electrochemical Methods*; John Wiley &Sons: New York, 1980; Chapter 12.

(79) Fujiwara, S.; Honda, S. *Anal. Chem.* **1987**, *59*, 487.

(80) Lambert, W.; Middleton, D. *Anal. Chem.* **1990**, *62*, 1585.

(81) Jorgenson, J. W.; Rose, D. J., Jr. *J. Chromatogr.* **1988**, *447*, 117.

(82) Bocek, P.; Foret, F.; Deml, M.; Kahle, V. *Electrophoresis* **1986**, *7*, 430.

(83) Nakagawa, G.; Nomura, K.; Tuda, T. *J. Chromatogr.* **1982**, *248*, 241.

(84) Jorgenson, J.; Wahlbroehl, Y. *J. Chromatogr.* **1984**, *315*, 135.

(85) Green, J.; Jorgenson, J. *J. Chromatogr.* **1986**, *352*, 337.

(86) Green, J. S.; Jorgenson, J. W. *J. Liq. Chromatogr.* **1989**,*12*, 2527.

(87) Wallingford, R. A.; Ewing, A. G. *Anal. Chem.* **1988**, *60*, 258.

(88) Pentoney, S. L.; Zare, R. N.; Quint, J. F. *J. Chromatogr.* **1989**, *480*, 259.

(89) Ingle Jr., J. D.; Crouch, S. R. *Spectrochemical Analysis*; Prentice Hall: Englewood Cliffs, 1988; Chapter 5.

(90) Jorgenson, J.; Lukacs, K. D. *JHRC & CC* **1985**, *8*, 407.

(91) Huang, X.; Coleman, W.; Zare, R. *J. Chromatogr.* **1989**, *480*, 95.

(92) Altria, K.; Simpson, C. *Analytical Proceedings* **1986**, *23*, 453.

(93) Foret, F.; Fanali, S.; Ossicini, L.; Bocek, P. *J. Chromatogr.* **1989**, *470*, 288.

(94) Walbroehl, Y.; Jorgenson, J. *Anal. Chem.* **1986**, *58*, 479.

(95) Terabe, S.; Yashima, T.; Tanaka, N.; Araki, M. *Anal. Chem.* **1988**, *60*, 1673.

(96) Bushey, M. M.; Jorgenson, J. W. *J. Microcol. Sep.* **1989**, *1*, 125.

(97) Nickerson, B.; Jorgenson, J. *J. Chromatogr.* **1989**, *480*, 157.

(98) Nishi, H.; Tsumagari, N.; Kakimoto, T.; Terabe, S. *J. Chromatogr.* **1989**, *477*, 259.

(99) Otsuka, K.; Terabe, S.; Ando, T. *J. Chromatogr.* **1985**, *348*, 39.

(100) Otsuka, K.; Terabe, S.; Ando, T. *J. Chromatogr.* **1985**, *332*, 219.

(101) Terabe, S.; Otsuka, K.; Ichikawa, K.; Tsuchiya, A.; Ando, T. *Anal. Chem.* **1984**, *56*, 111.

(102) Jones, A.; Gruska, E. *J. Chromatogr.* **1989**, *466*, 219.

(103) Grushka, E.; McCormick, R.; J., K. *Anal. Chem.* **1989**, *61*, 241.

(104) Otsuka, K.; Terabe, S. *J. Chromatogr.* **1989**, *480*, 91.

(105) Grushka, E.; McCormick, R. *J. Chromatogr.* **1989**, *471*, 421.

(106) Wallingford, R. A.; Ewing, A. G. *Anal. Chem.* **1987**, *59*, 678.

(107) Tsuda, T.; Mizuno, T.; Akiyama, J. *Anal. Chem.* **1987**, *59*, 799.

(108) Huang, X.; Gordon, M.; Zare, R. *Anal. Chem.* **1988**, *60*, 375.

(109) Wang, T.; Champlin, P.; Hartwick, R. *J. Chromatogr.* **1989**, *462*, 147.

(110) Nishi, H.; Tsumagari, N.; Kakimoto, T.; Terabe, S. *J. Chromatogr.* **1989**, *465*, 331.

(111) Nishi, H.; Fukuyama, T.; Matsuo, M.; Terabe, S. *J. Chromatogr.* **1990**, *498*, 313.

(112) Steiner, R. F.; Weinryb, I. *Excited States of Proteins and Nucleic Acids*; Plenum Press: New York, 1971; Chapter 1.

(113) Martin, M.; Guiochon, G.; Walbroehl, Y.; Jorgenson, J. *Anal. Chem.* **1985**, *57*, 559.

(114) Jorgenson, J.; Lukas, K. *Science* **1983**, *222*, 226.

(115) Mikkers, F.; Everaerts, F.; Verheggen, T. *J. Chromatogr.* **1979**, *169*, 1.

(116) Williams, J.; Elleman, T.; Kingston, I.; Wilkins, A.; Kuhn, K. *Eur. J. Biochem.* **1982**, *122*, 297.

(117) Edelman, G.; McClure, W. *Acc. Chem. Res.* **1968**, *1*, 65.

(118) Brand, L.; Gohlke, J. *Annu. Rev. Biochem.* **1972**, *41*, 843.

(119) Chakrabarti, S.; Ware, W. *J. Chem. Phys.* **1971**, *55*, 5494.

(120) Brand, L.; Gohlke, J. *J. Biol. Chem.* **1971**, *246*, 2317.

(121) Camerman, A.; Jensen, L. *J. Amer. Chem. Soc.* **1970**, *92*, 550.

(122) Turner, D.; Brand, L. *Biochemistry* **1968**, *7*, 3381.

(123) Hinze, W. *Organized Surfactant Assemblies in Separation Science* in Order Media in Chemical Separation; Hinze, W. L., Armstrong, D. W. Eds.; American Chemical Society: Washington, D.C., Vol. 342, 1987, p 2.

(124) Dorsey, J. *Chromatographic Capabilites of Micellar Mobile Phases* in Ordered Media in Chemical Separations; Hinze, W. L., Armstrong, D. W. Eds.; American Chemical Society: Washington, D.C., Vol. 342, 1987, p105.

(125) Hatton, T. *Extraction of Proteins and Amino Acids using Reverse Micelles* in Ordered Media in Chemical Separations; Hinze, W. L., Armstrong, D. W. Eds.; American Chemical Society: Washington, D.C., Vol. 342,1987 p170.

(126) Nakada, K. *Jpn. Kokai Tokkoyo Koho JP 02 39,021* **1990**, Chemical Abstracts 113: 8472.

(127) Egawa, J.; Asachi, K.; Noboru, N.; Sugaya, Y.; Mizutani, C. *Jpn. Kokai Tokkyo Koho JP 02 90,936* **1990**, Chemical Abstracts, 113: 178031.

(128) Haage, K.; Welder, C.; Kriwanek, J.; Paetzelt, D.; Wasow, G. *Ger. (East) DD 273,264* **1990**, Chemical Abstracts 113: 65062.

(129) Takeru, F.; Seiichi, S.; Shigeyuki, S.; Toru, H.; Akiya, Y. *Eur. Pat. Appl. EP 332,222* **1990**, Chemical Abstracts 113: 29263.

(130) Gabriel, D.; Mulley, V. *Detection, Separation, and Isolation of Anionic Surfactants* in Anionic Surfactants-Chemical Analysis; Cross, J. Ed.; Marcel Dekker Inc.: New York, 1977, p 1.

(131) Trehy, M.; Gledhill, W.; Orth, R. *Anal. Chem.* **1990**, *62*, 2582.

(132) Zhu, P.; Su, K. *Org. Mass Spectrom.* **1990**, *25*, 260.

(133) Uno, T.; Nakagawa, T. *Gas Chromatography for the Analysis of Anionic Surfactants* in Anionic Surfactants-Chemical Analysis; Cross, J. Ed.; Marcel Dekker Inc.: New York, 1977, p 109.

(134) Kudoh, M.; Tsuji, K. *J. Chromatogr.* **1984**, *294*, 456.

(135) Candau, S. *Light Scattering* in Surfactant Solutions; Zana, R. Ed.; Marcel Dekker Inc.: New York, Vol. 22, 1987,p 147.

(136) Zana, R. *Luminescence Probe Methods* in Surfactant Solutions; Zana, R. Ed.; Marcel Dekker Inc.: New York, Vol. 22, 1987, p 241.

(137) Meguro, K.; Muto, Y.; Sakurai, F.; Esumi, K. *A Study of Mixed Aqueous Solutions of Hydrocarbon and Fluorocarbon Surfactants Using 1-Anilonaphthalene Sulfonic Acid Ammonium Salt* in Phenomena in Mixed Surfactant Systems; Scamehorn, J. Ed.; American Chemical Society: Washington D.C., Vol. 311, 1987, p 61.

(138) Lindeman, B.; Solderman, O.; Wennerstrom, H. *NMR Studies of Surfactant Solutions* in Surfactant Solutions; Zana, R. Ed.; Macel Dekker Inc.: New York, Vol. 22, 1987, p 295.

(139) Konig, H. *Nuclear Magnetic Resonance Spectrometry of Anionic Surfactants* in Anionic Surfactants-Chemical Analysis; Cross, J. Ed.; Marcel Dekker Inc.: New York, 1977, p 141.

(140) Bodenmiller, J.; Latz, H. *Anal. Chem.* **1971**, *43*, 1354.

(141) Hayes, M.; Curry, P.; Ewing, A. *Paper 415* Pittsburgh Conference, Chicago IL **1991**.

(142) Gobel, L.; Rasmussen, H.; McNair, H. *Paper 425P* Pittsburgh Conference, Chicago IL **1991**.

(143) Huang, X.; Luckey, J.; Gordon, M.; Zare, R. *Anal. Chem.* **1989**, *61*, 766.

(144) Dasgupta, P.; Soroka, K.; Vithange, R. *J. Liq. Chromatogr.* **1987**, *10*, 3287.

(145) Soroka, K.; Vithanage, R.; Phillips, D.; Walker, B.; Dasgupta, P. *Anal. Chem.* **1987**, *59*, 629.

(146) Kotrly, S.; Sucha, L. *Handbook of Chemical Equilibria in Analytical Chemistry* ; John Wiley & Sons: New York, 1985.

(147) *Lange's Handbook of Chemistry*; Dean, J. A. 13th eds., McGraw-Hill Book Company: New York 1985.

(148) Cunnane, S. *Zinc: Clinical and Biochemical Significance* ; CRC Press Inc.: Boca Raton, 1988.

(149) Atkins, P. W. *Physical Chemistry* ; W. H. Freeman and Company: San Fransico, 1982, Chapter 27.

(150) Lee, M.; Jackson, W.; Richter, B.; Fjeldsted, J. *J. Chromatogr.* **1983**, *423*, 279.

(151) Cheng, Y.; Piccard, R.; Vo-Dinh, T. *App. Spectroc.* **1990**, *44*, 755.

(152) Goedert, M.; Guiochon, G. *Chromatographia* **1973**, *6*, 76.

(153) Guiochon, G.; Sepaniak, M. *Anal. Chem.* **1991**, *63*, 73.

(154) Novotny, M.; Shelly, D.; Gluckman, J. *Anal. Chem.* **1985**, *57*, 1546.

VITA

David F. Swaile was born in Oil City, Pennsylvania on September 1, 1964. After graduation from Southwestern Central High School in Jamestown New York, he entered Wake Forest University in the fall of 1982. He graduated in May 1986 with a Bachelor of Science in Chemistry. In the fall of 1986 he entered Clemson University, but after one year of study he entered the University of Tennessee. While at the University of Tennessee he married Beverly Ann Hanes of Winston Salem, North Carolina on July 16, 1988. He successfully completed the requirements for a Doctor of Philosophy Degree in Chemistry in the summer of 1990 and graduated in December.